DIAGONAL TENSION CRACKING IN REINFORCED CONCRETE BEAMS

by

Desmond Williams

A thesis submitted to the Faculty of Graduate Studies and Research in partial fulfilment of the requirements for the degree of Master of Engineering.

Department of Civil Engineering
and Applied Mechanics,
McGill University,
Montreal. July, 1961

ABSTRACT

Nine rectangular reinforced concrete beams, without web reinforcement but with varying amounts of longitudinal tensile reinforcement, were tested under simple span concentrated loading at a shear span to effective depth ratio of three. The results of this investigation indicated that increased resistance to diagonal tension cracking was associated with increased amounts of longitudinal reinforcement.

A stress function, derived to describe the state of stress in a homogeneous elastic beam, enabled an estimate to be made of the local effects of a concentrated load on a "shear" beam. Strain measurements made adjacent to the support point of a reinforced concrete beam bore a reasonable similarity with the above theoretical values for a homogeneous beam.

Measurements made of the slip of longitudinal reinforcing bars showed this to be relatively small. Strain measurements made above diagonal tension cracks indicated major stress redistributions at formation of the cracks.

CONTENTS

FIGURES

FIGURES (Concluded)

PLATES

TABLES

APPENDIX B

ACKNOWLEDGEMENTS

The tests reported in this thesis were carried out in the laboratory of the Department of Civil Engineering, McGill University.

The author wishes to express his appreciation for help given by Prof. P. Harris, under whose direction this thesis was written, both in the investigation in general and with regard to the theory of elasticity in particular.

Prof. Wilson and the staff of the laboratory gave invaluable assistance in conducting the test program.

Thanks are due also to Prof. R. Yong, Dept. of Civil Engineering, for his assistance in photographing the beams.

The author wishes to express thanks to Mr. M. McNaughton, Vice-President, Mount Royal Paving and Supplies Ltd., for his advice on concrete mixing and placing; also to Mount Royal Paving and Supplies Ltd., who generously provided the concrete for the test program.

Finally, to my wife, for her infinite patience and assistance.

DEFINITIONS AND NOTATION

CRITICAL SECTION is the section of potential shear compression failure in a beam containing a diagonal tension crack. In a beam under concentrated loading,this is the vertical cross section through the edge of a load or support bearing block, inside a shear span.

DIAGONAL TENSION CRACK is a well-defined inclined crack,extending from the tension steel to the critical section.

DIAGONAL TENSION FAILURE is a failure occurring simultaneously with the formation of a diagonal tension crack.

INITIAL INCLINED CRACK is that hairline crack through which the diagonal tension crack eventually "opens up".

MAXIMUM MOMENT to SHEAR MULTIPLIED by EFFECTIVE DEPTH RATIO (M/Vd ratio) in a beam under concentrated loading is the ratio of the maximum moment in a shear span to shear force in that span multiplied by the effective beam depth. For a simply supported beam, this ratio reduces to a/d ratio.

SHEAR BLOCK in a simple beam is that portion of the beam above a diagonal tension crack, extending from the crack to the support point.

SHEAR COMPRESSION FAILURE is that failure occurring at crushing of the compression zone at the critical section.

SHEAR SPAN in a beam under concentrated loading is that span across which the shear force has a constant value (not zero).

SHEAR SPAN to DEPTH RATIO (a/d ratio) is the ratio of shear span length to effective beam depth, for a simple beam.

α = a factor describing the cycles of a trigonometric or hyperbolic series $= 2\pi m/\ell$

∞ = infinity

A_s = area of tension steel reinforcement

A_v = area of web steel reinforcement

a = length of shear span in a simple beam

a/d = shear span to depth ratio. See definitions above.

b = width of a rectangular beam

c = half depth of a beam

d = effective depth of a reinforced concrete beam; it is the distance from the centroid of the tension reinforcement to the compression face.

$\delta_{℄}$ = deflection at the centre of a reinforced concrete beam.

E = east side electric strain gage on a beam

E_c = modulus of elasticity of concrete

E_s = modulus of elasticity of steel

$\epsilon_1 \rightarrow \epsilon_7$ = maximum strains in the compression zone and on the tension steel, of a reinforced concrete beam.

f'_c = compressive strength of a 6 by 12 inch concrete cylinder.

f_s = stress in tension reinforcement.

f'_t = modulus of rupture of concrete.

f_v = allowable tensile stress in web reinforcement.

g = position of a line of electric strain gages in relation to a load point, Fig. 10.

h_f & h_o = length of the overhang beyond the support point at the end of the shear span forming the first and second (if any) diagonal tension cracks respectively, Fig. 6.

I = moment of inertia of a beam's cross section with respect to its centroid.

jd = internal moment arm of a reinforced concrete beam, computed by "Cracked Section Theory".

k_1, k_2, k_3 & k_s = coefficients defining magnitude and position of the internal compressive force in a reinforced concrete beam failing by destruction of the compression zone, Fig. 1.

ℓ = total length of a beam.

L = length between the supports of a beam.

M = bending moment

M/Vd = maximum moment to shear multiplied by effective depth ratio -- see definitions above.

$(M/V)_c$ = ratio of the moment around the centroid of the compressive force to the shear at the section where the diagonal tension crack starts.

M_s = moment at the critical section of a beam at shear compression failure.

m = the number of the cycle to be added into the summation of a trigonometric or hyperbolic series.

micro-inch = .000,001 inch

μ = Poisson's ratio

p = tension steel ratio = A_s/bd

n = modular ratio = E_s/E_c

P = machine load on a test beam

q = position of a uniformly applied load pressure on a homogeneous beam, Fig. 2.

r = width of uniformly applied load pressure on a homogeneous beam, Fig. 2.

s = position of a uniformly applied support pressure on a homogeneous beam. Fig.2.

S = spacing of web bars along axis of beam

S_f & S_o = position of slip gages in the shear span forming the first and the second (if any) diagonal tension cracks respectively, in relation to the load points, Fig. 6.

$\sum$ = summation sign

σ_x, σ_y + τ_{xy} = horizontal and vertical stress components in a homogeneous beam.

σ_x' = difference between the horizontal stress components in a homogeneous beam given by elementary beam theory and by a stress function.

t = width of a uniformly applied support pressure on a homogeneous beam, Fig.2.

u = magnitude of a uniformly applied support pressure on a homogeneous beam, Fig.2.

Ø = stress function

V = external shear force = $\frac{1}{2}P$

V_c = external shear force at diagonal tension crack formation

V_u = external shear force at shear compression failure

v = nominal shear stress = V/bjd

v_c = nominal shear stress at diagonal tension crack formation.

W = west side electric strain gages on a beam.

w = magnitude of a uniformly applied load pressure on a homogeneous beam, Fig. 2.

$\overline{X}$, $\overline{Y}$ & $\overline{T}$ = factors used in computations of stress components in a homogeneous beam.

X & Y = rectangular coordinates.

INTRODUCTION

It has been known for a good number of years that so-called "shear" failures in reinforced concrete beams are the result of excessive principal tensile stresses in the concrete. Shear stress combines with flexural stress to form a resultant diagonal tension stress. Relatively short, deep beams have been found to be more susceptible to failure from such stresses than have longer, slimmer beams. Both shear and flexural stress can only be estimated approximately, yet shear stress is widely used as a measure of a beam's resistance to principal tensile stresses.

Object

Varying the steel ratio in a reinforced concrete beam moves the neutral axis, changing the tensile stresses in both the steel and concrete, including the principal tensile stresses in the concrete.

The primary purpose of this investigation was to show that a decrease in the amount of longitudinal reinforcement in a deep concrete beam is accompanied by decreased resistance to the formation of a diagonal tension crack.

The second objective was the evaluation of the local state of stress adjacent to a concentrated load point on a homogeneous elastic beam.

Included in this investigation were two secondary objectives:

Firstly, to show that steep diagonal tension cracks could only develop with considerable slippage of the longitudinal reinforcing bars.

Secondly, to determine the stress distribution at the critical section (see Definitions and Notation) above a diagonal tension crack.

Review of Earlier Research

Among the earliest studies made on the design of web reinforcement for reinforced concrete beams was one by Ritter*. In 1899 he suggested the "truss analogy" method of stirrup design:

$$V = \frac{A_v f_v jd}{s}$$

Between the years 1902 and 1909, Mörsch* made extensive contributions to our knowledge of the behavior of reinforced concrete beams under shear loads. He pointed out that principal tensile stresses are the cause of "shear" failures and that the action of web reinforcement is analogous to that of the diagonals in a truss and must be stressed in tension, not in shear as had earlier been believed. He derived the well known equation for shear stress, $v = \frac{V}{bjd}$

* Source for this is an abstract made by Hognestad (1).

and introduced the idea of analyzing as a free body that portion of a beam to one side of a diagonal crack--the shear block.

In the investigations which shaped the German Building Code requirements with respect to shear (thus influencing our own code), the names of O. Graf* and C. Bach* should be mentioned. They carried out much of the testing for the German Committees, under Mörsch's chairmanship.

In the United States, A. N. Talbot (2) was one of the earlier investigators. After conducting several series of tests between 1906 and 1909, he demonstrated that the nominal shearing strength of a reinforced concrete beam is improved by: increased cement content and age of concrete, increased amounts of longitudinal reinforcement, decreased shear span to effective depth ratio, and by adding stirrups and bent up bars. He also noted that stirrup stresses, as calculated by the truss analogy, were considerably higher than the measured stresses, and suggested modifying design practice to have the stirrups carry only two-thirds of the shear load.

In 1927 and 1928, Frank E. Richart (3) and Richart & Larson (4) presented the results of an extensive test program which was mainly concerned with the behavior of simple and restrained concrete beams with various types and arrangements of web reinforcement. Among other things, they found increased shear strength with: decreased shear

---

*Source for this is an abstract made by Hognestad (1).

span (in beams of the same depth), increased amounts of longitudinal reinforcement, and especially with web reinforcement. In connection with their findings on web reinforcement they noted that web reinforcement stresses were very small until diagonal tension cracking commenced; that there was considerable variation of web reinforcement stress with position in the shear span; and that the point of intersection with the diagonal tension cracks produced the greatest stresses in the stirrups. Even this maximum value was less than that given by the truss analogy equation, so Richart presented a modification to the equation.

Two topics which received a great deal of attention in this report were bond and anchorage. It was found that hooks and bends on bent-up bars caused considerable crushing -- often destruction of the beam. Richart indicated that adequate anchorage was essential to realize the reinforcement's full capacity, both for research purposes and in general design practice.

Dating from 1945, there has been a considerable amount of research done on shear failures at the University of Illinois. The earliest of this research was reported by Oreste Moretto (5), who made a study of welded stirrups in simply supported beams. His approach was to analyze the failures in terms of two stages -- the first being yielding of web reinforcement; the second being ultimate capacity. Both stages were found to be affected by the web reinforcement, the cylinder compressive strength of the concrete, and the amount of longitudinal reinforcement. Later, Arthur P. Clark (6) conducted similar tests, and showed that the ultimate shear capacity was greatly influenced by the a/d ratio as well as the other factors listed by Moretto.

In a 1951 report, E. Hognestad described modes of failure and stress redistribution* in restrained beams. These are basically the same as in simple beams. Fig.1(a) shows a beam containing a well-developed diagonal tension crack -- but with considerable load-carrying capacity remaining. A redistribution of stress has occurred as the crack formed -- the original beam action and stress distribution no longer exist. The longitudinal steel stress at section b-b has increased sharply, the local stress between sections a-a and b-b being governed by the bending moment at section a-a.

In considering a restrained beam, it can be noted that with one crack stress redistribution is only partially accomplished in the span. Part of the span is still behaving as a normal beam. On the condition that adequate ultimate capacity remains at the first diagonal tension

---

* These phenomena are fully described by Moody et al.(9), pp. 329 & 429 and Laupa et al.(8), p. 45. The original description appeared in an unpublished report,"Shear Failures in Concrete Beams", Department of Theoretical and Applied Mechanics, University of Illinois, 1951; see Laupa et al.(8) footnote, p. 45.

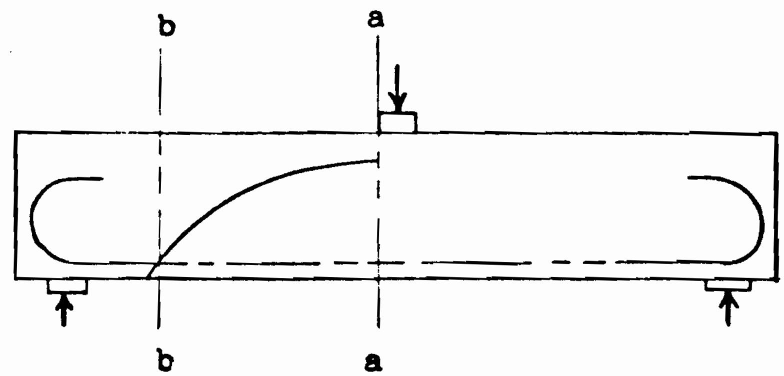

(a) Simply Supported beam with a diagonal crack.

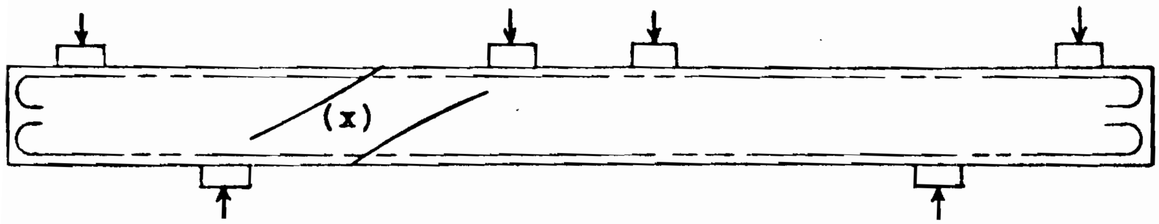

(b) Restrained beam with two diagonal cracks.

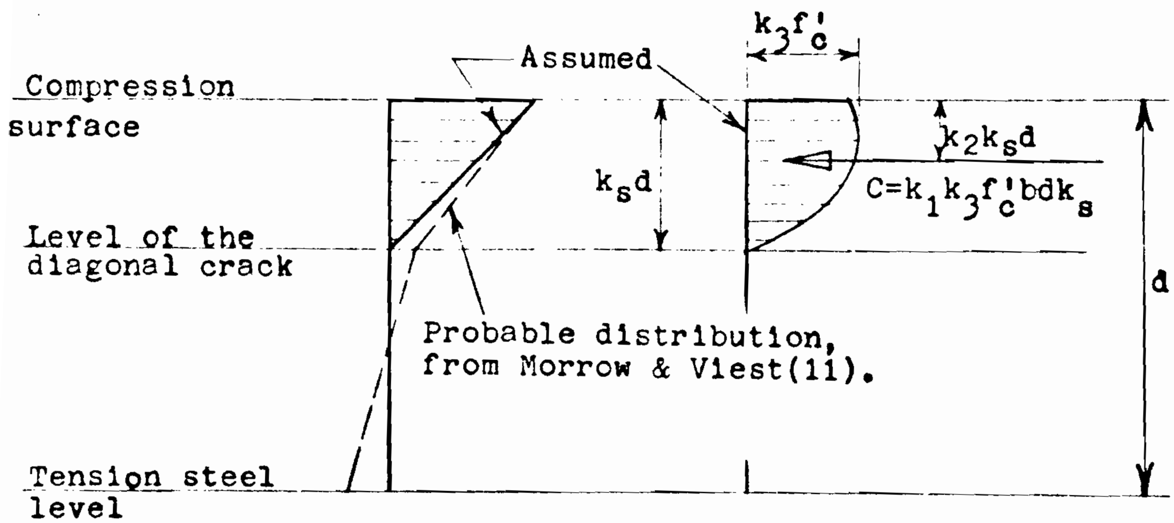

(i) Compressive strain distribution (ii)Stress Block

(c) Hypothetical distribution of stress and strain at the critical section of a beam failing in shear compression, as given in current literature.

Fig.1-Redistribution of Internal Stresses after Diagonal Crack Formation.

crack, a second will often form on the opposite side of the point of contraflexure, Fig. 1(b). This then, represents complete stress redistribution. For short shear spans, the two cracks are quite close together, often resulting in local bond failures through the uncracked zone, marked (x), causing the reinforcement to be in tension completely across the span. The zone (x) is now acting as a compression strut and the ultimate capacity of the beam is greatly reduced.

In 1953, E. M. Zwoyer (7) noted the similarity between flexural compression failures and that failure occurring in a diagonally cracked beam when the compression zone crushes at a considerably greater load than that at which the crack formed. This type of failure has been termed a "shear compression" failure.

An extensive analytical study of existing data was undertaken by Laupa, Siess and Newmark (8), and published in 1955. They were mainly concerned with compressive type failures at the critical section near the load point of a beam containing a fully developed diagonal tension crack -- shear compression failures. They considered that the criterion for the ultimate capacity of such a beam was a limiting moment rather than a shear stress. Their studies indicated that this ultimate moment capacity was influenced mainly by the cross sectional dimensions of the beam, the amount of longitudinal reinforcement, and the cylinder compressive strength of the concrete, but not by the shear span to depth ratio. By considering the state of stress existing in the zone under compression, they derived a relatively simple equation for ultimate moment capacity. This equation involved the empirical determination of the depth of the compression zone and the average compressive stresses in it, both of which they concluded to be primarily a function of the cylinder compressive strength of the concrete, and only secondarily of the amount of longitudinal reinforcement. This equation was adapted to fit various types of beams and loadings.

In 1954, following several series of test programs, Moody, Viest, Elstner & Hognestad (9) published a four part report dealing with reinforced concrete beams under concentrated loads. They envisaged the failure to be composed of two stages -- diagonal tension cracking and stress redistribution, followed by a shear compression failure at some higher load. But this mode of failure was found to depend on the ratio of the maximum moment in the effective shear span to the maximum shear multiplied by the effective depth of the beam (M/Vd); for beams of small M/Vd ratio, i.e. less than 3.5, the above mentioned failure pattern did occur. In fact, the smaller the M/Vd ratio, the greater the capacity beyond diagonal crack formation. For intermediate M/Vd ratios, they found that diagonal crack formation was accompanied by immediate collapse -- termed "diagonal tension" failures. Large M/Vd ratios resulted in flexural failures.

With some variations, diagonal tension crack growth or formation is reasonably similar in the descriptions given by current authors. Diagonal tension cracks coincided either with inclined flexural cracks or with cracks which appeared slightly above the level of the longitudinal reinforcement. In the case of restrained beams, there was added the possibility of cracks appearing at mid-depth. For smaller M/Vd ratios, crack growth and stress redistribution were slow -- the exact load at which an inclined crack could be called a diagonal tension crack,appeared to be arbitrary. Increasing M/Vd ratios served to more definitely pinpoint the formation of a diagonal tension crack. For the M/Vd ratios at which diagonal tension failures occurred, crack formation was, of course, defined by the failure. The presence of web reinforcement served to disperse the diagonal tension cracks -- to produce a diagonally cracked zone -- but did not delay the crack formation to any noticeable degree.

Moody et al.(9) found that only the beam dimensions, M/Vd ratio, and cylinder compressive strength appeared to influence diagonal tension crack formation, and presented an empirical equation to predict shear stress at crack formation. In restrained beams, the diagonal tension crack which formed first was found to be nearer the load point at which maximum moment occurred. They noted that the ultimate moment capacity at a shear compression failure was influenced primarily by the beam dimensions, amount of longitudinal reinforcement, cylinder compressive strength of concrete, and web reinforcement, but not by the M/Vd ratio. Although their basic equation involved the statics of the shear block, it contained several empirical parameters describing the stress distribution in the concrete above the diagonal crack (at the critical section) and the stress in the longitudinal reinforcement. This was a general equation to predict the failure moment of a restrained beam at any stage of stress redistribution.

In 1956, Phil M. Ferguson (10), at the University of Texas, pointed out that the increased ultimate capacity associated with beams of small M/Vd ratios must, to a considerable extent, be due to the local pressures caused by the load and support points -- that, in fact, it is the load points which stabilize diagonal crack development in order to produce a shear compression failure. By applying load and reaction to test beams as shears on the sides of the beams, rather than as pressures on the top and bottom surfaces of the beams, he demonstrated that ultimate capacity was reduced appreciably.

This report also emphasized the use of combined stress calculations in shear studies, and presented a hypothesis of diagonal tension crack growth based on such thinking.

The results of another of the University of Illinois test programs were reported in 1957 by Morrow and Viest (11). They presented an expression for the diagonal tension cracking load based on the principle of combined stresses and involving the modulus of rupture of concrete. It contained the dimensionless quantity $\frac{(M/V)_c}{npd}$, $(M/V)_c$ being the moment-shear ratio at the section where the diagonal crack intersected the longitudinal tension reinforcement. Also included was an expression for shear compression moment capacity, quite similar in derivation to that of Moody et al. (9). This program included frames loaded with a certain amount of axial load, but the authors concluded that this affected the shear and diagonal tension strengths only in that it changed the conditions of statics. With respect to the M/Vd ratio -- shear stress at diagonal tension failure was not affected too greatly by it, but limiting moments in shear compression failures increased with decreasing values of the ratio.

Charles S. Whitney (12), in reviewing the above data, noted that diagonal tension cracking loads appeared to be proportional to the ultimate flexural capacity of the section, and presented an expression in which the shear stress at diagonal tension crack formation was a function of only a/d ratio and ultimate flexural moment capacity. He also stressed his belief that the criterion for any future ultimate shear strength design method should be based on diagonal tension cracking capacity rather than shear compression capacity.

Two further reports concerning tests of beams and frames without web reinforcement were published at the University of Illinois in 1960. The first of these, by R. Diaz De Cossio and C. P. Siess (13), was a study of stub beams, and beams and frames under simulated uniform load (multiple load points). With respect to the uniform loadings -- crack development and beam behavior were essentially the same as those found for beams under concentrated loadings; shear compression failures were found for the shorter beams, and diagonal tension failures for the longer beams. It was found, however, that under uniform loads, the beams possessed around 150% greater diagonal tension cracking and ultimate capacities than when under concentrated loads. An obvious point, brought out by the authors, was that for uniform loading, the diagonal tension crack does not form at either the sections of maximum shear or moment, but at some intermediate location.

The other investigation, by J. E. Bower and I. M. Viest (14), consisted of a study of restrained beams with the object of ascertaining the effects of the M/Vd ratio and the ratio of maximum negative to maximum positive moment in the shear span. Of importance is their definition of the "effective" shear span. As previously described, the shear span is that portion of the beam between the load and support points, whereas Bower and Viest define effective shear span as that portion of the shear span between the point of contraflexure and the load or support points. The length of an effective shear span equals the maximum moment to shear ratio (M/V) of that particular span.

Bower and Viest demonstrated that a diagonal tension crack formed in one effective shear span, never crossing a point of contraflexure. Also noted was the fact that, although a shear span could contain two diagonal tension cracks, the crack which formed first was in that effective shear span with the larger moment. The ratio of negative to positive moment had no effect on either diagonal tension cracking load or ultimate load, but did have a small effect on ultimate moment capacity in shear compression failure. The M/Vd ratio influenced the diagonal tension cracking load, but not the ultimate moment capacity in shear compression failure. Neither the lengths of the effective shear span nor true shear span affected the cracking or failure behavior.

Authors of current literature appear to be divided as to the contribution of the amount of longitudinal tension reinforcement to the diagonal tension cracking strength of reinforced concrete beams. Moody et al.(9) found that the amount of longitudinal reinforcement had no effect on shear at the formation of diagonal tension cracks in either simple or restrained beams, with or without web reinforcement. Nor could Al-Alusi (15), testing T-beams at an M/Vd ratio of four, or Hanson (16), testing lighweight aggregate beams, find any correlation between the two, although the Hanson report is accompanied by the discussions of several authors who mention this point.

On the other hand, an examination of the Morrow-Viest (11) data shows a definite trend toward increased diagonal tension cracking load with increased amounts of longitudinal reinforcement. In the report, the analysis of diagonal crack formation included this factor in the dimensionless quantity $\frac{(M/V)_c}{npd}$. Whitney (12), in an analysis of the same data, introduced this factor by relating diagonal tension cracking strength to ultimate flexural moment capacity, which, for underreinforced beams, is largely a function of p. Ferguson (10) pointed out that increased amounts of reinforcement reduce both the amount of and height of flexural cracking and that this effect is accompanied by increased resistance (in rectangular beams) to the formation of diagonal tension cracks. J. Taub and A. M. Neville (17), in their examination of current literature, considered that the contribution of the amount of longitudinal reinforcement was limited to beams of larger M/Vd ratios, say three to five. At small M/Vd ratios, varying the steel area produced no noticeable effect on diagonal cracking load.

The fact that increased amounts of longitudinal reinforcement increases a beam's resistance to a shear compression failure was universally accepted. Increased steel area tends to slow widening of the diagonal tension crack, reducing the consequent rotation in the compression zone and thus increasing ultimate capacity.

In the various analyses of shear compression failures, assumptions have beem made as to the stress distribution in the compression zone at the critical section (see Definitions and Notation). Moody et al.(9) and Laupa et al.(8) have assumed the compressive stress distribution in this zone to be of the same shape as that for reinforced concrete beams failing in flexural compression and that it could be described with the aid of similar parameters, see Fig. 1(c). Morrow and Viest (11), while using the same assumption, indicated that some compressive strain would probably exist at, and even below, the level of the diagonal tension crack.

Scope of Research

The test program in its final form included two series (Series I and II) of reinforced concrete beams, each consisting of four shear beams with varying amounts of longitudinal reinforcement. No web reinforcement or compression reinforcement was used. The beams were of rectangular cross section, similar in dimensions, and had an a/d ratio of 3. In addition, two smaller beams were tested to supplement the information gathered from tests on the above beams. The results of this investigation included nominal shear stress at formation of a diagonal tension crack, slip measurements of the longitudinal reinforcement at one point in each shear span, and strain measurements. Concrete strains were measured above the base block of one beam and at one cross section in each of four shear spans. The original object of the shear span strain measurements was to determine the stress distribution at the critical section above a well-developed diagonal tension crack. However, at the a/d ratio chosen for this investigation, it was found that most of the beams failed upon formation of the diagonal tension crack, making it impossible to obtain the desired measurements.

A stress function in the form of a trigonometric series was derived to describe the state of stress in a homogeneous elastic beam of similar proportions to those of this investigation. Strain measurements near the base blocks were made during the test program, and compared to those resulting from the stress function.

Design

Originally, a set of four short shear beams and one long, shallow beam had been intended, but due to the very poor condition of the concrete in the first set, it was thought desirable to include a duplicate set of beams. These two sets differed only in concrete compressive strength; they are labelled Series I and Series II respectively. The long beam was later chopped in half to produce two more shear specimens; both are part of Series I.

The design of the shear beams eliminated all variables except that of steel ratio. Thus, all were given the same nominal cross sectional dimensions and length. In order to eliminate as much as possible any variation in the quality and strength of the concrete, all beams of each series were poured from a single batch of ready-mix concrete. It was thus possible to use a single cylinder compressive strength to describe each series.

To facilitate handling, the cross section size finally selected had a width of 7 inches and effective depth of 10 inches. For purposes of obtaining strain measurements above a well-developed diagonal tension crack, it was essential that the beam have considerable capacity beyond that load causing the crack. To insure this, it was thought that an a/d ratio of 3 would be adequate. Using the above a/d ratio and third point loading, the required span length was set at 7 feet 6 inches.

The steel ratio was varied from 1.7% to 3.9%. The larger ratios required two layers of reinforcing bars, thus introducing an unavoidable variable into the program. Studies of the diagonal tension cracking and flexural capacities of the beams by means of equations presented by several authors in the current literature on shear studies, indicated the possibility that the failure of those beams with the smaller steel ratios could be triggered by yielding of the steel rather than by a diagonal tension crack. However, this danger was reduced by the use of a hard grade steel in the beams with the lowest steel ratio. An added feature introduced in varying the steel ratio was the use of butt-welded reinforcing bars in one beam. By splicing together, in the central span, bars of differing cross sectional areas, it was possible to obtain different steel ratios in either shear span of a single beam. In this way it was possible to extend the range of the major variable. However, due to the large bond stresses expected in the concrete at the point where the load in the larger bar was transferred to the smaller bar, this method was found to be practical for only one specimen.

THEORY

In order to describe the state of stress in the rectangular, homogeneous, elastic beam shown in Fig.2, a stress function in the form of a trigonometric series has been derived. This is a simply supported beam under

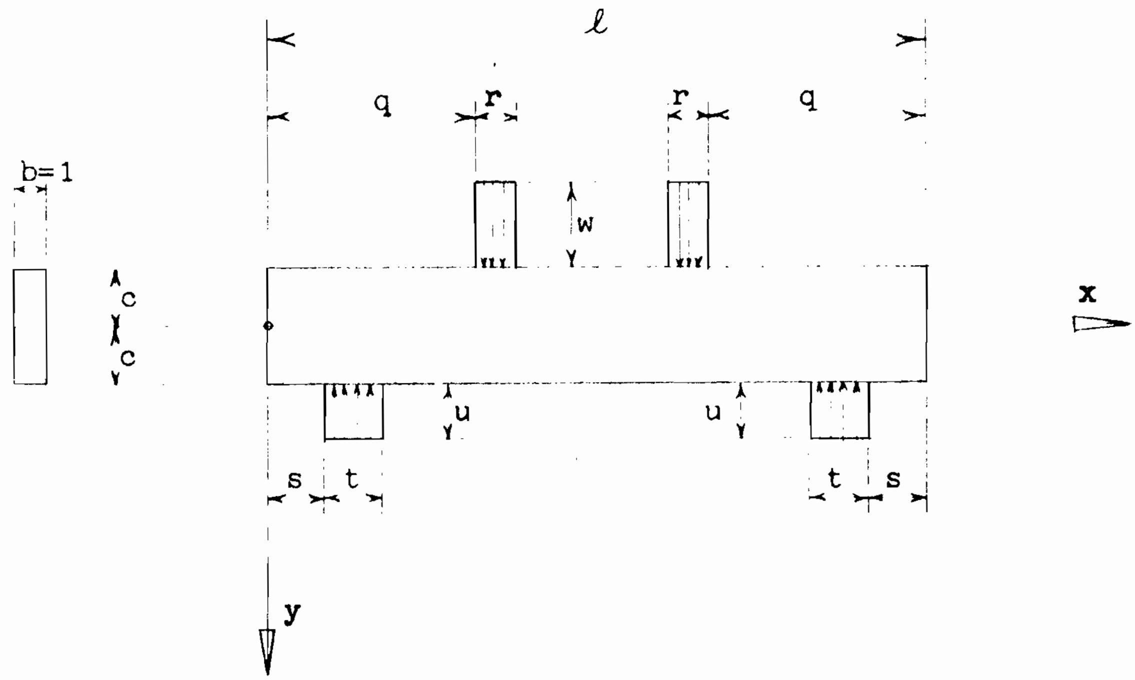

Fig.2.- Homogeneous Beam Under Discontinuous, Uniform Loading Pressures.

two point loading and can be assumed to be a case of plane stress. The boundary conditions involve discontinuous, uniform loads. Such a distribution of vertical loading, f(x), along the top and bottom surfaces of the beam can be represented by the following Fourier Series:

$$f(x) = A_o + \sum_{m=1}^{m=\infty} a_m \sin \alpha x + \sum_{m=1}^{m=\infty} b_m \cos \alpha x \qquad (1)$$

where $A_o = 1/\ell \int_0^\ell f(x)\, dx$

$$a_m = 2/\ell \int_0^\ell f(x) \sin \alpha x \, dx$$

and $b_m = 2/\ell \int_0^\ell f(x) \cos \alpha x \, dx$

with ℓ = length of the cycle.

m = the number of the cycle to be added into the summation.

and $\alpha = 2\pi m/\ell$

Considering the top surface of the beam:

$$A_o = 1/\ell \int_q^{q+r} w \, dx + 1/\ell \int_{\ell-q-r}^{\ell-q} w \, dx = 2rw/\ell$$

$$a_m = 2/\ell \int_q^{q+r} w \sin \alpha x \, dx + 2/\ell \int_{\ell-q-r}^{\ell-q} w \sin \alpha x \, dx = 0$$

$$b_m = 2/\ell \int_q^{q+r} w \cos \alpha x \, dx + 2/\ell \int_{\ell-q-r}^{\ell-q} w \cos \alpha x \, dx$$

$$= \frac{4w}{\pi m} \sin \alpha r/2 \ \cos \alpha (r/2 + q)$$

Therefore, for the top surface of the beam,

$$f(x) = \frac{2rw}{\ell} + \sum_{m=1}^{m=\infty} \left[\frac{4w}{\pi m} \sin \alpha r/2 \ \cos \alpha (r/2 + q)\right] \cos \alpha x \qquad (2)$$

Similarly, the boundary conditions on the bottom of the beam can be described by the function:

$$\frac{2tu}{\ell} + \sum_{m=1}^{m=\infty} \left[\frac{4u}{\pi m} \sin \alpha t/2 \ \cos \alpha (t/2 + s)\right] \cos \alpha x \qquad (3)$$

The stress function , ϕ, must satisfy the equation

$$\frac{\partial^4 \phi}{\partial x^4} + 2\frac{\partial^4 \phi}{\partial x^2 \partial y^2} + \frac{\partial^4 \phi}{\partial y^4} = 0 \tag{4}$$

and the boundary conditions as given by eqs.(2) and (3).

Take $\phi = \cos \alpha x [f(y)]$ (a)

Substitution of this into eq.(4) results in the equation

$$\alpha^4 f(y) - 2\alpha^2 \frac{\partial^2 f(y)}{\partial y^2} + \frac{\partial^4 f(y)}{\partial y^4} = 0 \tag{5}$$

The general integral of this linear differential equation with constant coefficients is, as suggested in Timoshenko and Goodier (18), page 47,

$$f(y) = C_1 \cosh \alpha y + C_2 \sinh \alpha y + C_3 y \cosh \alpha y + C_4 y \sinh \alpha y \tag{b}$$

The substitution of this into eq.(a) gives the following stress function:

$$\phi = \cos \alpha x [C_1 \cosh \alpha y + C_2 \sinh \alpha y + C_3 y \cosh \alpha y + C_4 y \sinh \alpha y] \tag{c}$$

while the stress components become

$$\sigma_x = \frac{\partial^2 \phi}{\partial y^2} = \cos \alpha x [C_1 \alpha^2 \cosh \alpha y + C_2 \alpha^2 \sinh \alpha y + C_3(\alpha^2 y \cosh \alpha y + 2\alpha \sinh \alpha y) + C_4(\alpha^2 y \sinh \alpha y + 2\alpha \cosh \alpha y)] \tag{d}$$

$$\sigma_y = \frac{\partial^2 \phi}{\partial x^2} = -\alpha^2 \cos \alpha x [C_1 \cosh \alpha y$$
$$C_2 \sinh \alpha y + C_3 y \cosh \alpha y + C_4 y \sinh \alpha y]$$

$$\tau_{xy} = -\frac{\partial^2 \phi}{\partial x \partial y} = \alpha \sin \alpha x [C_1 \alpha \sinh \alpha y + C_2 \alpha \cosh \alpha y$$
$$+ C_3(\alpha y \sinh \alpha y + \cosh \alpha y)$$
$$+ C_4(\alpha y \cosh \alpha y + \sinh \alpha y)]$$

The constants C_1, C_2, C_3 and C_4 can be determined from the boundary conditions of the beam, for any given cycle "m".

At $y = \pm c$, $\tau_{xy} = 0$. Therefore at $y = +c$

$$\alpha \sinh \alpha x [C_1 \alpha \sinh \alpha c + C_2 \alpha \cosh \alpha c + C_3(\alpha c \sinh \alpha c$$
$$+ \cosh \alpha c) + C_4(\alpha c \cosh \alpha c + \sinh \alpha c)] = 0 \qquad \text{(e)}$$

and at $y = -c$

$$\alpha \sinh \alpha x [C_1 \alpha \sinh(-\alpha c) + C_2 \alpha \cosh(-\alpha c) + C_3(-\alpha c \sinh(-\alpha c)$$
$$+ \cosh(-\alpha c)) + C_4(-\alpha c \cosh(-\alpha c) + \sinh(-\alpha c))] = 0 \qquad \text{(f)}$$

At $y = \pm c$, σ_y is given by eqs.(2) and (3), which contain both a trigonometric series term and a constant: $2rw/\ell$ or $2tu/\ell$. These constants represent a uniform load across the complete length of the beam.However the stress function is best derived to include only the loading due to the trigonometric term, the effects of the uniform load being added afterward to the stress components. Thus at $y = +c$

$$\sigma_y + \frac{2tu}{\ell} = -\frac{4u}{\pi m}[\sin \alpha t/2 \, \cos \alpha (t/2 + s)] \cos \alpha x$$
$$= -\alpha^2 \cos \alpha x [C_1 \cosh \alpha c$$
$$+ C_2 \sinh \alpha c + C_3 c \cosh \alpha c + C_4 c \sinh \alpha c] \qquad \text{(g)}$$

and at $y = -c$,

$$\sigma_y + \frac{2rw}{l} = -\frac{4w}{\pi m}\left[\sin\alpha r/2\ \cos\alpha(r/2+q)\right]\cos\alpha x$$

$$= -\ \alpha^2\cos\alpha x\left[C_1\cosh(-\alpha c)\right.$$

$$\left.+ C_2\sinh(-\alpha c) - C_3 c\cosh(-\alpha c) - C_4 c\sinh(-\alpha c)\right] \qquad \textbf{(h)}$$

Solving eqs.(e), (f), (g) and (h) results in the following values for the constants:

$$C_1 = \frac{1}{\alpha^2}\left[\frac{4w}{\pi m}\sin\alpha r/2\ \cos\alpha(q+r/2) + \frac{4u}{\pi m}\sin\alpha t/2\ \cos\alpha(s+t/2)\right]\times$$
$$\times\left[\frac{\sinh\alpha c + \alpha c\cosh\alpha c}{\sinh 2\alpha c + 2\alpha c}\right]$$

$$C_2 = -\frac{1}{\alpha^2}\left[\frac{4w}{\pi m}\sin\alpha r/2\ \cos\alpha(q+r/2) - \frac{4u}{\pi m}\sin\alpha t/2\ \cos\alpha(s+t/2)\right]\times$$
$$\times\left[\frac{\cosh\alpha c + \alpha c\sinh\alpha c}{\sinh 2\alpha c - 2\alpha c}\right] \qquad \textbf{(k)}$$

$$C_3 = \frac{1}{\alpha^2}\left[\frac{4w}{\pi m}\sin\alpha r/2\ \cos\alpha(q+r/2) - \frac{4u}{\pi m}\sin\alpha t/2\ \cos\alpha(s+t/2)\right]\times$$
$$\times\left[\frac{\alpha\cosh\alpha c}{\sinh 2\alpha c - 2\alpha c}\right]$$

$$C_4 = -\frac{1}{\alpha^2}\left[\frac{4w}{\pi m}\sin\alpha r/2\ \cos\alpha(q+r/2) + \frac{4u}{\pi m}\sin\alpha t/2\ \cos\alpha(s+t/2)\right]\times$$
$$\times\left[\frac{\alpha\sinh\alpha c}{\sinh 2\alpha c + 2\alpha c}\right]$$

Substituting the constants into eq.(c) gives the stress function:

$$
\begin{aligned}
\phi = \frac{\cos\alpha x}{\alpha^2}\Bigg\{ & \left[\frac{4w}{\pi m}\sin\frac{\alpha r}{2}\cos\alpha\left(q+\frac{r}{2}\right)+\frac{4u}{\pi m}\sin\frac{\alpha t}{2}\cos\alpha\left(s+\frac{t}{2}\right)\right]\times \\
& \times\left[\frac{\cosh\alpha y(\alpha c\cosh\alpha c+\sinh\alpha c)-\alpha y\sinh\alpha y\sinh\alpha c}{\sinh 2\alpha c+2\alpha c}\right] \\
& -\left[\frac{4w}{\pi m}\sin\frac{\alpha r}{2}\cos\alpha\left(q+\frac{r}{2}\right)-\frac{4u}{\pi m}\sin\frac{\alpha t}{2}\cos\alpha\left(s+\frac{t}{2}\right)\right]\times \\
& \times\left[\frac{\sinh\alpha y(\alpha c\sinh\alpha c+\cosh\alpha c)-\alpha y\cosh\alpha y\cosh\alpha c}{\sinh 2\alpha c-2\alpha c}\right]\Bigg\} \qquad (6)
\end{aligned}
$$

The stresses resulting from this stress function thus become:

$$
\begin{aligned}
\sigma_x = \sum_{m=1}^{m=\infty}\cos\alpha x\Bigg\{ & \left[\frac{4w}{\pi m}\sin\frac{\alpha r}{2}\cos\alpha\left(q+\frac{r}{2}\right)+\frac{4u}{\pi m}\sin\frac{\alpha t}{2}\cos\alpha\left(s+\frac{t}{2}\right)\right]\times \\
& \times\left[\frac{\cosh\alpha y(\alpha c\cosh\alpha c-\sinh\alpha c)-\alpha y\sinh\alpha y\sinh\alpha c}{\sinh 2\alpha c+2\alpha c}\right] \\
& -\left[\frac{4w}{\pi m}\sin\frac{\alpha r}{2}\cos\alpha\left(q+\frac{r}{2}\right)-\frac{4u}{\pi m}\sin\frac{\alpha t}{2}\cos\alpha\left(s+\frac{t}{2}\right)\right]\times \\
& \left[\frac{\sinh\alpha y(\alpha c\sinh\alpha c-\cosh\alpha c)-\alpha y\cosh\alpha y\cosh\alpha c}{\sinh 2\alpha c-2\alpha c}\right]\Bigg\} \qquad (7)
\end{aligned}
$$

$$
\begin{aligned}
\tau_{xy} = \sum_{m=1}^{m=\infty}\sin\alpha x\Bigg\{ & \left[\frac{4w}{\pi m}\sin\frac{\alpha r}{2}\cos\alpha\left(q+\frac{r}{2}\right)+\frac{4u}{\pi m}\sin\frac{\alpha t}{2}\cos\alpha\left(s+\frac{t}{2}\right)\right]\times \\
& \times\left[\frac{\alpha c\sinh\alpha y\cosh\alpha c-\alpha y\cosh\alpha y\sinh\alpha c}{\sinh 2\alpha c+2\alpha c}\right] \\
& -\left[\frac{4w}{\pi m}\sin\frac{\alpha r}{2}\cos\alpha\left(q+\frac{r}{2}\right)-\frac{4u}{\pi m}\sin\frac{\alpha t}{2}\cos\alpha\left(s+\frac{t}{2}\right)\right]\times \\
& \times\left[\frac{\alpha c\cosh\alpha y\sinh\alpha c-\alpha y\sinh\alpha y\cosh\alpha c}{\sinh 2\alpha c-2\alpha c}\right]\Bigg\} \qquad (8)
\end{aligned}
$$

$$\sigma_y = -\sum_{m=1}^{m=\infty} \cos \alpha x \left\{ \left[\frac{4w}{\pi m} \sin \frac{\alpha r}{2} \cos \alpha (q + r/2) + \frac{4u}{\pi m} \sin \frac{\alpha t}{2} \cos \alpha (s + t/2) \right] \times \right.$$

$$\times \left[\frac{\cosh \alpha y (\alpha c \cosh \alpha c + \sinh \alpha c) - \alpha y \sinh \alpha y \sinh \alpha c}{\sinh 2\alpha c + 2\alpha c} \right]$$

$$- \left[\frac{4w}{\pi m} \sin \frac{\alpha r}{2} \cos \alpha (q + r/2) - \frac{4u}{\pi m} \sin \frac{\alpha t}{2} \cos \alpha (s + t/2) \right] \times$$

$$\left. \times \left[\frac{\sinh \alpha y (\alpha c \sinh \alpha c + \cosh \alpha c) - \alpha y \cosh \alpha y \cosh \alpha c}{\sinh 2\alpha c - 2\alpha c} \right] \right\} \qquad (9a)$$

However , these stresses satisfy only the boundary conditions as described by the trigonometric terms of eqs.(2) and (3). To them must be added the stresses resulting from the uniformly applied loads on both top and bottom surfaces of the beam: $2rw/\ell$ and $2tu/\ell$ respectively. In order to satisfy the condition that there not be any shear stress over the ends of the beam, the relationship $rw=tu$ must be true. Thus

$$\frac{2rw}{\ell} = \frac{2tu}{\ell}$$

The stresses due to this uniformly applied pressure on the top and bottom of the beam are:

$$\sigma_x = 0$$
$$\tau_{xy} = 0 \qquad (1)$$
$$\sigma_y = -2rw/\ell$$

Therefore, σ_x and τ_{xy} for the required case are as given in eqs.(7) and (8). σ_y becomes:

$$\sigma_y = -\frac{2rw}{\ell} - \sum_{m=1}^{m=\infty}(\cos \alpha x) \times$$

$$\times\left\{\left[\frac{4w}{\pi m}\sin \frac{\alpha r}{2} \cos\alpha(q+r/2) + \frac{4u}{\pi m}\sin \frac{\alpha t}{2} \cos\alpha(s+t/2)\right]\times\right.$$

$$\times\left[\frac{\cosh\alpha y(\alpha c \cosh\alpha c + \sinh\alpha c) - \alpha y \sinh\alpha y \sinh\alpha c}{\sinh 2\alpha c + 2\alpha c}\right]$$

$$-\left[\frac{4w}{\pi m}\sin \frac{\alpha r}{2} \cos\alpha(q+r/2) - \frac{4u}{\pi m}\sin \frac{\alpha t}{2} \cos\alpha(s+t/2)\right]\times$$

$$\left.\times\left[\frac{\sinh\alpha y(\alpha c \sinh\alpha c + \cosh\alpha c) - \alpha y \cosh\alpha y \cosh\alpha c}{\sinh 2\alpha c - 2\alpha c}\right]\right\} \qquad (9)$$

The stress function given in eq.(6) can be rounded out to include the effects of the uniform load of eq.(1) by the addition of the term: $-(rw/\ell)x^2$. The stress function now satisfies the boundary conditions that τ_{xy} be zero on the top, bottom, and ends of the beam and that σ_y on the top and bottom surfaces of the beam be given by eqs.(2) and (3). However, the stress function is a periodic function; the discontinuous uniform loads shown in Fig. 2 are repeated every span length "ℓ". This then, is a case of a continuous beam on an infinite number of supports; there will be restraining moments on the ends of the beam.

Computations

Stresses for a specific case have been computed from eqs. (7), (8) and (9). The dimensions selected were those of the reinforced concrete beams tested in this investigation:

ℓ	= 9 feet 6 inches	q	= 39.5 inches
c	= 6 inches	s	= 9.5 inches
b	= unit width	u = w	= 1 psi.
r=t	= 5 inches	α	= $2\pi m/\ell$

Computations were carried to 20 cycles (m = 20). On lines at y = 0, ± 2, ± 4 and ± 6 inches, the stresses were calculated for values of x from 0 to 28.5 inches; these values apply equally well to the zone around the load point, x = 42 inches, although the y coordinate must be changed from positive to negative (or vice versa). σ_y and τ_{xy} are presented in Figs. 3 and 4, exactly as given by the equations. For purposes of presentation, σ_x was broken down into two parts. From the σ_x stresses resulting from eq. (7), (which gives the stresses for a continuous beam on an infinite number of supports), were subtracted the flexural stresses given by elementary beam theory. The differences, σ_x', represent the local effects of the load point; these are presented in Fig. 5. Thus $\sigma_x = \sigma_x' + \frac{My}{I}$ (for either a simple or a continuous beam).

While not converging exactly to zero, the τ_{xy} and σ_x' curves do indicate, in regions more remote from the support point, that elementary beam theory is very accurate for this particular case. σ_x' shows the greatest divergence from zero --- this is most likely due to the limited number of cycles to which the calculations were carried (20 cycles). The τ_{xy}, σ_y and σ_x' curves are symmetrical about the support point to within 2, 7, and 10 thousandths of a psi. respectively, over nearly the whole range of the computations.

In order to carry out the computations for eqs. (7), (8) and (9), a system of tabulated calculations was used. This is explained more fully in APPENDIX A, which also contains the constants for the final stage of the computations.

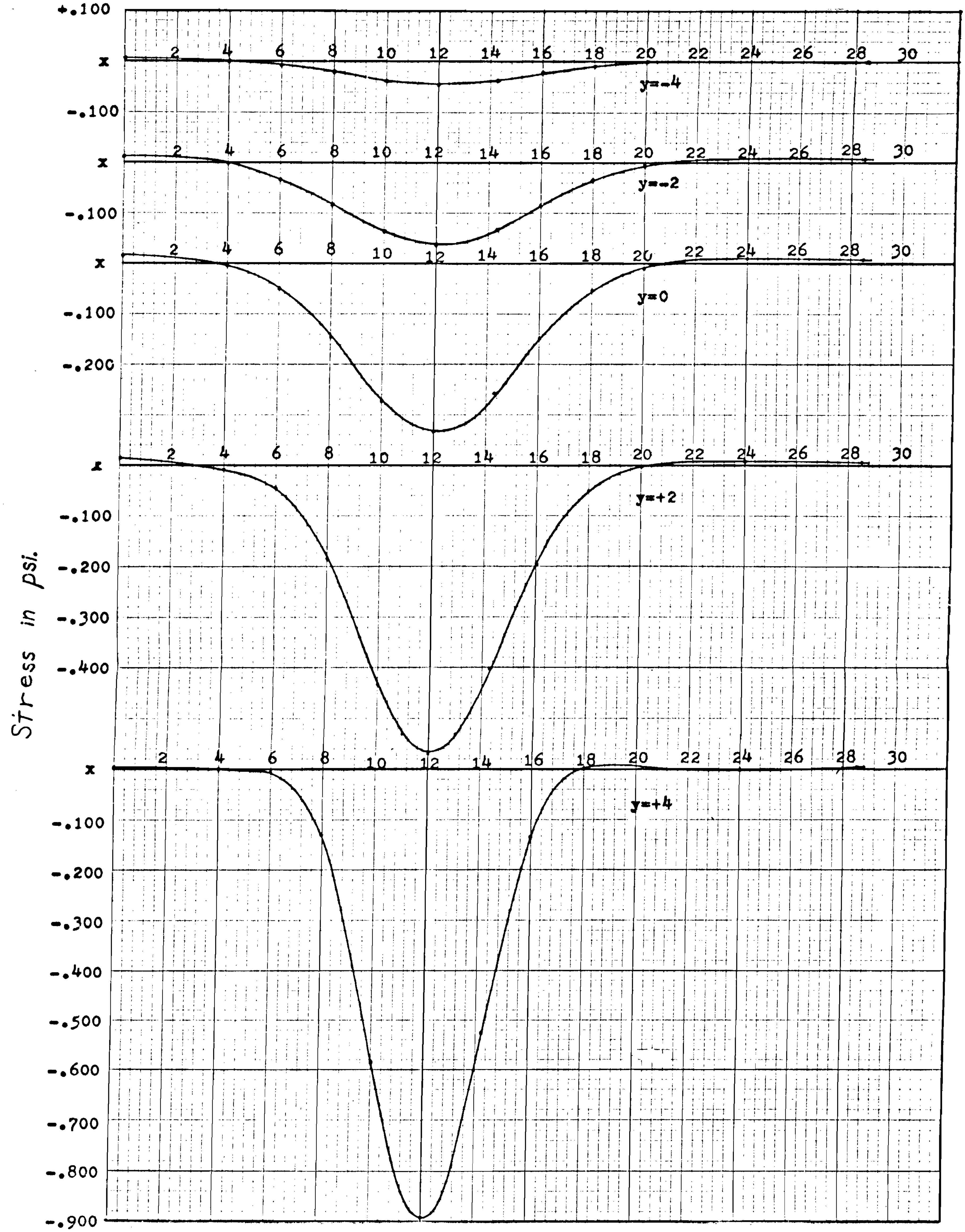

Fig.3- σ_y Due to Base Block Pressure.

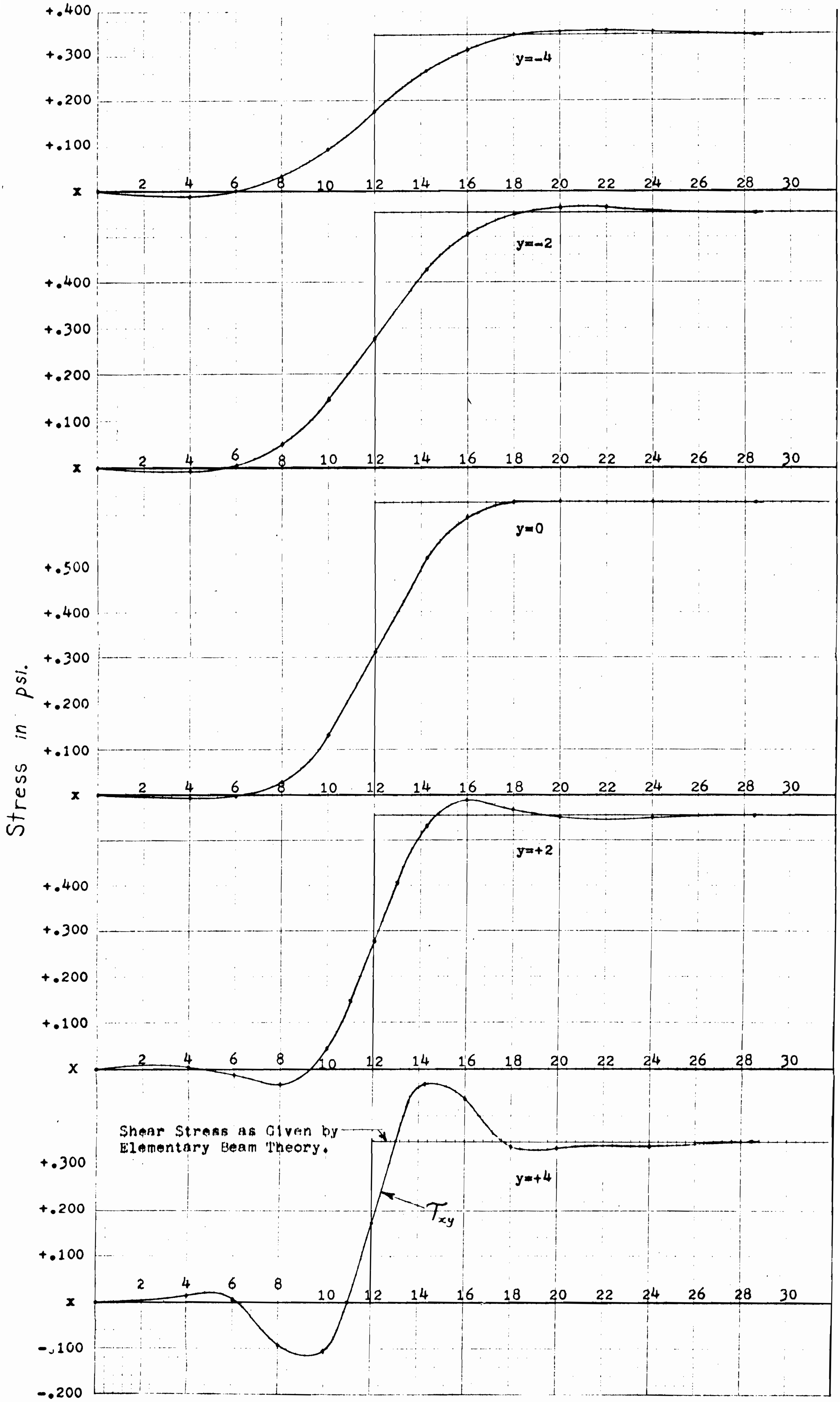

Fig.4- τ_{xy} Due to Base Block Pressure.

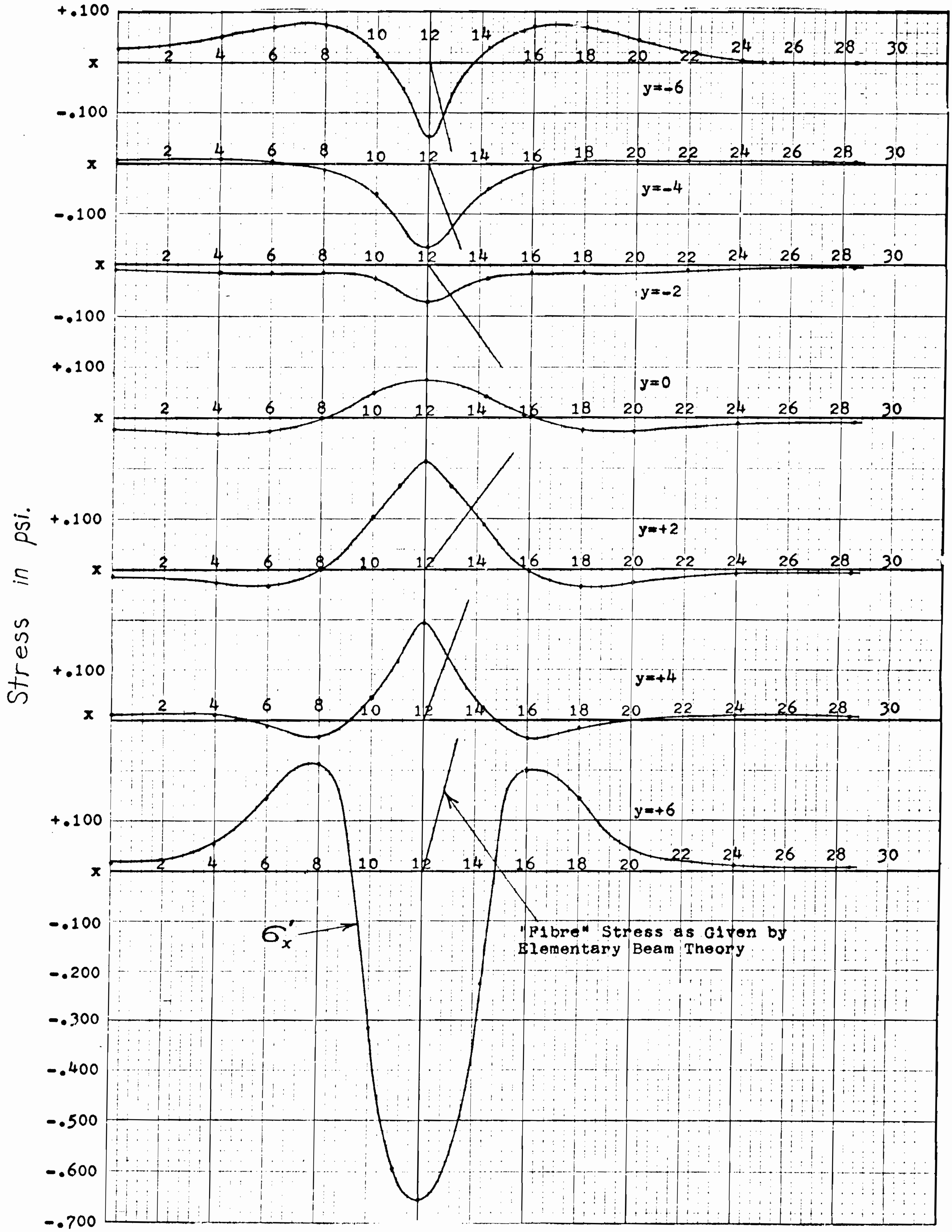

Fig.5- σ_x' Due to Base Block Pressure.

SPECIMENS AND TEST PROCEDURE

Fabrication

Details of the beams are shown in Fig. 6 and dimensions are given in Table 1. The beams of Series I and II were 8 feet 6 inches long. Due to the difficulty in selecting a suitably smooth surface on the beams on which to glue the strain gages, it was found necessary to juggle the position of the beam in relation to the support and load points. Beams 5A and 5B were made by chopping in half a long beam. Considerable damage was done at the location of the cutting, but an estimated 10 to 15 inches of bonded reinforcing bar remained outside the support points.

The bars of Series I beams had hooks to insure adequate anchorage in the shear block formed by the diagonal tension crack; hooks were not supplied for Series II. The bars were supported at $\frac{3}{4}$ inches or in the case of double layers, at $\frac{3}{4}$ and $2\frac{1}{2}$ inches, above the bottom of the beam at three points. In the case of Series I, bar chairs of the types clearly seen in Plate 23 were used. Bars of Series II beams were supported by means of horizontal transverse rods which passed through the formwork to be supported in turn by adjustable wooden hangers. In all beams, the bars were held rigidly in place with baling wire. Clearances between bars, as shown in Fig. 6, were greater than 1 inch except in the case of Beams 1 and 11 where four bars reduced spacing to

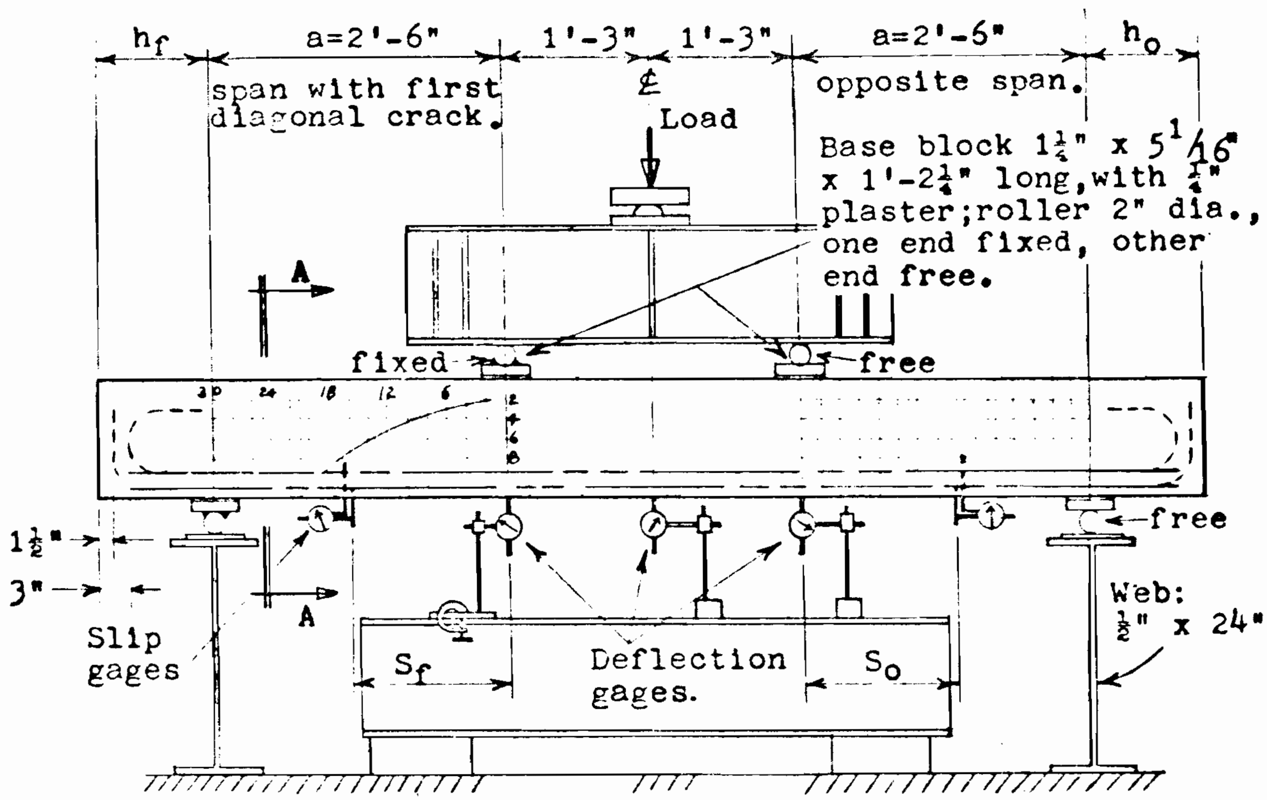

(a) Beams-SERIES I and II

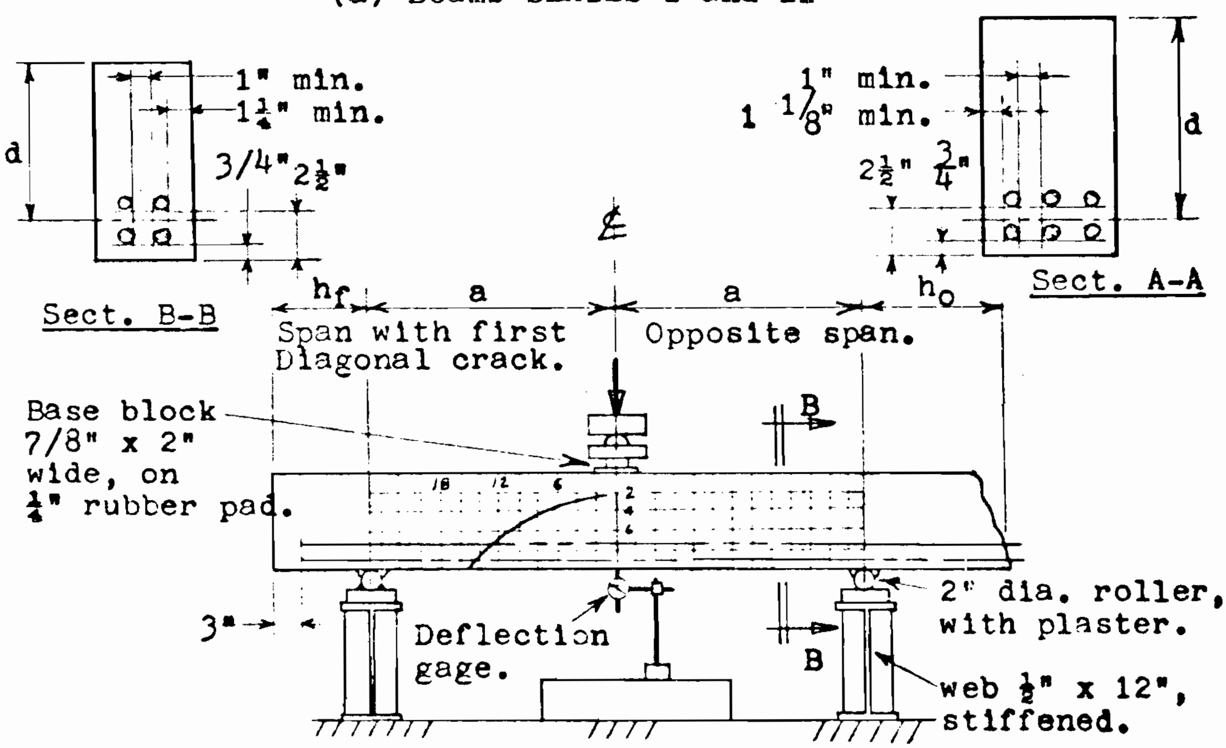

(b) Beams 5A and 5B-SERIES I

Fig.6-Details of Beams and Testing Arrangements.

TABLE 1.-Beam Dimensions

BEAM	Series	f'$_c$ (psi.)	b (i) (in.)	d (ii) (in.)	a (iii) (in.)	Bars & Size (iV)	p (V) %	Layers of Bars	S_f (in.)	S_o (in.)	Hooks	h_f (in.)	h_o (in.)
1	I	4540	7.09	10.0	30	4#5	1.75	1	14	14	yes	12	12
2	I	"	7.15	10.3	"	2#6 1#7	2.03	1	17½	18	"	12	12
3	I	"	7.19	10.1	"	2#4 4#6	2.98	2	14	14	"	12	12
4	I	"	7.13	10.1	"	5#6 1#7(B)	3.87	2	12	16	"	10	14
11	II	3710	7.02	10.2	"	4#5	1.75	1	18	18	No	12	12
12	II	"	7.14	10.2	"	2#6 1#7	2.03	1	19	9	"	17	7
13	II	"	7.04	10.1	"	2#4 4#6	3.05	2	8	14	"	9	15
14	II	"	7.05	10.1	"	5#6 1#7(B)	3.94	2	11¼	10¾	"	12	12
5A	I	4540	5.08	8.5	25.5	2#5(T) 2#6(B)	3.45	2	--	--	"	9	10-18
5B	I	"	5.11	8.5	21.3	2#5(T) 2#6(B)	3.45	2	--	--	"	12	11-15

(i) Average of six readings in each span forming a diagonal tension crack.
(ii) Effective depth d is computed to the centroid of the reinforcing bars.
(iii) a/d ratio is 3 for all beams except 5B, which has a ratio of 2.5.
(iV) Beams 2 and 12 contain spliced bars; opposite span has 3#7 bars, p = 2.49%.
(V) Based on nominal bar area.

$\frac{3}{4}$ inch clear. Spliced bars to provide differing steel area in either shear span were used in the case of Beams 2 and 12. One No. 7 bar was carried completely through, while two No. 6 bars were spliced to 2 No. 7's. Details are given in Fig.7(a).

Strain gages were attached to the longitudinal reinforcing bars at the time of testing; access was gained through core holes formed in the bottom of the beams at the time of pouring. It was thought that this method was preferable to applying gages to the bars prior to pouring the concrete, because both moisture proofing and protection during compaction would be required. The bar deformations over a distance of about 2 inches were ground off with a power grinder, then the area was smoothed up with files and sandpaper. Micrometer measurements showed insignificant losses in cross sectional area at the points of grinding. Finally, tape was placed over the finished surface to protect it from mortar and rust. The access holes were formed with blocks approximately $2\frac{1}{2}$ by $1\frac{1}{2}$ by $\frac{3}{4}$ inches -- loose cork in Series I but stronger, more manageable wood in Series II.

The slip measuring apparatus consisted of a dial gage bolted to an anchorage in the concrete on the bottom surface of the beam. The plunger of the dial gage bore against a metal prong extending down, through a core hole in the concrete, from one of the reinforcing bars of the bottom layer. Thus, readings represented horizontal motion of the bar relative to the anchorage point, see Fig. 7(b). There was one such

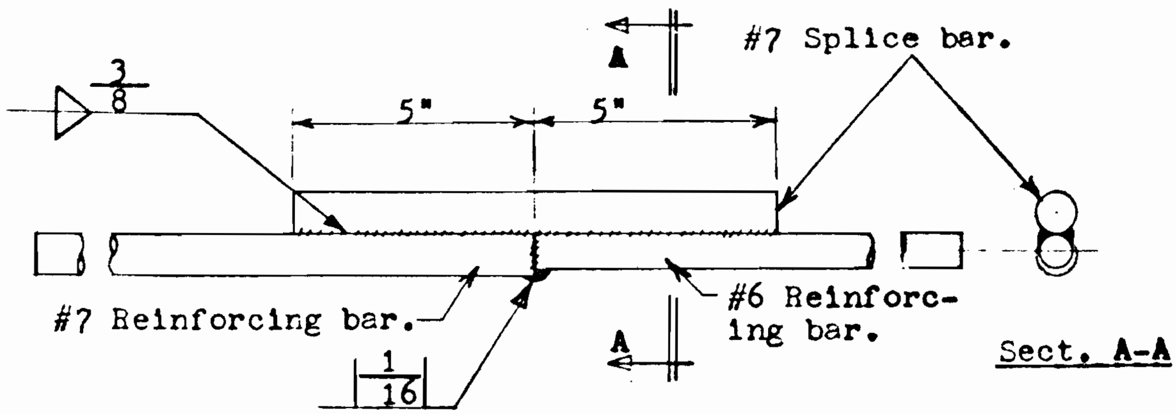

(a) Details of splice located in the pure moment spans of Beams 2 and 12.

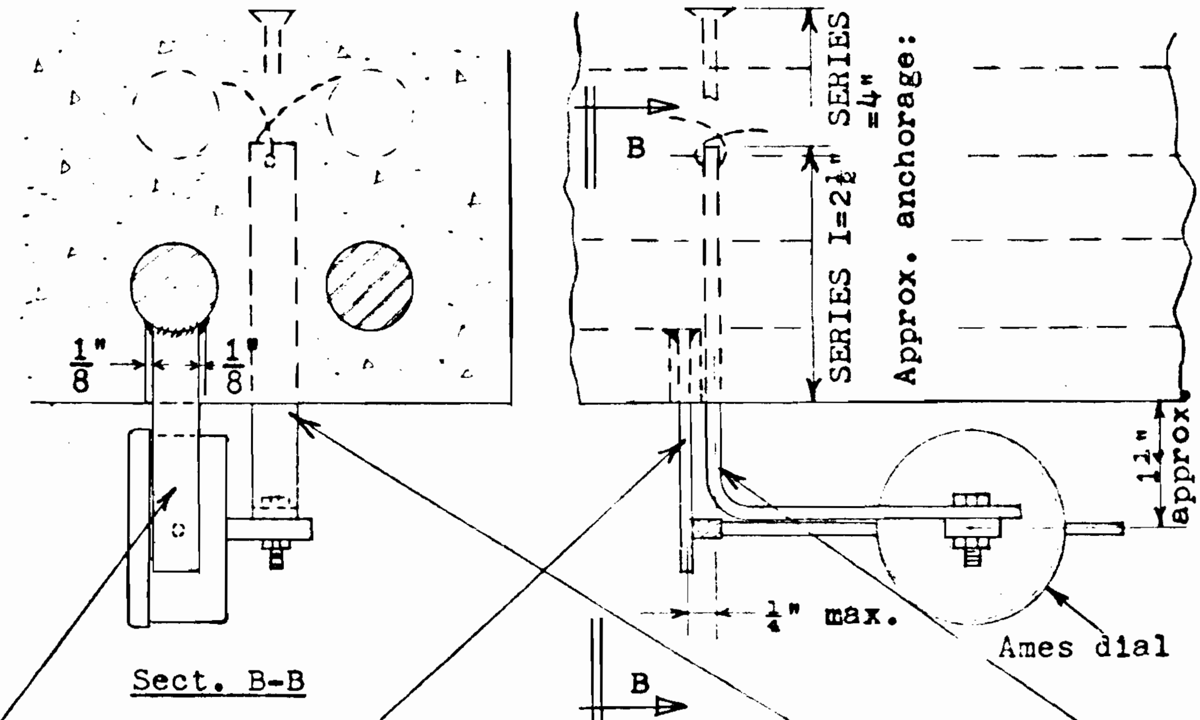

Metal prong welded to reinforcing bar and separated from surrounding concrete by 1/8".
SERIES I : Prong 1/8" x ½" flat, protected by cork wrapping.
SERIES II: Prong 3/16" dia. bolt, protected by a removable copper sleeve.

Anchorage:
SERIES I : 1/8" x ½" bent flat.
SERIES II: 3/16" dia. vertical bolt with 1/8" x ½" horizontal support arm for the dial gage.

(b) Details of the slip gage arrangement.

Fig.7-Splice and Slip Gage Details.

arrangement in each shear span, located as shown in Fig. 6. Ten thousandth dial gages were used on all beams except 1 and 2, where measurements were made to only .001 inch.

The formwork for the beams was of wood, the sides being 1 inch lumber with 2 x 2 inch bracing. Bottom joists were at one foot intervals, studs at 2 feet with 45 degree props back down to extended joists. Some shrinkage and warpage occurred leaving $\frac{1}{8}$ inch gaps between the two boards used on a side, thus causing small but troublesome ridges at the level of a few of the strain gages.

Concrete was delivered by ready-mix trucks, transferred to the forms by means of a wheelbarrow, then shoveled into place. Compaction was achieved by rodding vigorously with $\frac{3}{4}$ inch diameter bars. The concrete for the Series I beams, with less than 1 inch slump midway through the pouring operation, was placed in 3 inch lifts, accompanied by rodding through at least two lifts at a time. More care was exercised in placing the concrete of Series II, which had a slump of 7 inches at the start and 4 inches at the completion of pouring. Placing proceeded in 3 inch lifts from one end toward the other. The leading end of the concrete was carefully rodded ahead, under the bars, to insure good bond. When the first lift was completed, a second was begun. In this manner the form was half filled, then allowed to settle while the other forms were being poured. Later, the form was filled and screeded off with a steel trowel; then lifting hooks were inserted near the ends of the beam. Total pouring time was

$1\frac{1}{4}$ hours for both series. Two cylinders were made at the time of pouring each beam.

The beams were cured by keeping them covered with double layers of damp sacking, which covered both the top surface and most of the sides. The sacking was dampened at least twice a day; in addition, plastic sheeting slowed evaporation from several of the beams. Formwork was removed four or five days later; damp curing was stopped at 7 and 11 days for Series I and II respectively, leaving the beams to finish curing in air. The cylinders were handled in the same way, but probably they were better cured because the steel or cardboard molds used were watertight.

Removal of the forms from the Series I beams revealed serious honeycombing in Beams 3, 4, 5A and 5B, these being the beams with the double layers of reinforcement. The worst honeycombing occurred directly under the lower layer of reinforcing bars and was estimated to expose the following percentages of the lengths of the bars' lower surfaces -- Beams 3 & 4: 30-50%; Beam 5A: 50%; and Beam 5B: 70%.

Materials

STEEL: Deformed bars meeting ASTM* Specification 305-56T were used for the longitudinal reinforcement; Plate 1 shows typical bars. Tension tests were made on three coupons taken from the bars of Series I beams. The results are shown

---

* American Society for Testing Materials.

in Table 2.

TABLE 2 - Physical Properties

of Reinforcing Bars

Bar Size	Number of Tests	Yield Point (psi.)	Ultimate Strength (psi.)	Elongation in 8 inches (%)
4	1	53,100	92,800	6.6
5	1	67,000	104,500	8.5
7	1	41,300	71,300	17.9

When ordering, hard grade steel was specified for the No. 5 bars (Beam 1); the others were to be of intermediate grade steel. But, as can be seen from the results, both the No. 4 and No. 5 coupons tested close to hard grade -- the elongations were somewhat less than that required by ASTM Specification A15-58T for billet steel reinforcing bars.

As the major variable studied in this investigation was the steel ratio, it was thought desirable to have a reasonable approximation of the true cross sectional area of the deformed bars, as opposed to the nominal area. Extensive micrometer measurements made on all bars of Series I showed that the cross sections were fairly irregular in shape and between 2% and 10% less than the nominal area. However, the transverse deformations would undoubtedly tend to stiffen the bars, suggesting the use of an "effective" area rather than a minimum area. Calculations made, using measurements

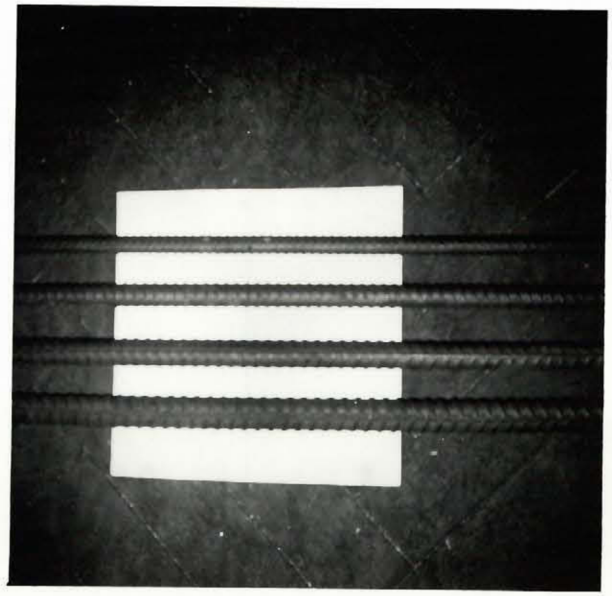

Plate 1 - Type of Deformed Bars Used in Tests.
From the Top Down Are Shown No. 4,5,6&7 Bars.

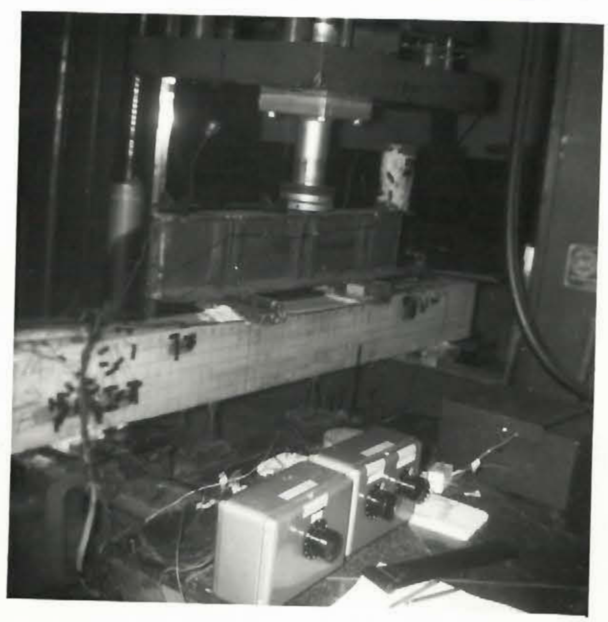

Plate 2 - Specimen in the Testing Machine.

of average deformation size, indicated that such an effective area differed little from the nominal area as given by ASTM specifications. Hence, nominal bar area has been used in all calculations in this investigation.

From two electric strain gages placed on the No. 7 coupon mentioned above, a modulus of elasticity of 30,000,000 psi. was obtained for the steel. However, the gages indicated considerable eccentricity of loading -- the individual gages gave linear stress-strain curves which differed up to 9% from the average. The Nos. 4 and 5 coupons, tested with only one gage each, also had linear stress-strain curves but the moduli of elasticity were up to 7% different from the expected value of 30,000,000 psi. Clearly, two gages (three if they will fit) should be used to obtain a reliable value for the modulus of elasticity.

CONCRETE: Table 3 gives the mix proportions for the concrete of Series I and II, while Table 4 gives the grading of the fine and coarse aggregates. The fine aggregate was river material from St. Gabriel de Brendon, Quebec; the coarse aggregate, crushed Trenton limestone. The cement was Type I, Canada Cement Company.

A total of ten concrete cylinders were tested with each series of beams, including approximately one cylinder compressive strength test per beam, and four cylinders tested to derive stress-strain curves for Series II concrete. A cylinder was tested usually within one day of a beam test at

TABLE 3 - Concrete Mix Proportions

Materials (lbs. per cu. yd.)	Series I	Series II
Cement	475	510
Sand (dry)	1,695	1,800
Gravel* - $\frac{1}{4}$"	--	575
" - $\frac{1}{2}$"	540	850
" - $\frac{3}{4}$"	1,070	--
Water	260	355
Total Weight	4,040	4,090
Slump	1"	4"--7"

* Includes sand sizes larger than No. 4.

a loading rate of either 1400 or 1800 psi. per minute. Fig. 8 shows cylinder compressive strengths plotted with respect to age of the concrete. Also included are the time of each beam test and ultimate strengths of cylinders used in obtaining the stress-strain curves. A record kept of which cylinders were poured from which portion of the concrete batch for Series I, indicated a trend toward a decrease in strengths for each successive load from the batch. Such a record was not kept for the concrete of Series II. As hoped, the variation in concrete strength during the test program

TABLE 4-Grading of Sand and Gravel

Sieve Size	Percent Retained			
	Sand	¼"Gravel	½"Gravel	3/4"Gravel
1 in.		0	0	0
3/4 in.		0	0	54.7
5/8 in.		0	4.8	95.6
1/2 in.		0	39.9	97.6
3/8 in.	---	15.8	83.5	98.3
No. 4	0	92.8	96.2	98.8
8	6.6	----	----	----
14	23.6			
28	50.2			
48	80.9			
100	95.6			
200	98.7			
Fineness Modulus	2.57			

was not great --- less than 4% of the average value. Thus, all the beams of each series are described by the following cylinder compressive strengths:

Series I, $f'_c = 3{,}710$ psi.

Series II, $f'_c = 4{,}540$ psi.

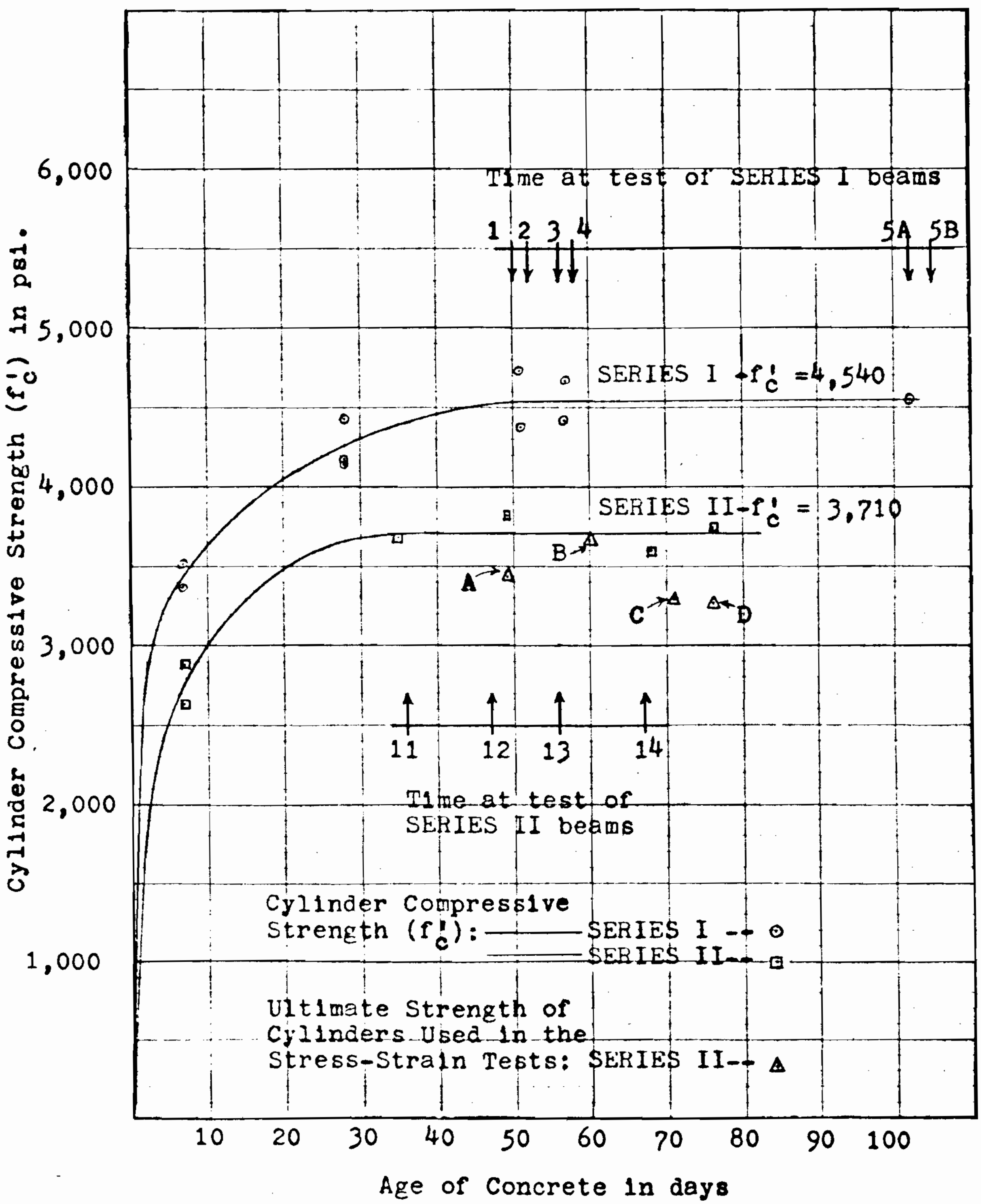

Fig.8-Increase in Concrete Strength with Time

Four cylinders of the Series II concrete were tested to obtain stress-strain curves. Age of concrete is shown in Fig. 8. Three A-3 electric strain gages were placed on each cylinder (at 120 degrees), with the exception of cylinder B, where two A-3's and one AX-5 were used. Strain in each cylinder was computed using the average reading of the three gages, including the AX-5, but excluding the readings of one erratic gage on cylinder D. Each cylinder was loaded to 50,000 pounds, unloaded, then reloaded to destruction in an effort to obtain as much of the stress-strain curve as possible. It appears that the curves that were obtained extended to a peak value, but failure always resulted before the descending branch could be evaluated.

As there seemed to be considerable variation among the strain gage readings on the first cylinder, an attempt was made at accurate centring of cylinders B and C in the test machine. Cylinders are normally centred by eye, so some eccentricity could be expected. However, by using a preliminary set of strain readings, the amount and direction of the supposed eccentricity can be calculated. Then, with the aid of a plumb bob, a correction can be made in the position of the cylinder. If necessary, this can be repeated till all eccentricity is eliminated. Unfortunately, this process did not work too well; in fact, in the case of cylinder B, a "correction" by eye was resorted to and this proved to be the most accurate setting achieved. The final correction to cylinder C put it 5/16 inches off centre -- near failure rotation of the loading head was clearly visible. For this reason the results of this cylinder were considered to be less reliable than the others. It would appear that the variation between the strain gage readings was due not only to eccentric loading but also to stress concentrations at the location of the gage itself. This is discussed more fully in the "Discussion of Test Methods".

The stress-strain curves for each cylinder are shown in Fig. 9. Both the tangent and secant moduli of elasticity vary widely for each cylinder -- anywhere from 3 to 5 million psi. There is such a wide variation in these values that a value of 3,750,000 psi. has been arbitrarily selected as the best approximation of this value. In the lower, more elastic ranges, this value fits within ± 25%, except in the case of cylinder C, where it is 40% low. The curves are relatively linear to a value of 500 micro-inches.

The variation between the strain gage readings was less than ± 5% on cylinders B and D, within ± 20% in the elastic range of cylinders A and C, but ± 50% in the plastic range of cylinder C.

Poisson's ratio was computed from a single A X-5 (two element) gage place on cylinder B; load versus Poisson's ratio is given in Fig. 9. In the load-unload range of the test, the ratio varied between 0.225 and 0.275, with an average value of 0.25.

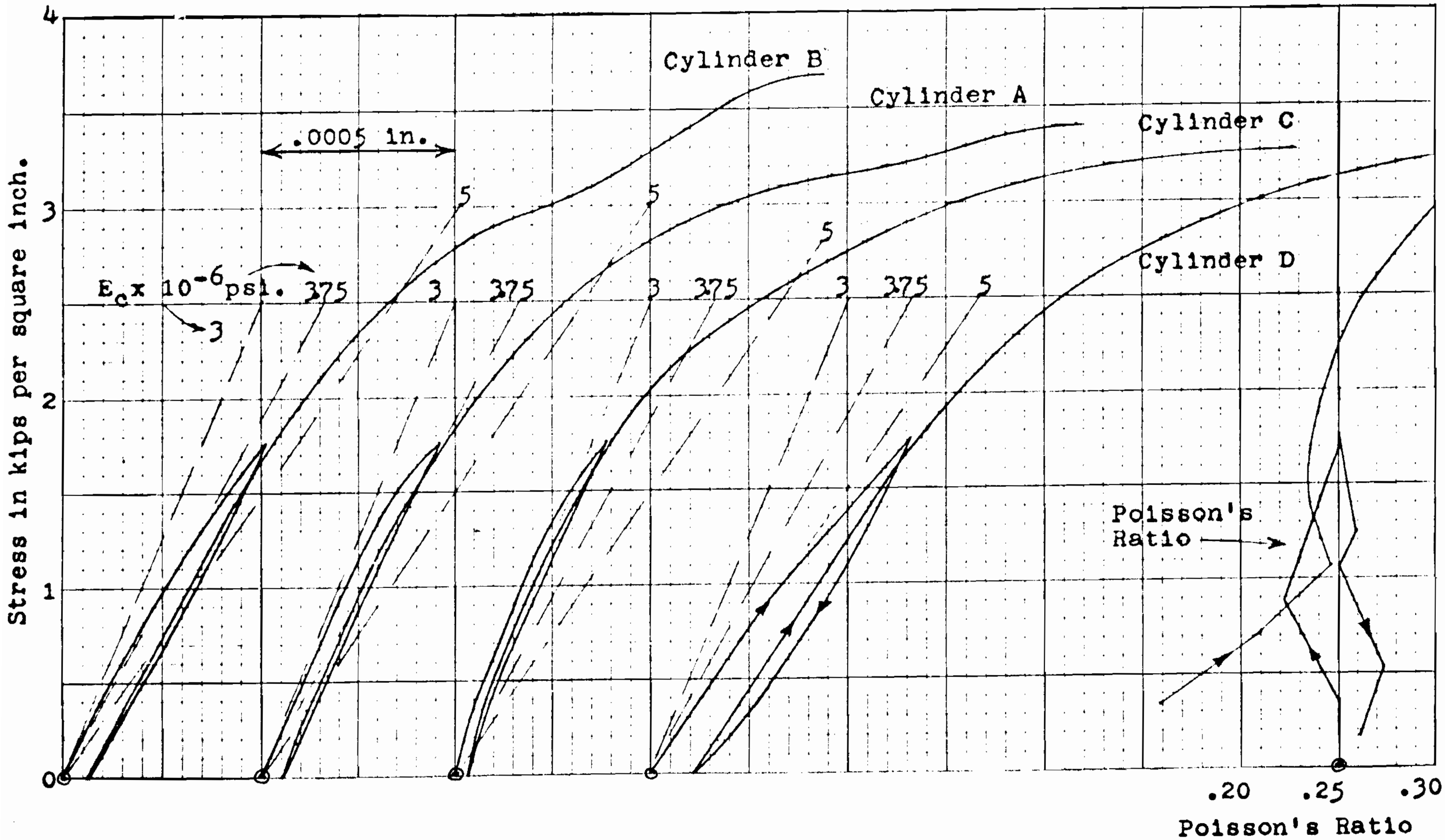

Fig.9-Stress-Strain Curves and Poisson's Ratio for Series II Concrete.

The loading rates varied considerably among the four cylinder tests. The strain gages generally remained quite steady up to between 2,000 and 3,000 psi., after which they began to show a continuous, steady strain increase under a constant load. The gage readings of cylinder A were taken as rapidly as was possible, those of cylinder B (continuous plastic flow not starting till near failure) were given more time to approach equilibrium. The reload curve of cylinder B encompassed about $1\frac{1}{2}$ hours, those of C and D, slightly longer. Cylinders C and D were loaded in a different manner: when stress had increased enough to start continuous plastic flow, a load was put on and left, allowing the cylinder to come to equilibrium, then load and strain were recorded. The rate of strain increase slowed but never became zero, partly because the machine load had a tendency to creep up unless continuously controlled.

The correlation between rate of loading and shape of the stress-strain curve is not too clear: cylinders C and D, loaded very slowly, show the two extreme values of "elasticity"; cylinder B was loaded quite rapidly, but shows greater plasticity than cylinder A. No doubt a constant rate of applied strain during each cylinder test would have produced more consistent results. There is a possible correlation between modulus of elasticity and age of concrete. Cylinders A, B and D were each tested at successively greater ages, and show decreasing moduli of elasticity; however cylinder C does not fit this pattern.

To summarize: A wide variation was found in the shapes of the stress-strain curves for the concrete of Series II, especially in the more elastic range. This variation was due partly to eccentric loading of the cylinders, partly to different ages of the samples, but more particularly to difficulties encountered with electric strain gages when applied to concrete. Another important factor was variation in the rate of loading (or straining) of the concrete. But none of these factors could obscure the fact that basic variations existed in the material itself. Therefore, for computational purposes, a modulus of elasticity for the range zero to 550 micro-inches has been selected:

$$E_c = 3.75 \times 10^6 \text{ psi.}$$

$$\mu = 0.25$$

Test Procedure

Fig. 6 shows the third point loading arrangement used for the beams of Series I and II. Base blocks 5 1/16 inches wide by $1\frac{1}{2}$ inches thick by $14\frac{1}{8}$ inches long separated from the beam by $\frac{1}{4}$ inch of plaster were used at the load and support points of the large beams. One end of each beam was on a roller; the other end was fixed. As can be noted in several of the beam photographs, special wooden adapter blocks were used in stabilizing the base blocks on the rollers to facilitate positioning of the beam. The base blocks of Beams 5A and 5B are as noted in Fig. 6. A set of strain gages, placed on Beam 14 above the base block at the support point, necessitated fairly accurate positioning of both the block and the roller. The block was positioned with the aid of marks on the beam. The presence of any eccentricity of the roller with respect to the base block had been expected to "show up" in the strain gage readings shown in Fig. 13. Therefore, a rather elaborate system of adjusting screws for the roller was contrived to correct trial readings taken prior to testing the beam (see Plates 19 and 20). However, the measured strains were found to be so small, in relation to the accuracy of the strain indicator, as to be unaffected by eccentric roller position. Later, by replacing the base block with a cast iron angle, legs $3\frac{1}{4}$ by $2\frac{1}{8}$ inches, readings were obtained for a support point which approximated a knife edge.

Deflections were measured at the mid-span and third points of the large shear beams, and at the mid-span of the small shear beams. The deflection dial gages were supported from a 12 inch wide flange beam placed on steel blocks resting on the bed of the test machine. The support mounts for two dial gages were of the magnetic type; the third gage was supported either from the arm of an 8 foot high stand or by means of a small stand clamped to the wide flange beam. Only mid-span deflections were taken for Beams 5A and 5B, the dial gage being mounted on a steel block resting on the bed of the test machine.

For ease in describing crack position on the beams, a coordinate system was used. A grid of two inch squares was marked out on the shear spans of all beams; the coordinates in inches were numbered from the load point toward the support point and from the top surface toward the bottom.

Considerable effort was expended in examining the beams for hairline cracking during the tests. This was found to be a very tedious task, requiring much concentration and time. Each of the four surfaces of the shear spans was illuminated by either two 60 or 100 watt bulbs, or one 150 watt flood lamp. Four to five minutes were spent on each surface (12 by 30 inches) locating cracks and tracing them up with the aid of a low power lens. It should be noted that the first beam, Beam I, was not as well examined as the others due to both the quantity of light used and the time taken in its examination. After each load increment was placed on, 2 or 3 minutes were allowed for the beam to come to equilibrium, then the cracks were traced up and marked with the load of that increment: e.g. the 27,000 pound increment was marked 27, and 27,500 pounds marked 275. Felt nib india ink pens, grease pencils and charcoal pencils were used, but the charcoal pencils were found to be the strongest and clearest on rough surfaces. Occasionally, the pure moment spans were examined. Besides amount of light and time, two other factors were important in detecting hairline cracks. The shaded light bulbs were on goose neck stands but required constant adjusting because the angle of the light or the amount of reflection and glare affected visibility of the cracks. Also of primary importance was the texture of the surface of the beam -- visibility of a hairline crack was directly proportional to smoothness of the surface. Beams 3, 4, 5A and 5B were very rough; the others were much smoother with local "fuzzy" areas. Beams 3 and 4 were white-washed to improve the surface, but this practice was discontinued for the remainder of the beams as it was felt that it introduced an unknown characteristic to crack identification. It is suggested that steel forms would be superior to wooden forms in leaving a shinier surface on the beams.

Strain measurements were made with three types of Baldwin SR 4 electric strain gages, all paper based. A-3 gages were used for concrete strain on cylinders and on the sides of beams; A-7's were used on reinforcing bars (small gages were necessary to reduce the amount of grinding required on the deformations); and finally, AX-5 two element rosettes were used for concrete strain above one base block. The gages were applied to concrete having an age of at least 7 weeks; for $5\frac{1}{2}$ of these weeks the beams were drying in air.

SR 4 nitrocellulose type cement, without precoat, was used in applying the gages to both steel and concrete. The reinforcing bars, prepared before pouring the beam, required cleaning only in order to apply the gages. Applying the $\frac{3}{4}$ inch long A-7 gages through the $2\frac{1}{2}$ inch hole was not found to be too difficult, but as these gages were not protected by felt pads, extreme care was necessary in handling them. It was found to be much easier to apply gages on horizontal surfaces; a system of supports and a lever made tipping of the beams quite simple.

Considerable difficulty was encountered in finding suitable spots on the concrete on which to locate gages. There were innumerable air voids on the surface, especially on the top 3 or 4 inches of the beam, so that after selection of the best gage line it was necessary to juggle the beam in relation to the support points in order to bring the gages into the desired position in the shear span. The rough standard maintained was that a gage should never placed on an air void larger than 1/16 inch diameter. Beam 13 was so rough that gage lines on opposite sides of the beam could not be matched up; on the other hand, the gages above the base block of Beam 14 were located on a perfectly smooth area. It is suggested that future investigators use metal forms, or if wood is used, that they line it with sheets of thin metal at the desired gage locations. Good compaction of the concrete while placing is also essential.

Preparation of the concrete surface was relatively simple, requiring only limited sandpapering; excessive sanding only ripped out fine aggregate, spoiling the surface. An exception to this was the top surface, which required the use of a power sander to smooth the hardened laitance. In order to smooth the sanded surfaces, a preliminary coat of glue was applied, and the air voids were carefully plugged. When this was dry, more glue was added and the gages applied. The glue dried in less than one minute, so the A-3 and A-7 gages could be held with the fingers. But this rapid drying was a disadvantage with the AX-5 gages, which were made of a very stiff, curly paper, slow to become saturated with glue. This difficulty was overcome by covering the gage with a sheet of cellophane, and holding it firmly on the concrete surface with foam rubber and weights. The cellophane not only prevented the foam rubber from becoming stuck to the gage but also prevented evaporation, thus delaying drying and allowing the paper to become impregnated with glue.

Readings of strain were made with a Type L or M Baldwin strain indicator with a tolerance of 3 micro-inches. As the gages were read individually, a ten and a twenty point switch box were used to facilitate readings. Lighting arrangements were such that the 60 or 100 watt bulbs would necessarily be as close as three inches to the shear span gage lines for one or two minutes at each increment of load, so heat protection for the gages was essential. This was accomplished by taping two or three sheets of paper very loosely over the gages, sealing the bottom and sides but leaving the top open to form a pocket. Experiments proved that this would be adequate to prevent gage drift during the time that the hot bulbs were close to the gages. Temperature compensating gages for the steel and concrete strain measuring gages were mounted on a bar coupon and on cylinders respectively, which were placed either on the beam or on the floor below the beam.

Location of the gages on all beams is shown in Fig. 10 and dimensions are given in Table 5. The gages were numbered in accordance with their relative distance from the top. Gage "1" is on the top surface; those on the sides have the suffix "E" or "W" to indicate east or west side; those on the reinforcing bars are always labelled "7". The gages over the base block were numbered in accordance with their relative distances from the end of the beam; e.g. the gage directly over the roller is at x = 12 in., etc.

A beam test consisted of the following readings: load, deflection, slip, strain gages and crack patterns. Slip was not measured on Beams 5A or 5B, and strain measurements were limited to four beams. A Baldwin-Tate-Emery Universal Type testing machine with a capacity of 400,000 pounds was used for all tests of beams, bars and cylinders. A typical test set-up is shown in Plate 2. The load was applied in increments,allowing time both for the beam to come to equilibrium and for readings. Hairline cracking was first marked, then dial gages were read; simultaneously the strain gages were read, allowing in the case of Beams 12 and 13, time for the beam to stabilize. At any given beam load, drift of strain reading over a time interval was rare, although the deflection readings did take time to become stationary. Total test time varied between 6 and 8 hours; the time of

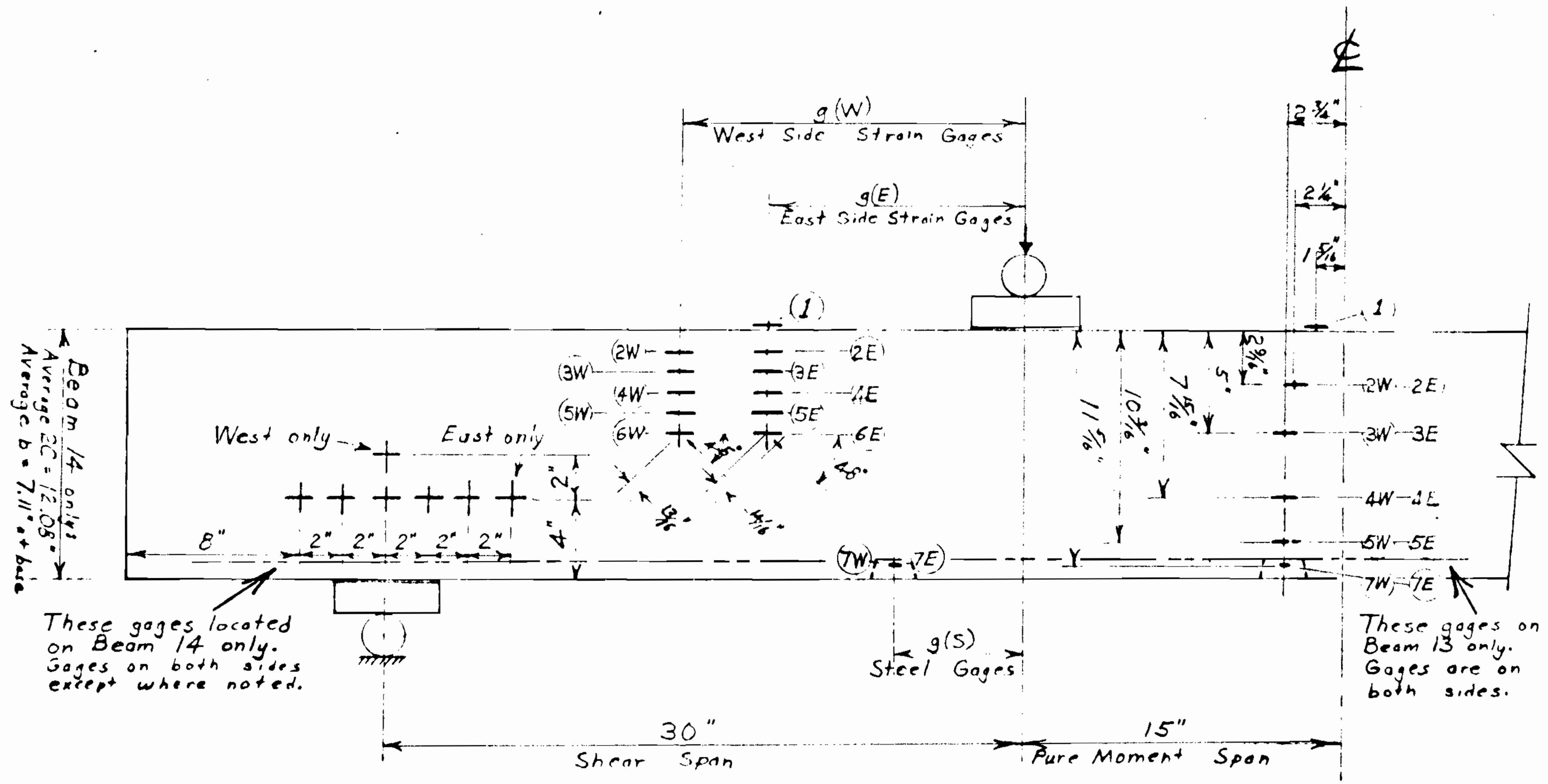

1. For dimensions of gage locations see Table 5.
2. Gage 7 is located on the reinforcing steel.
3. Gage 1 is a single gage on the top surface of the beam, located on the centre axis in all cases except on Beam 12, where it is offset to the east by 3/8".
4. SR4 electric strain gage symbols: A-3, A-7, AX-5

Fig. 10—Electric Strain Gage Location Details.

TABLE 5- Electric Strain Gage Location Dimensions

Gage No.	Distance of the gage from the top surface of the beam (inches)											
	Beam 12 Shear Span			Beam 13 Shear Span			Beam 13 Pure Moment Span	Beam 14 First Shear Span to Crack (34^k)		Beam 14 Second Shear Span to Crack (38^k)		Beam 14 Gages above Base Block
g	g(E)	g(W)	g(S)	g(E)	g(W)	g(S)	----	g(E&W)	g(S)	g(E&W)	g(S)	----
(in.)	11.63	11.63	9.50	15.00	15.94	6.25	----	15.75	5.69	14.00	---	----
1	0			0	--		As	0		0		As
2	.88	.88		1	1		Noted	1.38		2.5		Noted
3	--	1.5		2	2		in	2.75		---		in
4	2	--		--	--		Fig.10	4.13		---		Fig.10
5	3	3		--	--			---		---		
6	--	--		3	3			---		---		
7			10.56			11.38			11.31		----	

(i) For strain gage location details, see Fig.10

(ii) Gages 1 to 5 (including those in the pure moment span of Beam 13) are A-3 gages.

(iii) Gage 6 (in the shear span of Beam 13 only) consists of an AX-5 (two element) gage placed horizontally and an A-7 (single element) gage placed at an angle to the horizontal; see Fig. 10.

(iV) Gage 7 (including those in the pure moment span of Beam 13) consists of a pair of A-7 gages, placed on the reinforcing bars.

one load increment was usually 15 minutes for Series I and 20 minutes for Series II. Exceptions were the 10 minute increments of Beam 1, and of Beam 11 after the 24 kip load.

The load increment varied somewhat, depending on expected capacity of the beam. Increments of 2000 pounds were used till 16 to 26 kips, then either 500 or 1000 pounds till failure. There were exceptions made to this in order to shorten test time: 2000 pound increments were used for the last one or two increments on Beams 3, 4 and 13, but only Beam 13 failed while the load was being increased. Beams 5A and 5B were loaded roughly $2\frac{1}{2}$ times as rapidly as the others -- with 5000 pound increments to 20 kips, then with 1000 pound increments to failure. Beam 14 had a rather complicated loading history involving several repetitions of a 5 kip load, a sustained load of probably 5 kips lasting less than one day, followed by a beam test to produce the first diagonal tension crack, an overnight rest, to 15 kips then to zero, to 36 kips then zero, finally to failure in 2,000 pound increments.

Accuracy of Test Results

The accuracy of the various measurements made in this investigation is shown below:

Beam dimensions	b	± 1/16 inches
	d	± 1/8 inches
	Span lengths	± 1/4 inches

Area of Reinforcing bars (micrometer measurements)	$\pm$ 4%
Loads: Beams	$\pm$ 100 pounds
Bar coupons	$\pm$ 50 pounds
Cylinders	$\pm$ 250 pounds
Strain: A-3 and AX-5	$\pm$ 1% & 5 micro-inches minimum
A-7	$\pm$ 2% & 5 micro-inches minimum
Position	$\pm$ 1/32 inch
Dial Gages: Deflection	$\pm$ .001 inches
Slip	$\pm$ .0001 inches

The resulting accuracies of some test results are therefore:

Steel Ratio (p)	$\pm$ 6%
Average Shear Stress $\frac{V}{bd}$	$\pm$ 5%
Nominal Shear Stress $\frac{V}{bjd}$ (assuming n $\pm$ 30%)	$\pm$ 10-20% (increases with greater p)

RESULTS

Table 6 shows loads and nominal shearing stresses at which the diagonal tension cracks formed.

TABLE 6 - Test Results

Beam	f_c (psi)	p (%)	j (ii)	Diagonal Tension Cracking (1): V_c (iii) (lbs.)	Diagonal Tension Cracking (1): $v_c = \frac{V_c}{bjd}$ (iv) (psi)
1	4540	1.75	.874	13,950	225
2	4540	2.03	.866	15,450	245
3	4540	2.98	.847	17,950	290
4	4540	3.87	.832	18,950	315
11	3710	1.75	.865	14,950	240
12	3710	2.03	.856	13,950	225
13	3710	3.05	.835	16,450	280
14 (F)(v)	3710	3.94	.820	17,450	300
14 (S)(v)	3710	3.94	.820	19,450	335
5A (F)	4540	3.45	.839	11,100	305
5A (S)	4540	3.45	.839	12,100	335
5B (F)	4540	3.45	.839	10,600	290
5B (S)	4540	3.45	.839	12,600	340

(i) All beams failed in diagonal tension except Beam 14, which failed in shear compression above the second diagonal tension crack. For this failure, V_u = 23,450 lbs. and M_s = 710,000 inch-lbs.

(ii) Based on n=6.6 for f'_c=4540 psi. and n=8 for f'_c=3710.

(iii) Self weight of beams included.

(iv) b and d were nominally 7 by 10 inches except Beams 5A & 5B which had a b and d of 5 by 8.5 inches; a/d ratio was 3 for all beams except Beam 5B, where a/d = 2.5.

(v) "F" and "S" refer to first and second shear spans to crack diagonally.

Behavior Under Load

Before formation of the diagonal tension crack, the behavior of each specimen was characteristic of reinforced concrete flexural members. The flexural cracks began to make their appearance in the range 10 to 15 kips, and under continued loading, would grow upward and gradually incline toward the load points. When a relatively high load had been attained, the diagonal tension crack would form and the load would drop back to a smaller value. The crack always appeared quite suddenly and was unmistakable, due to its large size and extent. The formation of this crack, which would extend from the level of the reinforcement up to somewhere near the load point, was accompanied by a certain amount of "heaving" of the top surface of the beam and by splitting along the reinforcing bars toward the support point.

Most of the beams failed upon formation of the crack -- a diagonal tension failure. However, three, Beams 14, 5A and 5B, continued to take load and failed under some higher load after the formation of a diagonal tension crack in the other shear span.

FLEXURAL CRACKING: Flexural cracks were very fine (hairline cracks), with a spacing in the shear spans of between three and six inches. They grew at very erratic rates both in the upward direction and in spreading from the load points toward the support points. Their maximum height of growth was found to be roughly to the neutral axis, as computed by the Cracked Section Theory. The influence of increased amounts of longitudinal reinforcement could be seen both in the decreasing amount and height of flexural cracking which developed, and in the increasing load required to make the cracks visible. Beams 2 and 12 were quite interesting in this respect, having more reinforcement in one shear span than in the other. While Beam 2, Plates 5 and 6, showed greater flexural cracking in the span with the lesser amount of reinforcement, Beam 12, Plates 13 and 14, did not. Possibly this effect was hidden by the difficulty of observing cracks on a poor surface, or by twisting of the beam as it was loaded, causing higher cracks in one side than in the other.

All flexural cracks in the shear spans showed the effect of shear, gradually inclining toward the load points as they grew upward; the amount of inclination was greater for cracks at greater distances from the load points.

INITIAL INCLINED CRACKS: The crack which later grew to be the diagonal tension crack was a hairline crack like the others, differing only in that, as it was usually the most distant from the load point, it developed a greater angle of inclination. This crack, which will be referred to as the initial inclined crack, first appeared at either the bottom of the beam, or else at or slightly above the level of the reinforcing bars. This phenomenon of hairline cracks which first became visible above the level of the bars was not limited to initial inclined cracks; it occurred with equal frequency at any point on the beam. A few more increments in load would usually suffice to cause the crack to grow to the bottom of the beam.

The amount of growth of the initial inclined cracks before they "opened up" to form the diagonal tension cracks varied among the beams. Nearly half of them grew to about the level of the neutral axis (as calculated by Cracked Section Theory). In the case of Beams 2, 11 and 5B, the initial inclined crack could be traced well into the compression zone; the remainder of the beams contained only small cracking. With but few exceptions, the diagonal tension cracks "opened up" from hairline cracks closest to the support point.

DIAGONAL CRACK: The following pages contain photographs of both sides of every shear span which developed a diagonal tension crack. The locations of the load points are given by heavy vertical lines. Hairline cracks have been traced out with a charcoal pencil and the height of rise marked at every load increment; e.g. 27,000 lbs. is marked 27; 27,500 lbs. is marked 275. Two minor errors should be noted: on Beam 3, Plates 7 and 8, 33 should read 32; on Beam 13, Plates 15 and 16, 21 should read 22.

PLATES 3 to 24 ---

PHOTOGRAPHS OF TEST BEAMS AFTER DIAGONAL TENSION CRACK FORMATION AND FAILURE

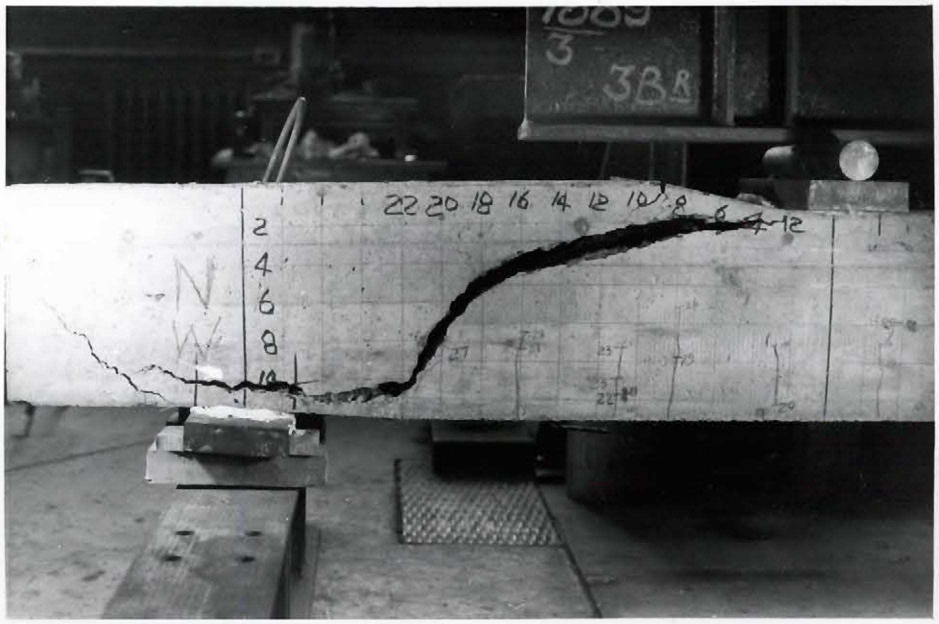

Plate 3 - Beam 1 (West).

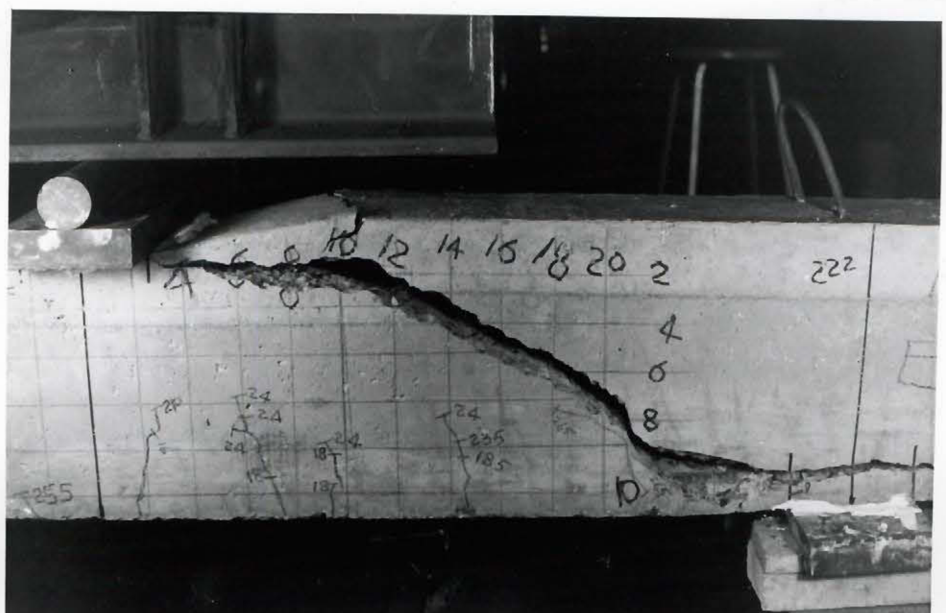

Plate 4 - Beam 1 (East).

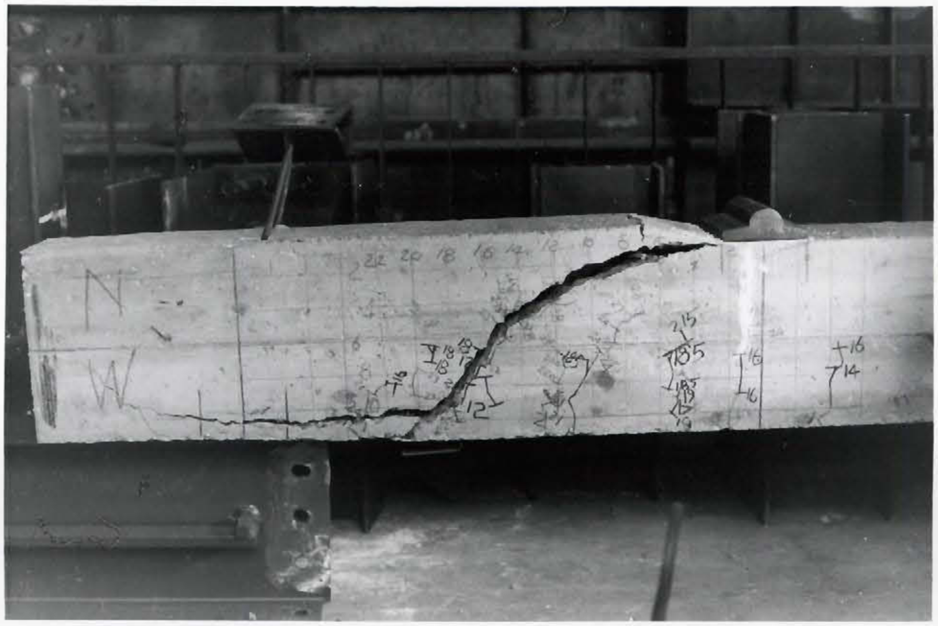

Plate 5 - Beam 2 (West).

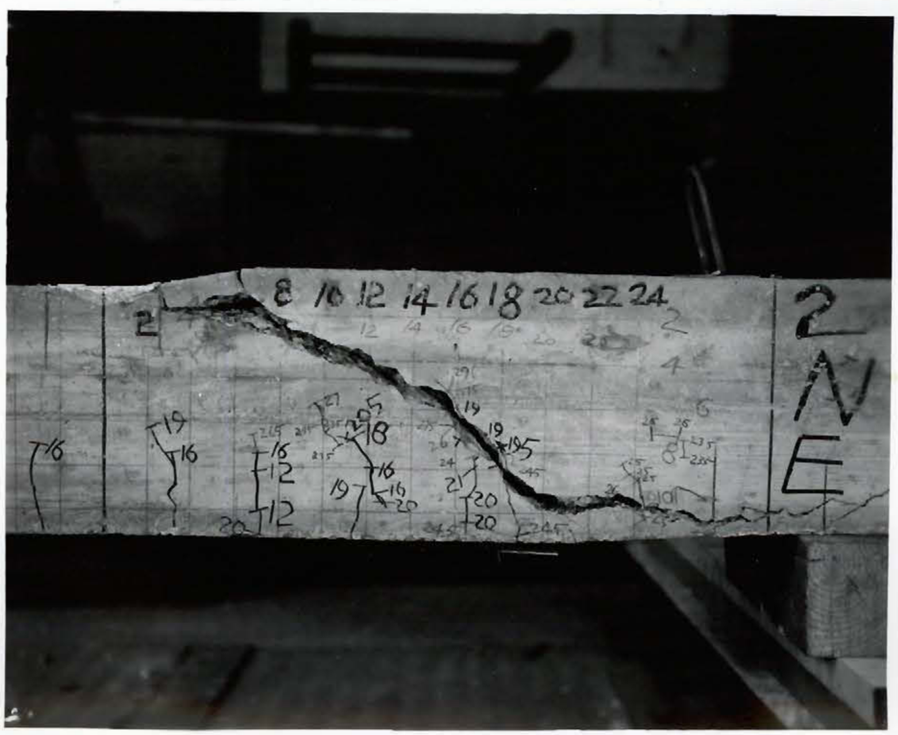

Plate 6 - Beam 2 (East).

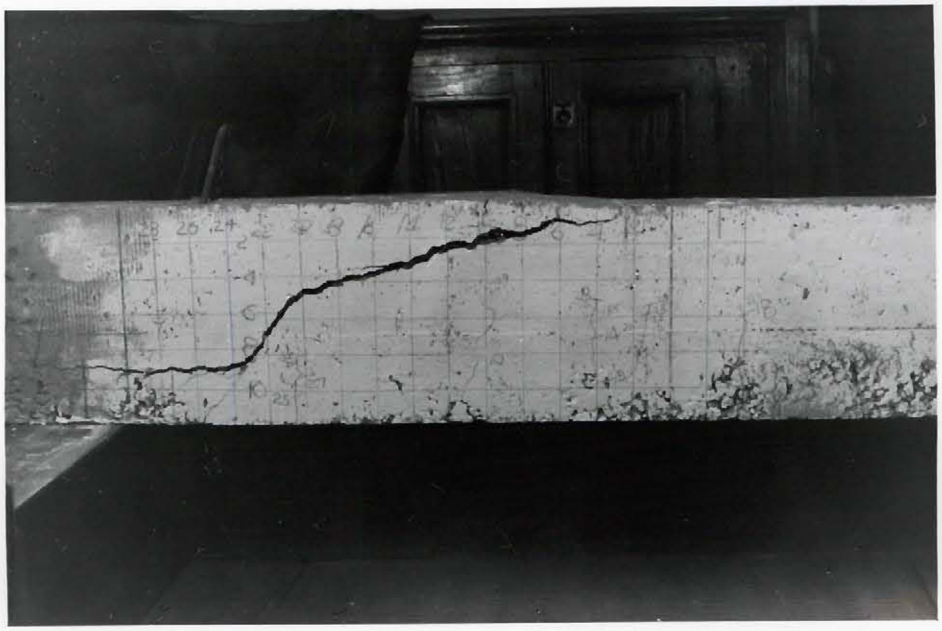

Plate 7 - Beam 3 (West).

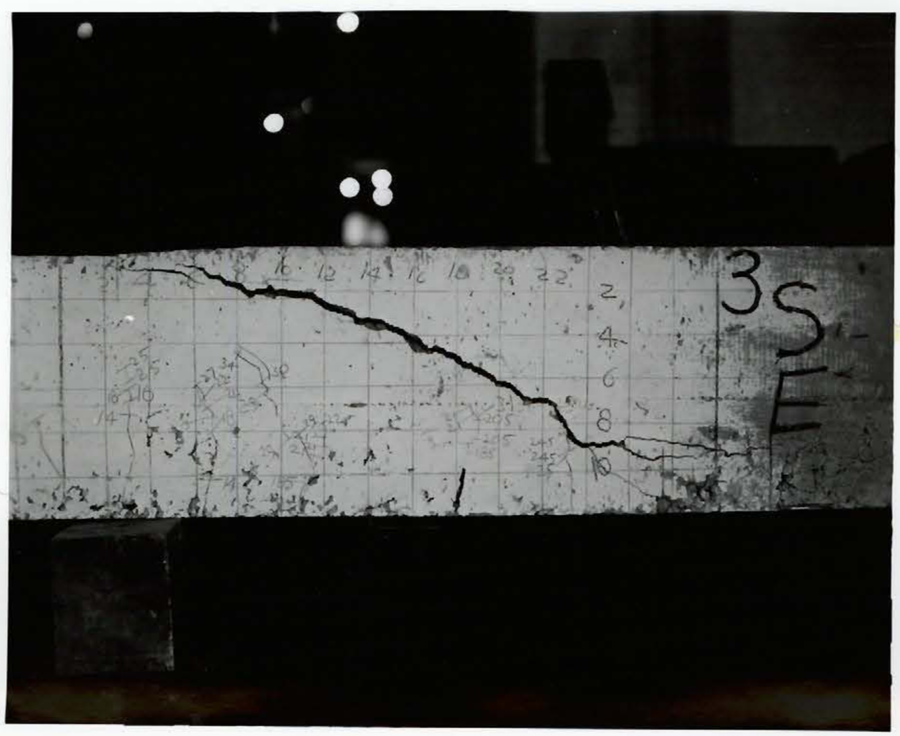

Plate 8 - Beam 3 (East).

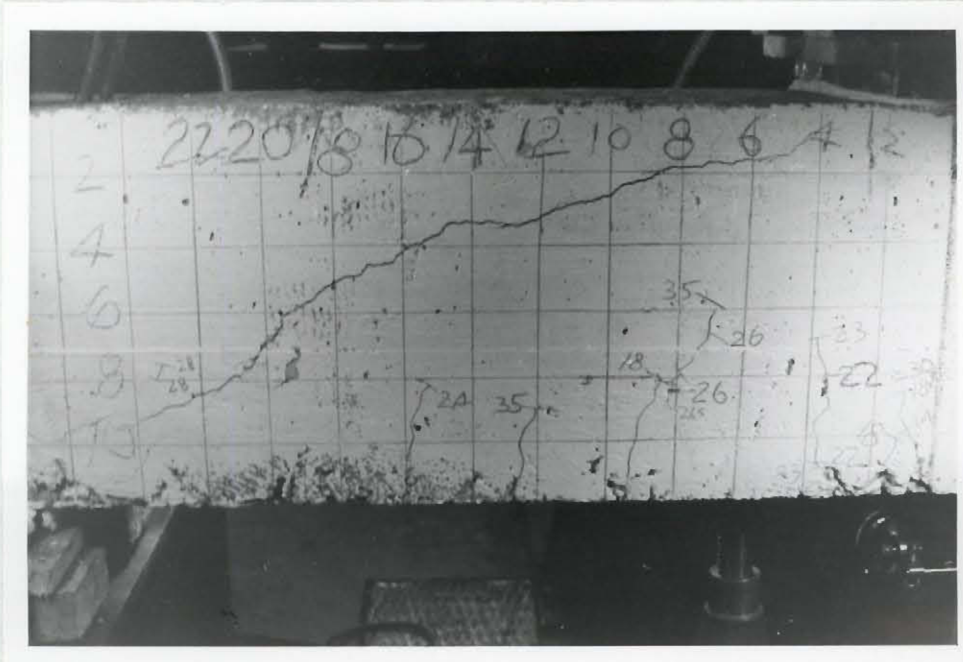

Plate 9 - Beam 4 (East).

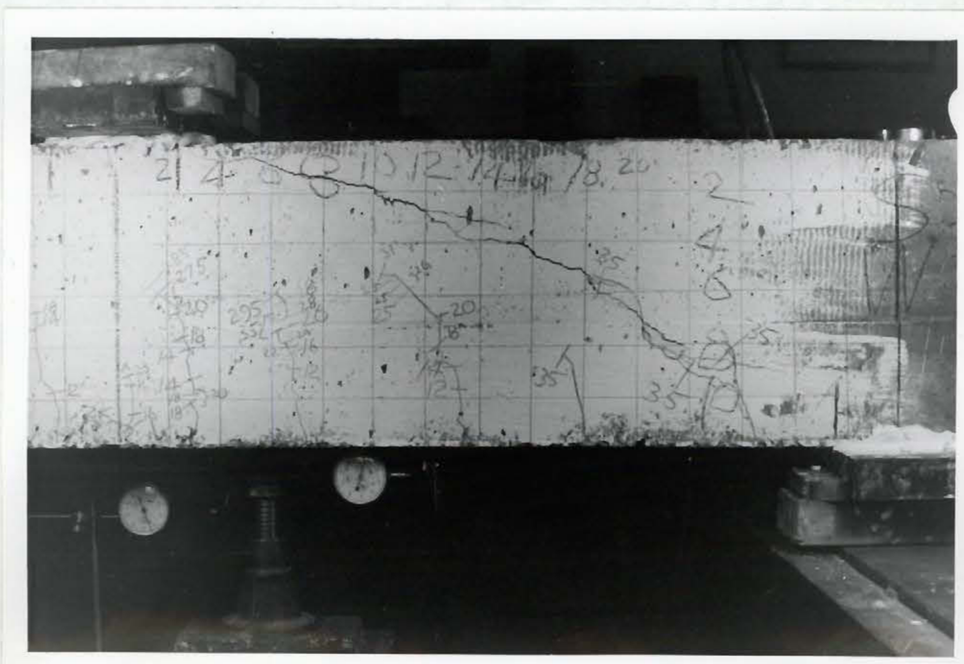

Plate 10 - Beam 4 (West).

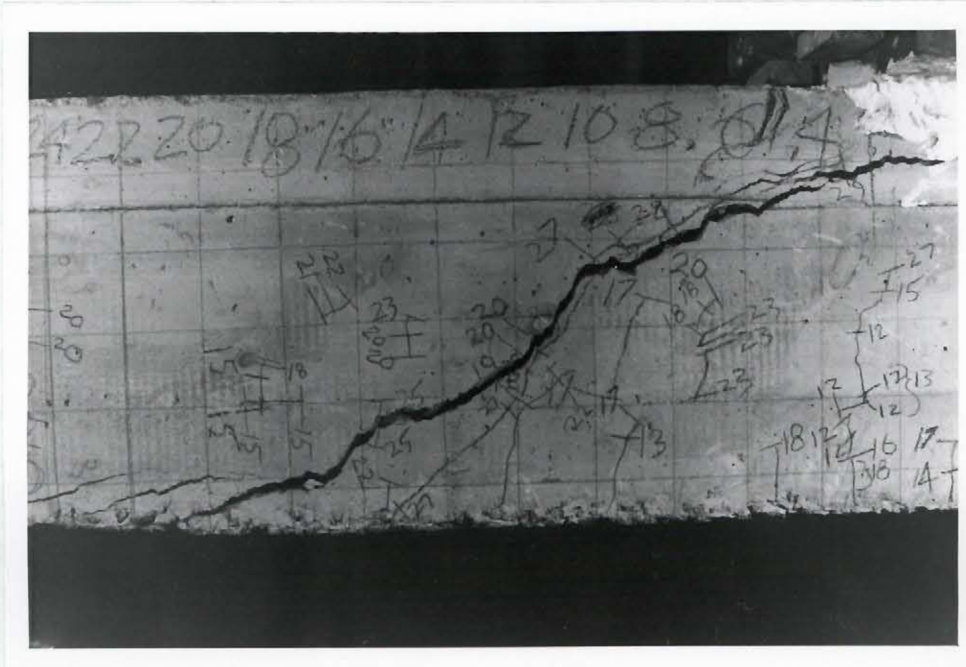

Plate 11 - Beam 11 (West).

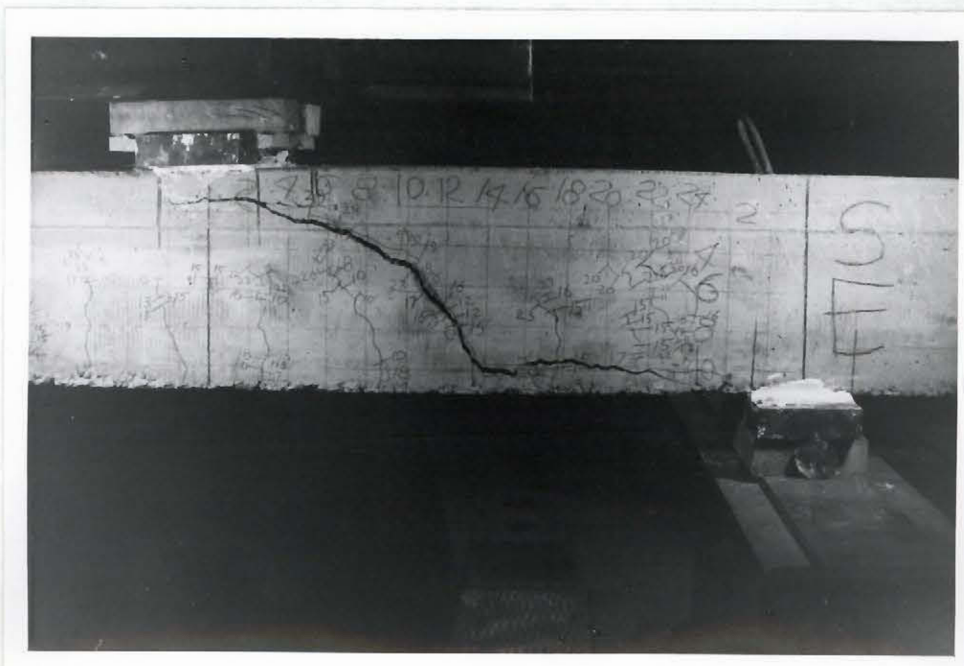

Plate 12 - Beam 11 (East).

Plate 13 - Beam 12 (West).

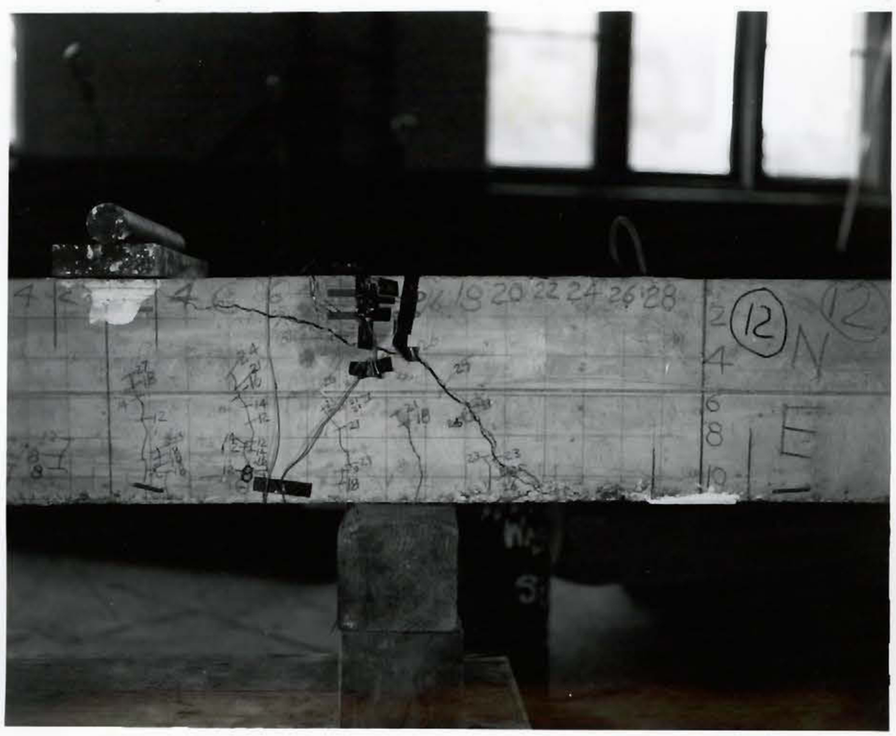

Plate 14 - Beam 12 (East).

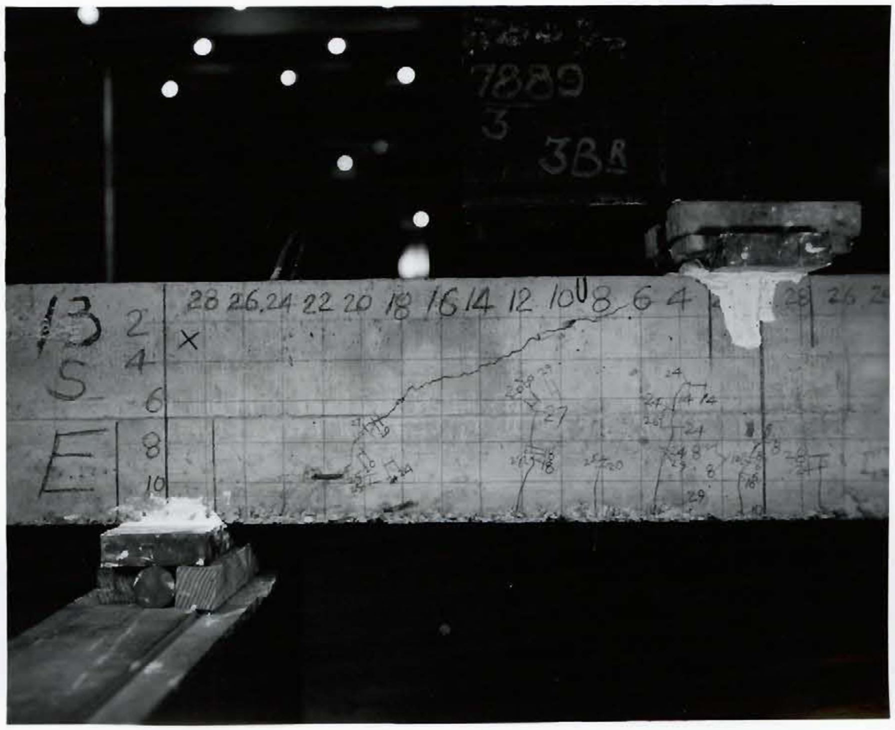

Plate 15 - Beam 13 (East).

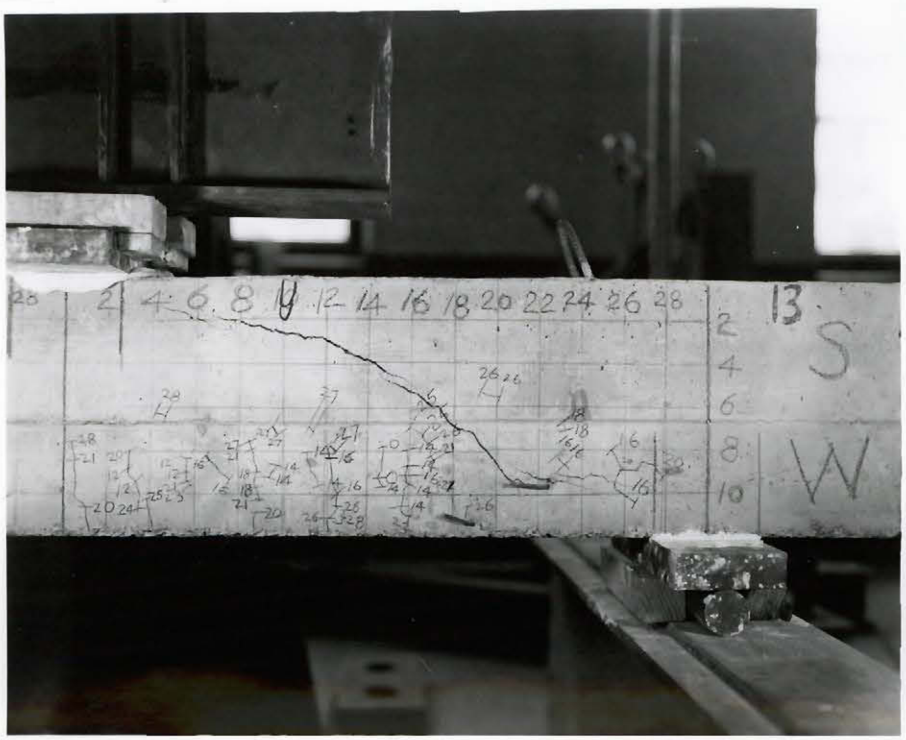

Plate 16 - Beam 13 (West).

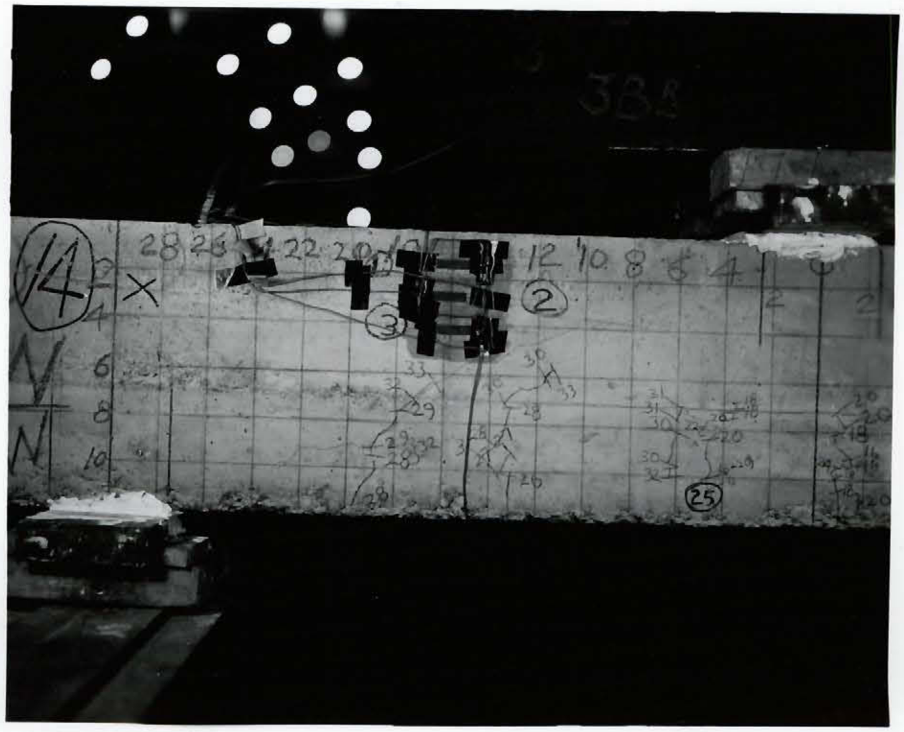

Plate 17 - Beam 14,
Span with First Diagonal Crack (34 kips),(West).

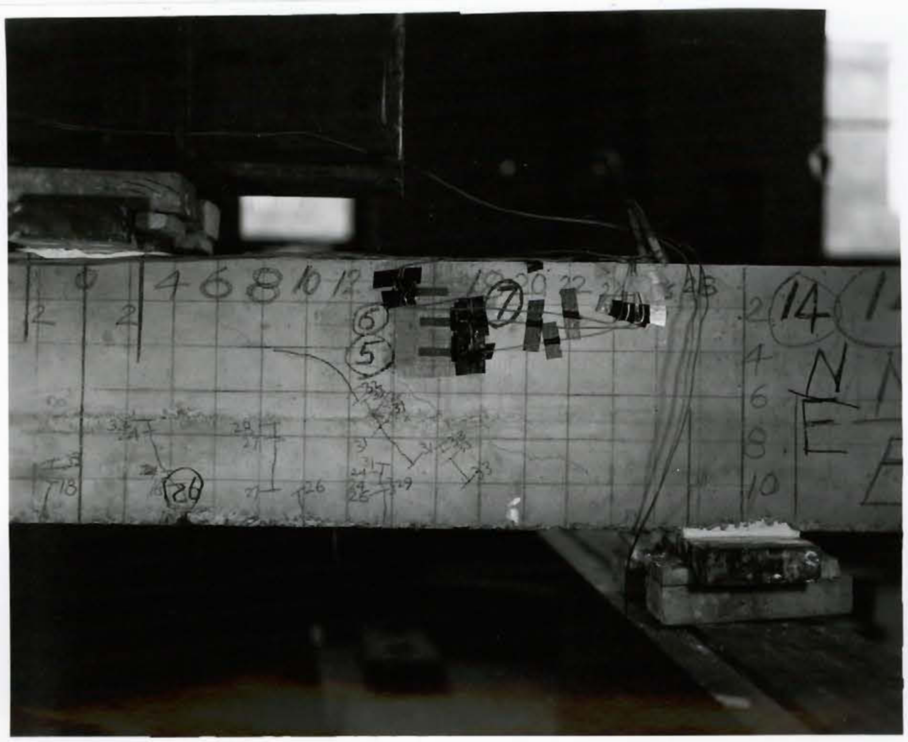

Plate 18 - Beam 14,
Span with First Diagonal Crack (34 kips), (East).

Plate 19 - Beam 14, Span with Second Diagonal Crack (38 kips),(East). Failure Span.

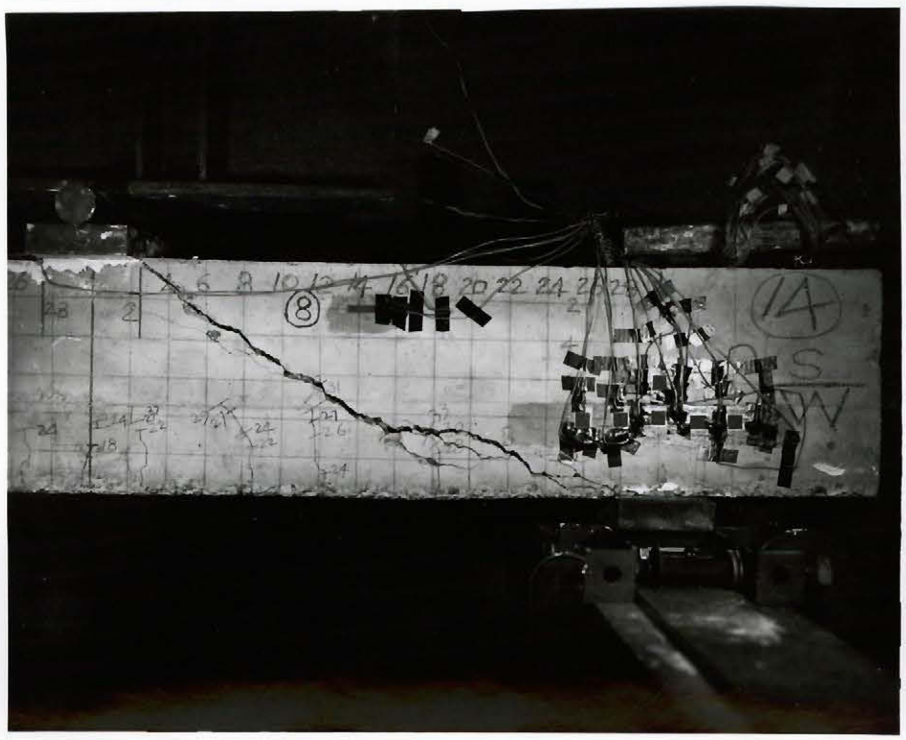

Plate 20 - Beam 14, Span with Second Diagonal Crack (38 kips),(West). Failure Span.

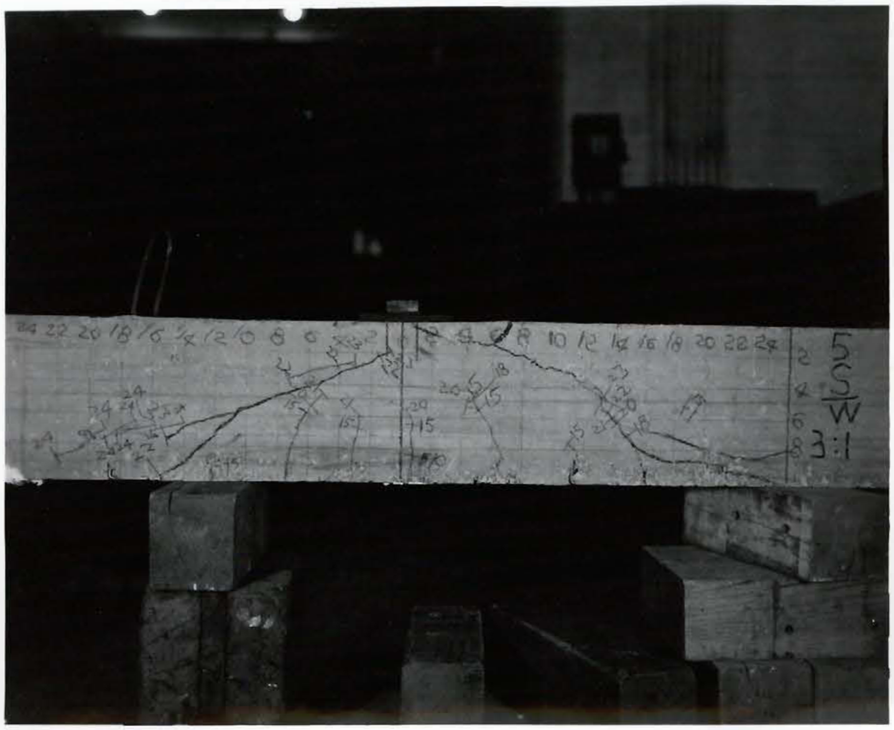

Plate 21 - Beam 5A (West). Failure Span on Right.

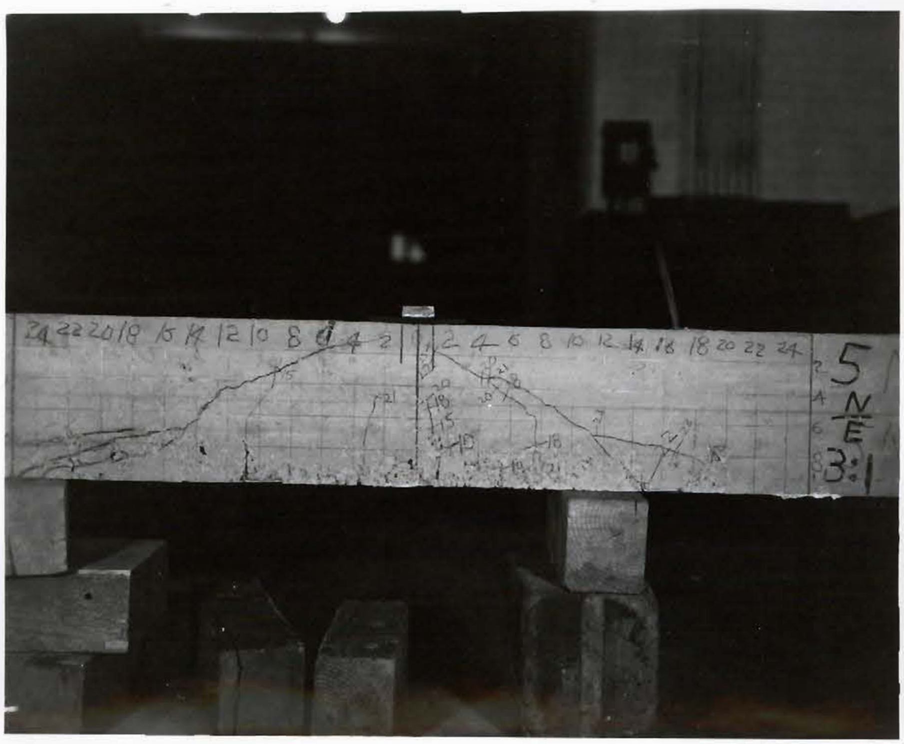

Plate 22 - Beam 5A (East). Failure Span on Left.

Plate 23 - Beam 5B (East). Failure Span on Right.

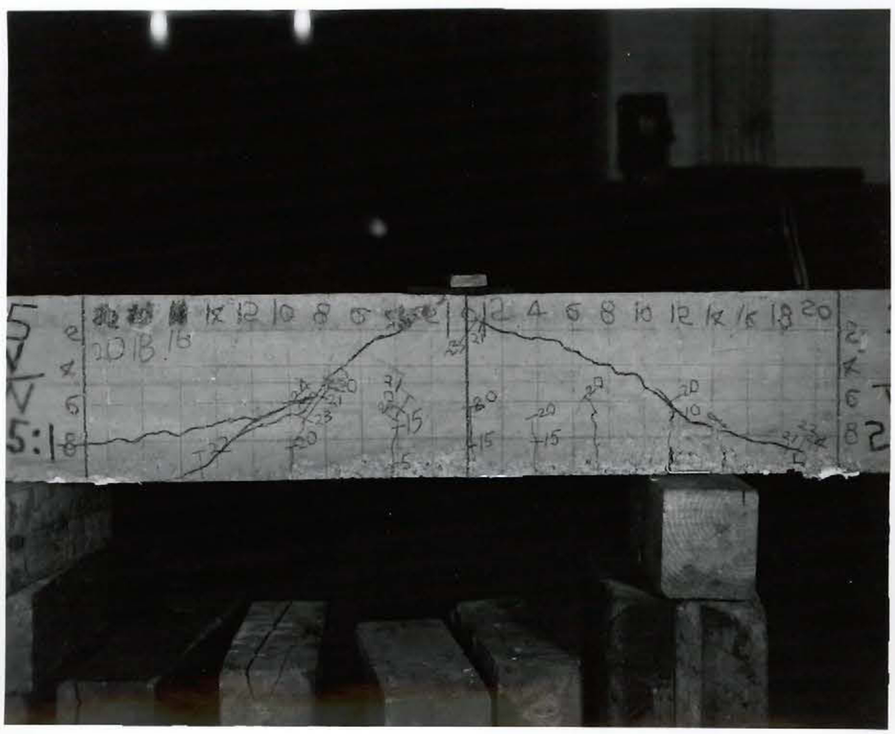

Plate 24 - Beam 5B (West). Failure Span on Left.

For convenience in description, the beams are grouped according to the location of the diagonal tension crack. Beams 1 to 4, 12, 13 and 5A all failed in diagonal tension due to a crack passing through an area designated as zone "Z", shown in Fig. 11. This figure is a composite picture of all the diagonal tension cracks of this test program. The final shapes shown are the averages of the two sides, which are within ± 1 inch of the average in the lower portion of the crack and nearly identical in the upper part. Zone "Y" is an area bordering zone "Z" and extending toward the load point; it includes the remaining diagonal tension crack positions.

In the case of Beam 11, the diagonal tension crack that opened up did not follow the original hairline crack completely on one side, but tore out a section of concrete along the reinforcing bars toward the support point, producing a flatter crack at the lower end (see Plate 11).

One side of the first shear span to crack, Beam 14, Plates 17 and 18, developed a diagonal tension crack with two branches, the minor one being quite steep. This minor crack joined the diagonal crack but was quite fine; on the opposite side there was a hairline crack but this did not join the diagonal tension crack, or "open up".

The zone "Z" diagonal tension cracks were not too jagged in shape; they could be approximated by two straight lines, steep at the lower end and considerably flatter in the upper part. The point of transition from steep to flat was

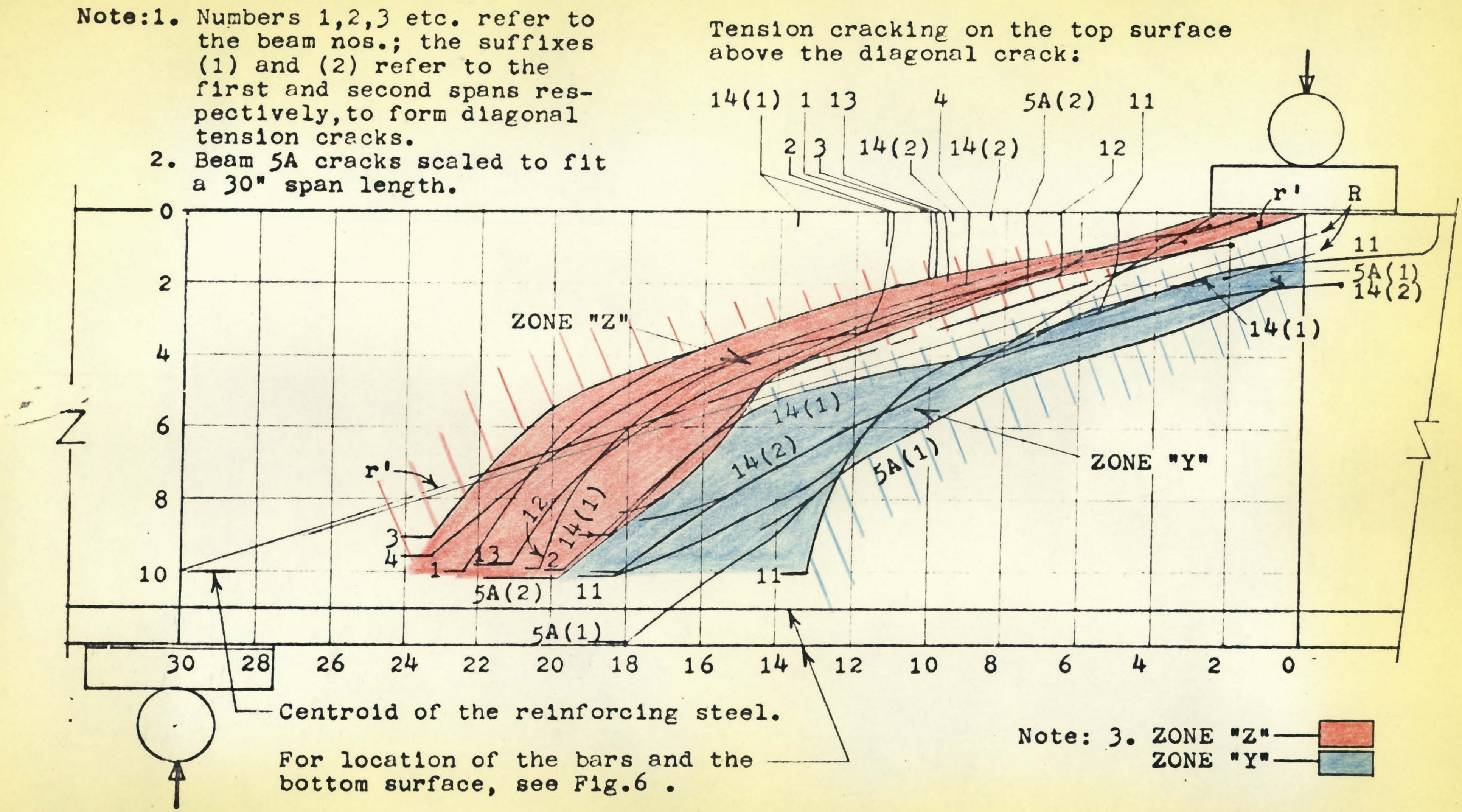

Fig.11-Composite Sketch of Diagonal Tension Cracks.

very often quite close to the neutral axis (as computed by Cracked Section Theory). The lower ends were inclined between 45° and 60° to the horizontal. The upper ends were inclined between 17° and 21°, thus making them roughly parallel to, but somewhat above, a line joining the intersection of the lines of the reinforcing bars and support point to the load point (marked r' in Fig. 11).

The diagonal tension cracks which formed in zone "Y" had more variety in angle at the lower end; the upper ends were parallel to, but below, the line marked r'.

FAILURE: All zone "Z" diagonal tension cracks produced immediate failure -- diagonal tension failure. The crack passed up through the compression zone, stopping at the load block and the thin strutlike portion above the crack heaved or buckled upward. Beam 1, Plate 3 is an exaggerated example of this latter action. Simultaneously with this, a split developed along the upper layer of the longitudinal reinforcement, toward the support point. The beams of Series I showed greater destruction than those of Series II. The diagonal tension cracks opened wider and more splitting ensued. In fact, in the case of Beam 1, the splitting passed almost all the way around the hooks, breaking off a large block of concrete below them.

The initial inclined crack of Beam 11 grew slowly and was very steep, having started relatively close to the load point. This beam eventually carried a much greater load than expected from an examination of the failure loads of the other beams. Failure occurred when the initial inclined crack suddenly "opened up" to form a diagonal tension crack. The thin strut above the crack heaved up adjacent to the load block -- there was crushing along the surface of the crack and tensile cracking on the top surface of the beam at this point. Splitting occurred along the longitudinal reinforcing bars. The crack passed completely under the base block, terminating in a crushed zone at about one inch from it, inside the pure moment span; Plate 12.

Beam 14 developed a diagonal crack in each shear span (these will be referred to as "First Crack (34 kips)" and "Second Crack (38 kips)"), accompanied by limited splitting along the upper layer of reinforcing bars. In this case, however, the beam continued to take load, failure occurring at a much higher load by violent punching-shear adjacent to the base block of the second crack (38 kips); Plates 19 and 20. Tension cracks within one foot of the base blocks could be discerned on the sides (Plate 17) and top surface above the first crack (34 kips), and on the top surface only, above the second crack (38 kips).

Beam 5A developed diagonal tension cracks in each span, diagonal tension failure resulting from the formation of the second crack, which was a zone "Z" crack; Plates 21 and 22.

Beam 5B also developed a diagonal crack in either span, but failure was due to a combination of diagonal tension and

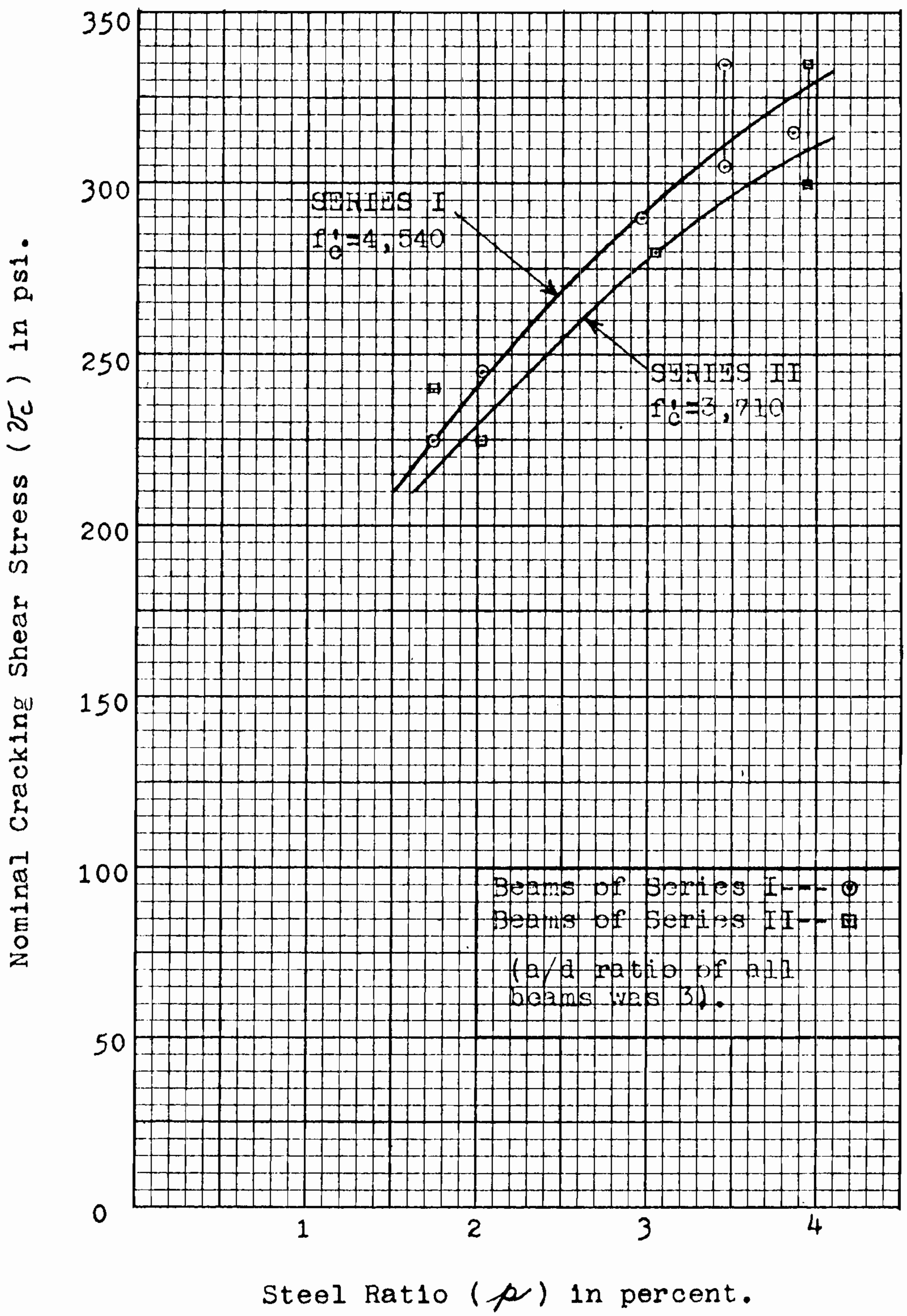

Fig.12-Percent of Tension Reinforcement versus Nominal Shear Stress at Diagonal Crack Formation.

shear compression as the second crack formed. The crack opened very slightly when the last increment of load was put on; the beam held for a few minutes then crushing occurred. In Plate 23 the compressive crushing can be seen clearly.

Test Data Compiled

Table 6 shows loads V_c and nominal shearing stresses, $v_c = V_c/bjd$, at which the diagonal tension cracks formed. v_c includes dead weight of the beam. The elastic value j was computed by the Cracked Section Theory using a modular ratio n = 6.6 for Series I and n = 8 for Series II. The modular ratio for Series II concrete was obtained by stress-strain measurements described previously. The modular ratio for Series I concrete was computed using an assumed E_c of 1,000 f'_c. Fig. 12 shows nominal shear stress v_c versus steel ratio p. When a beam has diagonal tension cracks in both spans, two points are shown for that steel ratio, and are connected with a light line.

Fig. 13 shows a comparison of measured stresses over the support point base block of Beam 14 with those theoretically occurring in a homogeneous beam of similar proportions (taken from Figs. 3 and 5, y = +2). Strain measurements were made at 2 inch intervals along a level 4 inches above the base block, or, using the coordinate system of the stress function, at y =+2 between x = 8 and 18. These measurements

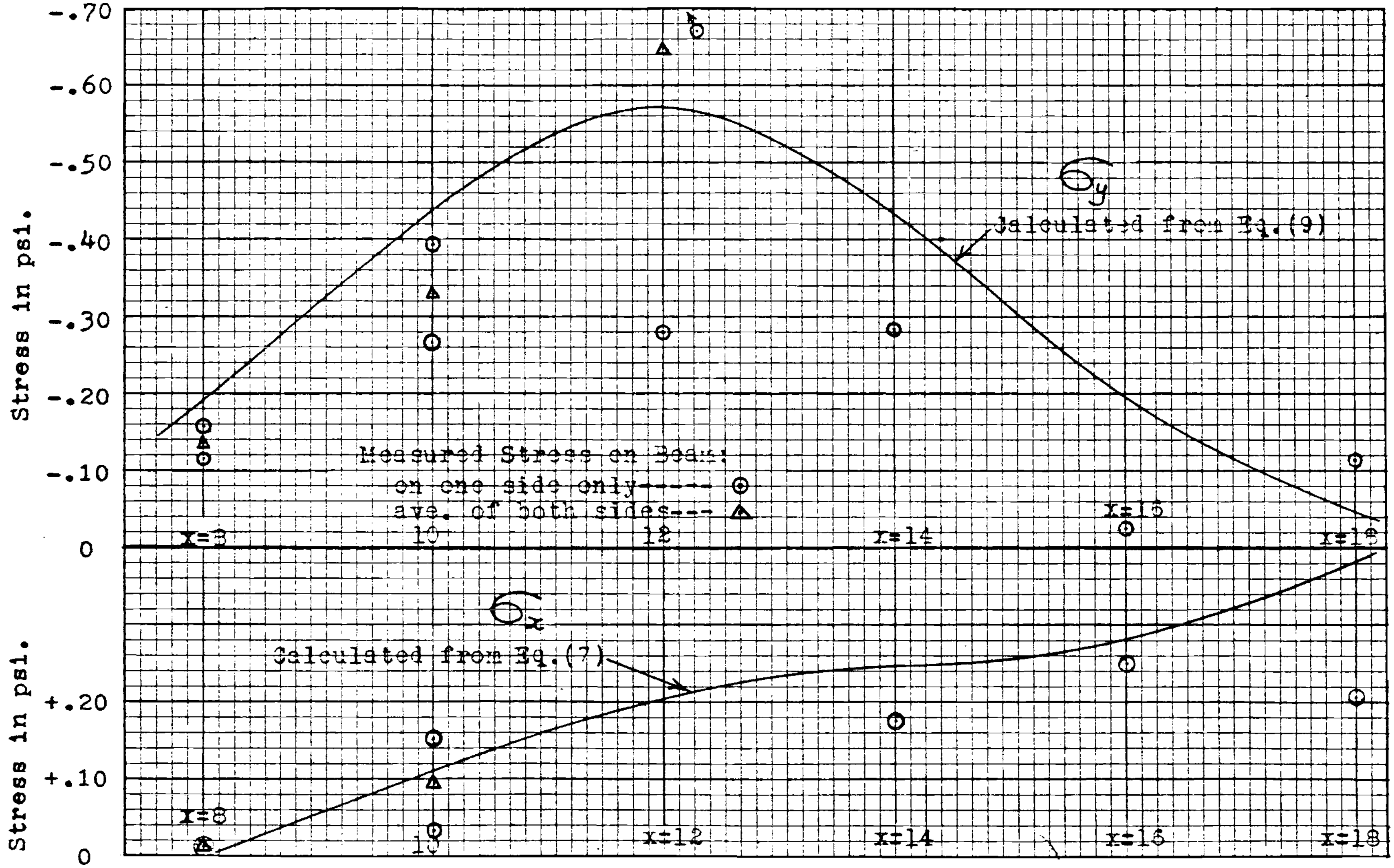

Fig.13-Measured σ_y and σ_x Stresses at y=+2 in., above a Base Block Support.

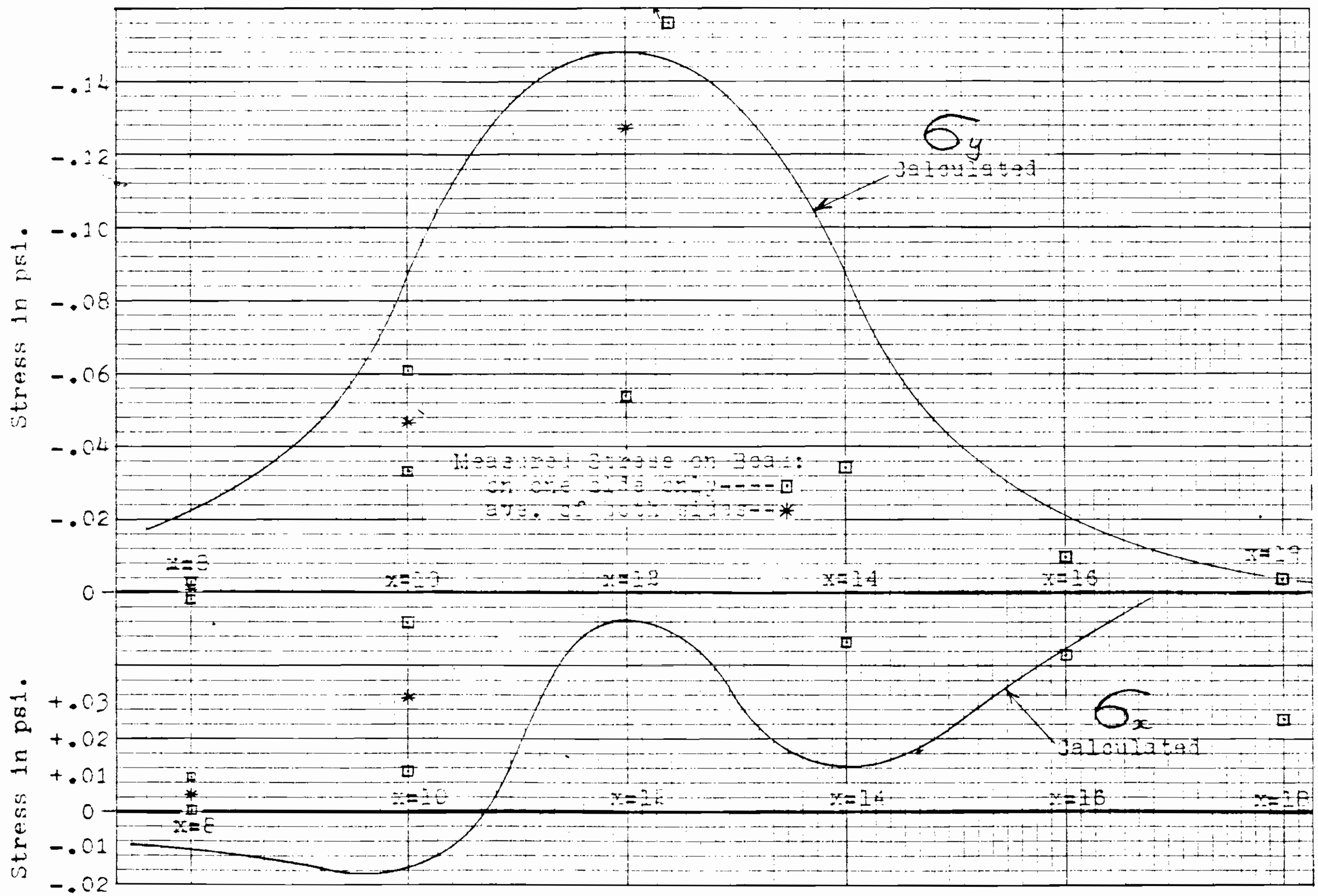

Fig.14-Measured σ_y and σ_x Stresses at y=+2 in.,above a Knife Edge Support.

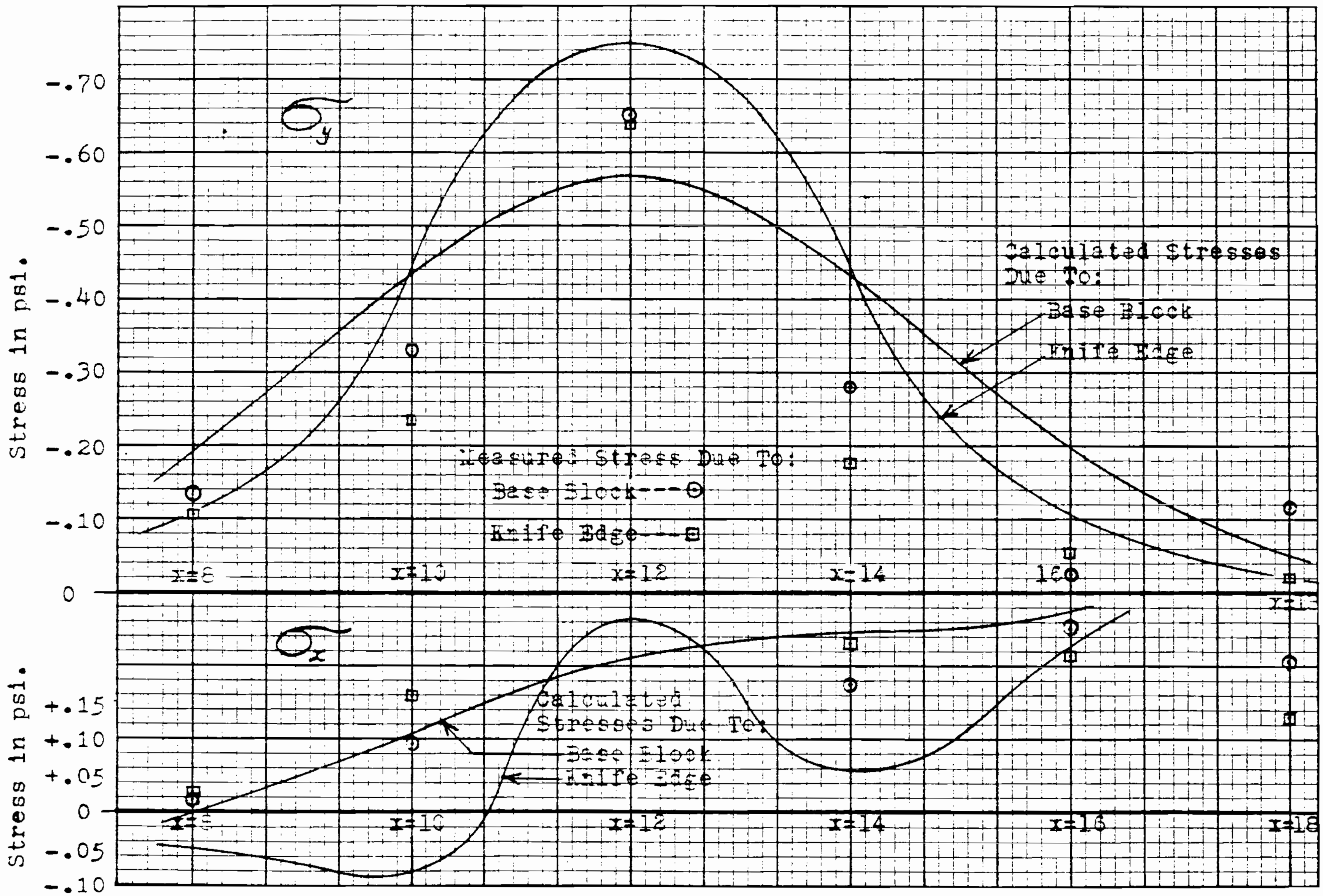

Fig.15-Comparison of σ_y and σ_x at y=+2 in.,above a Base Block and above a Knife Edge Support.

were plotted in load-strain curves, Fig. B-1, Appendix B, together with the theoretical strain given by Eqs. 7 and 9. The final rather than the initial zero readings (except σ_x, at x = 18) were used in plotting these load-strain curves, thus displacing the lower ends of several of the curves from their origins. Many of the curves showed changes of stiffness during the test -- a fitting line through the values at the higher loads was used to obtain overall strain during the test. This strain was then averaged with the strain on the opposite side of the beam, reduced to stress at unit base block pressure, and plotted in Fig. 13. The modulus of elasticity of 3,750,000 psi. was used for both tensile and compressive stress; a Poisson's ratio of 0.25 was used. The following gages were excluded from the averages: at x = 14, West and at x = 16, East. The gages at x = 12 gave widely divergent values for the σ_y stresses. The σ_x stress for this point has been omitted; the average σ_y stress, although only approximate, is included in order to illustrate that stress was probably considerably larger here than at adjacent gage locations.

A similar comparison is made in Fig. 14, where stress distribution caused by a knife edge support point is shown. The load-strain curves for this run were perfectly linear; calculations were the same as for the base block curves, except that strains were reduced to those at unit load on the knife edge. Those gages excluded from the calculations for the base block stresses were also excluded from the knife

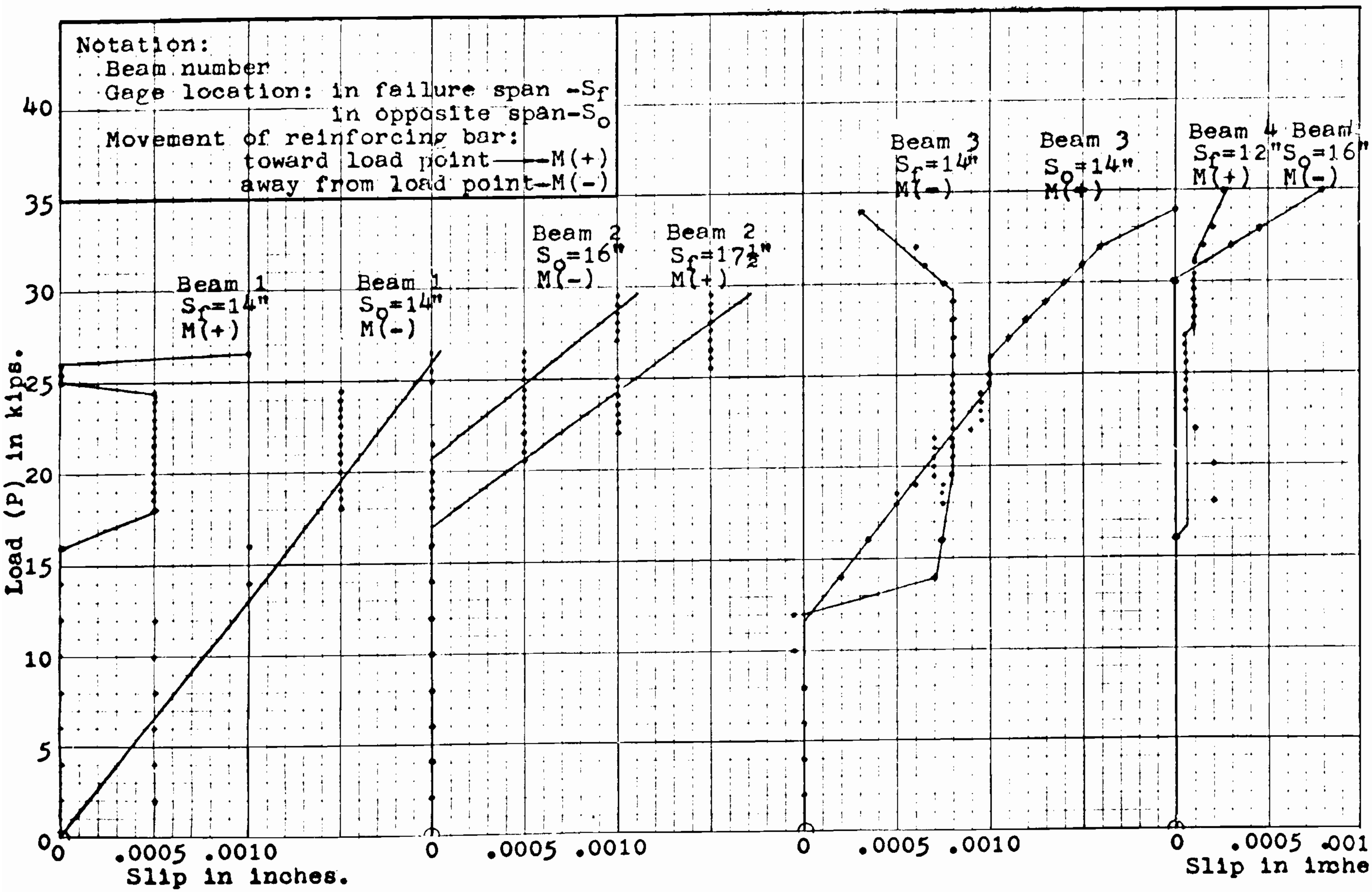

Fig.16- Load-Slip Curves for SERIES I Beams.

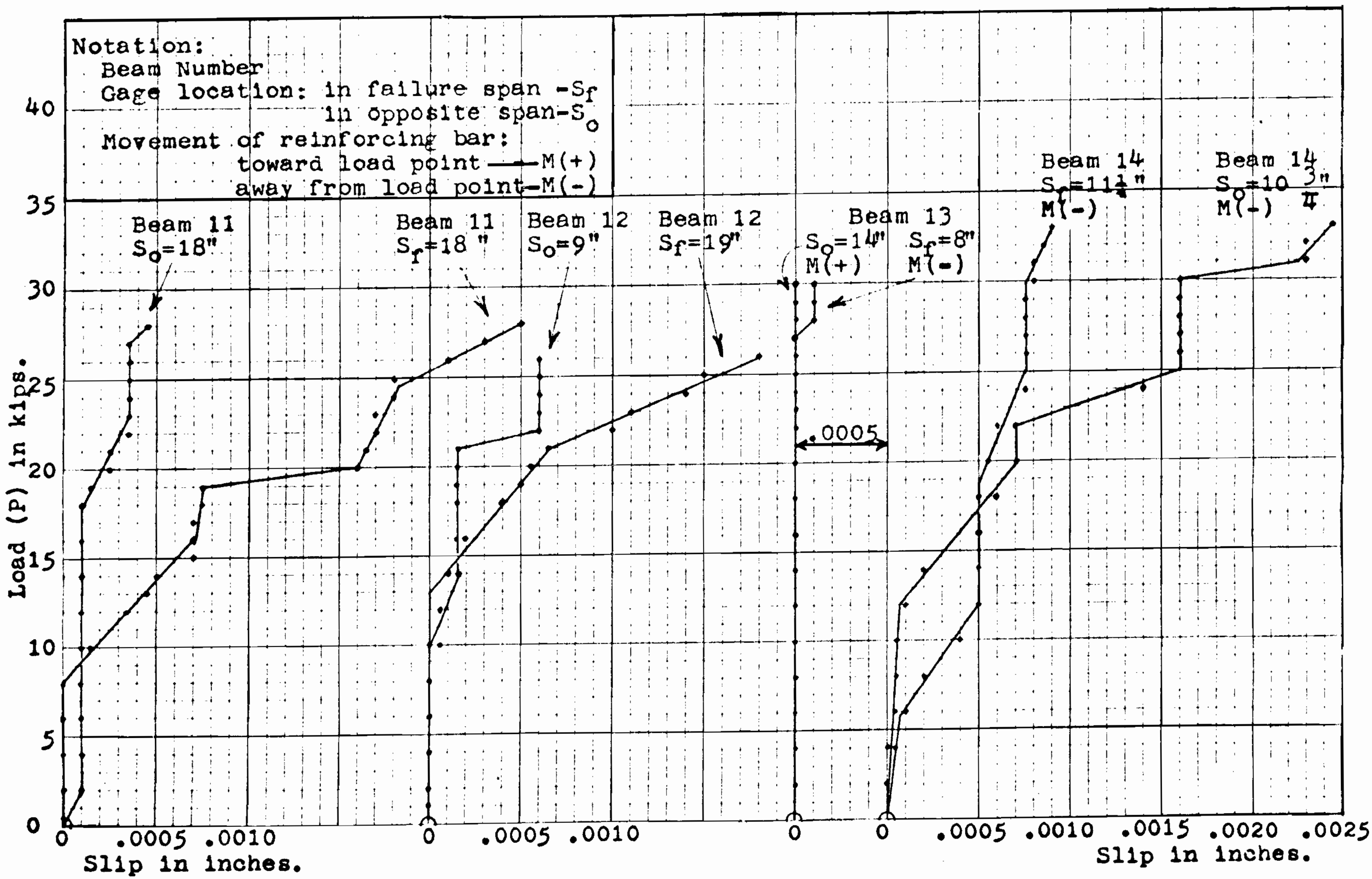

Fig.17-Load-Slip Curves for SERIES II Beams.

edge calculations. The theoretical values shown (at $y = +2$) were obtained from Sewald's curves, given in Timoshenko and Goodier (18) page 103, by a process of double interpolation. Fig. 15 is a comparison between stresses caused by the base block and by the knife edge, both under a total support point reaction of 5 pounds (per inch width of beam).

The load-slip curves are shown in Figs. 16 and 17. Also included are the distances from the load point to the gage location in that shear span to form the first diagonal tension crack (S_f), and the opposite span (S_o), respectively. The direction of the motion of the reinforcing bars is indicated. Direction of slip in Beams 11 and 12 was not recorded. Slip for Beams 1 and 2 was recorded with a .001 inch dial gage, hence a rather rough fitting curve.

The measured strain distributions on cross sections in the shear spans of Beams 12, 13, 14 - First Crack, and 14 - Second Crack, and in the pure moment span of Beam 13 are shown in Figs. 18 to 22. These were constructed from the averages of strains on opposite sides of the beams, measured at the indicated load increments. In several cases strains were measured at some distance from the desired section, as in the case of the steel strains. Therefore, the required strain has been calculated from the measured strain by direct ratio of the bending moment at the respective sections; the strains thus adjusted are marked with the superscript ', e.g. 7E'. With the exception of those on Beam 13, the gage

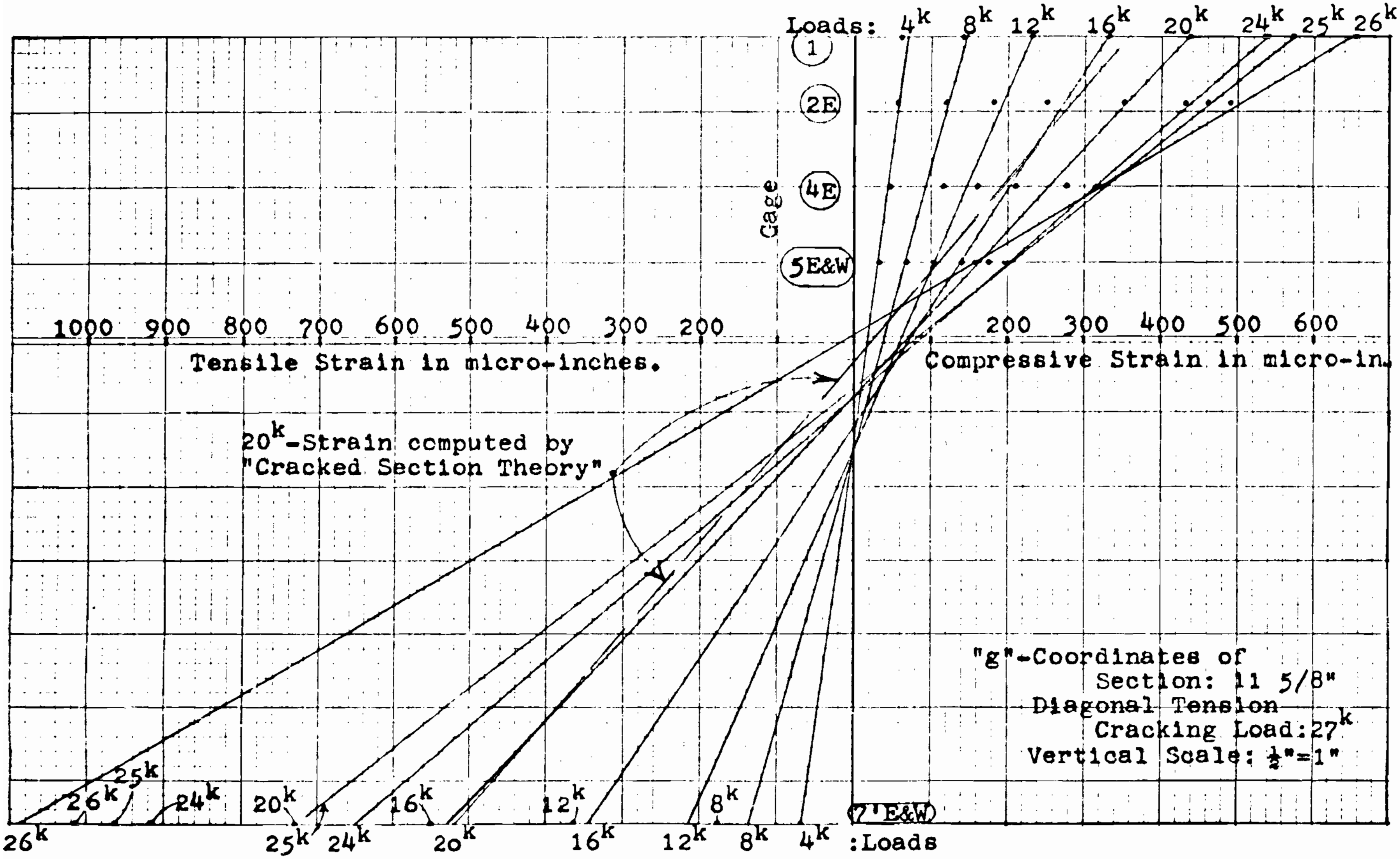

Fig.18-Strain Distribution in the Shear Span of Beam 12.

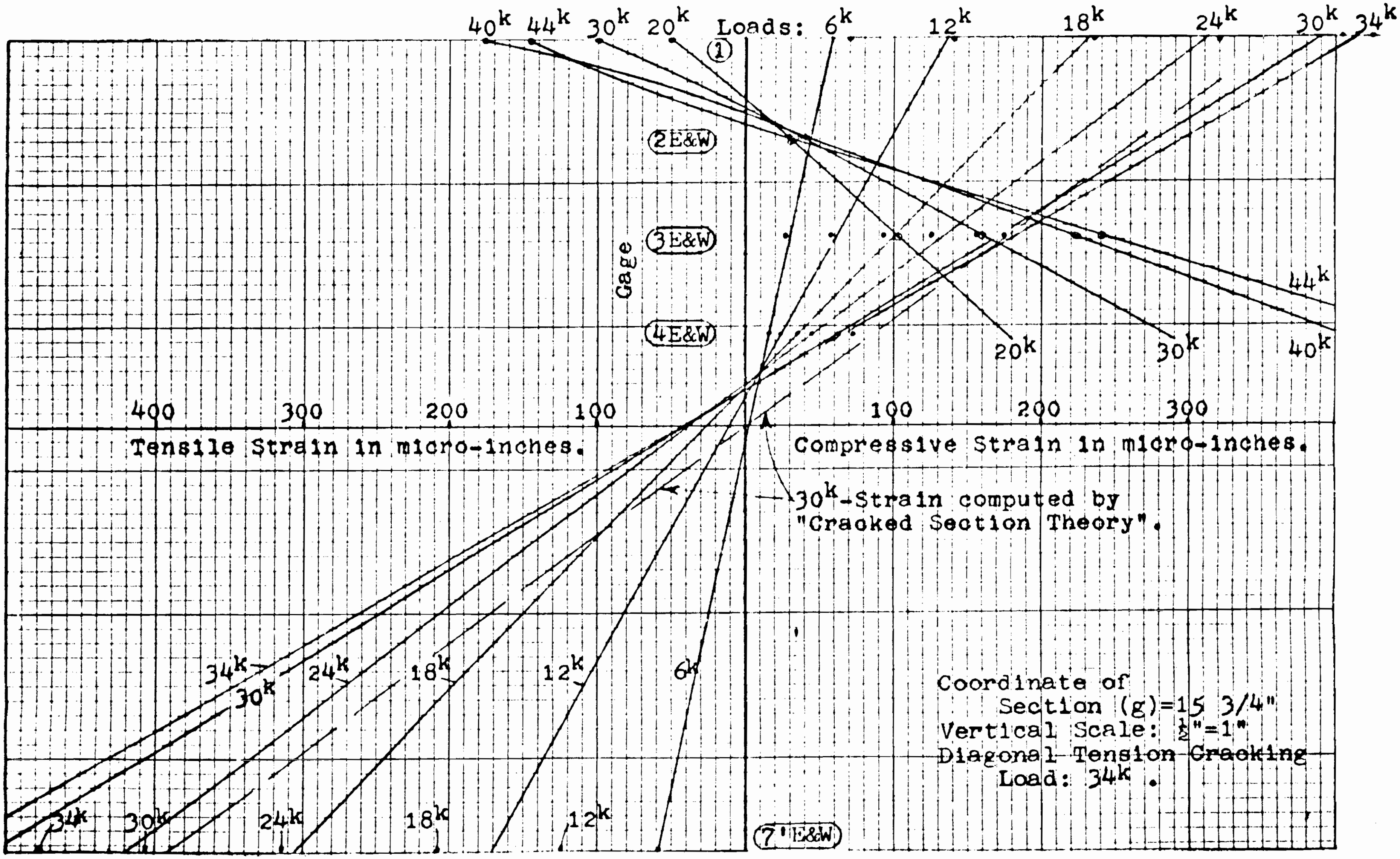

Fig.19-Strain Distribution in the Shear Span Forming the First Diagonal Tension Crack, Beam 14.

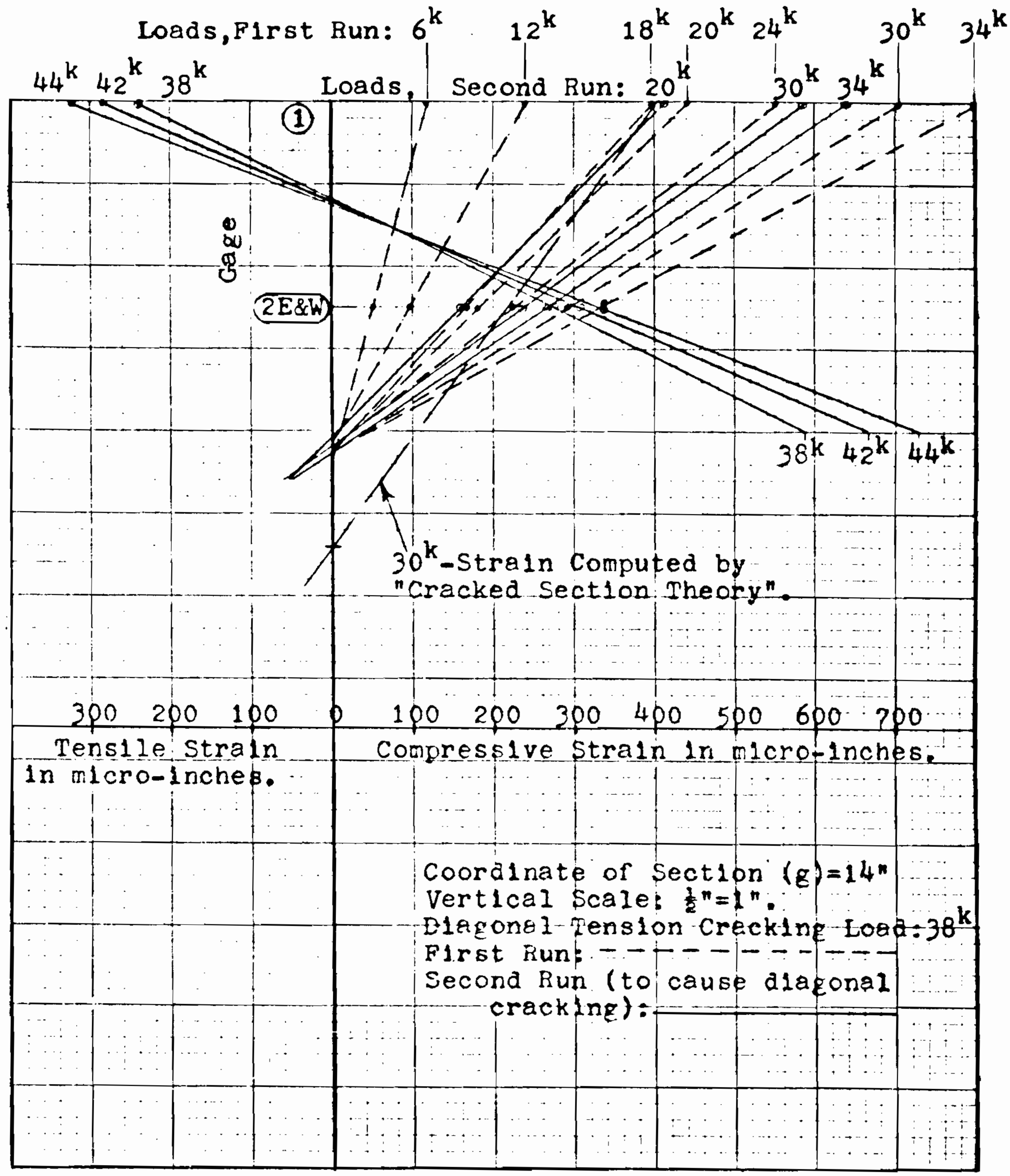

Fig.20-Strain Distribution in the Shear Span Forming the Second Diagonal Tension Crack, Beam 14.

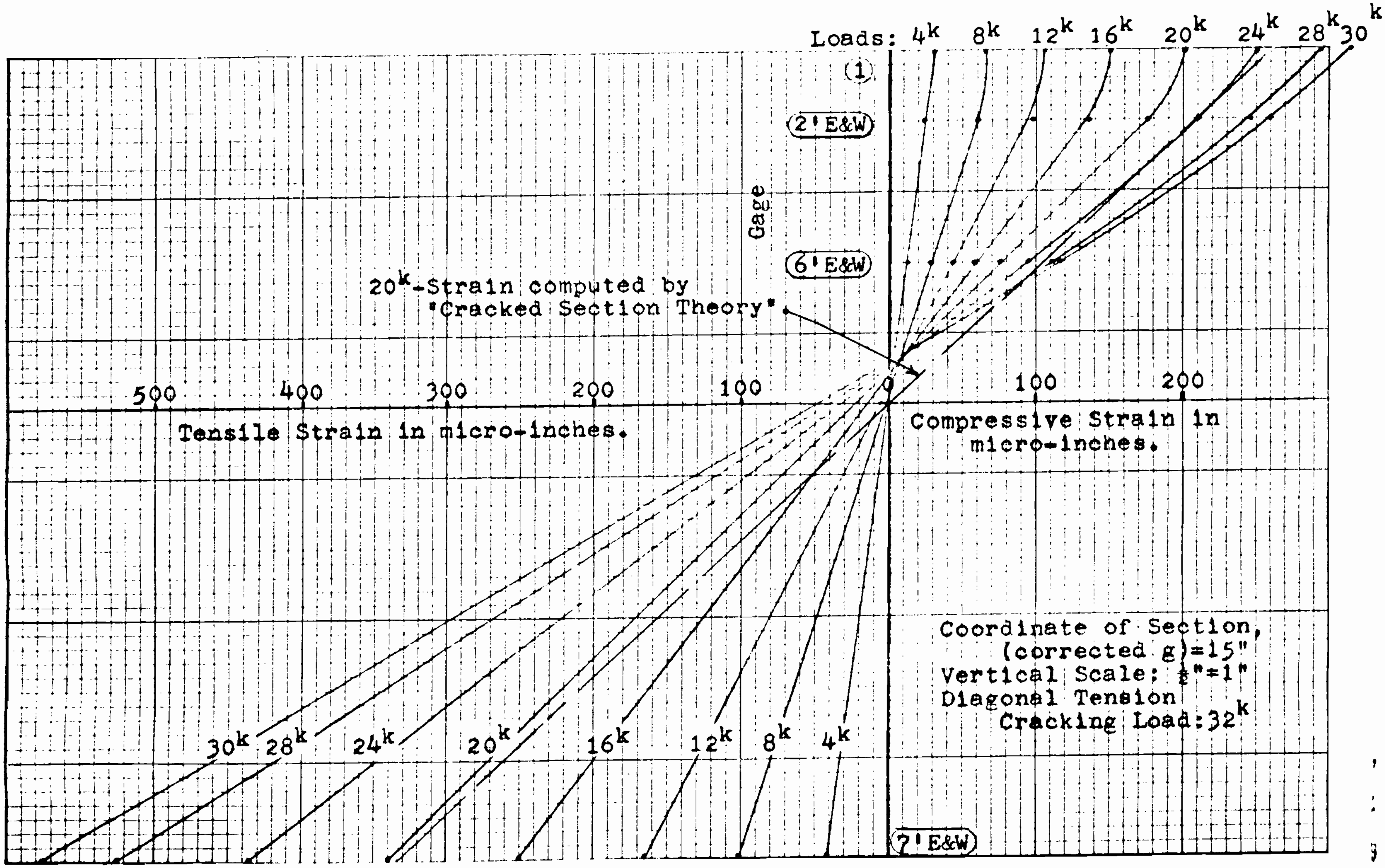

Fig.21-Strain Distribution in the Shear Span of Beam 13.

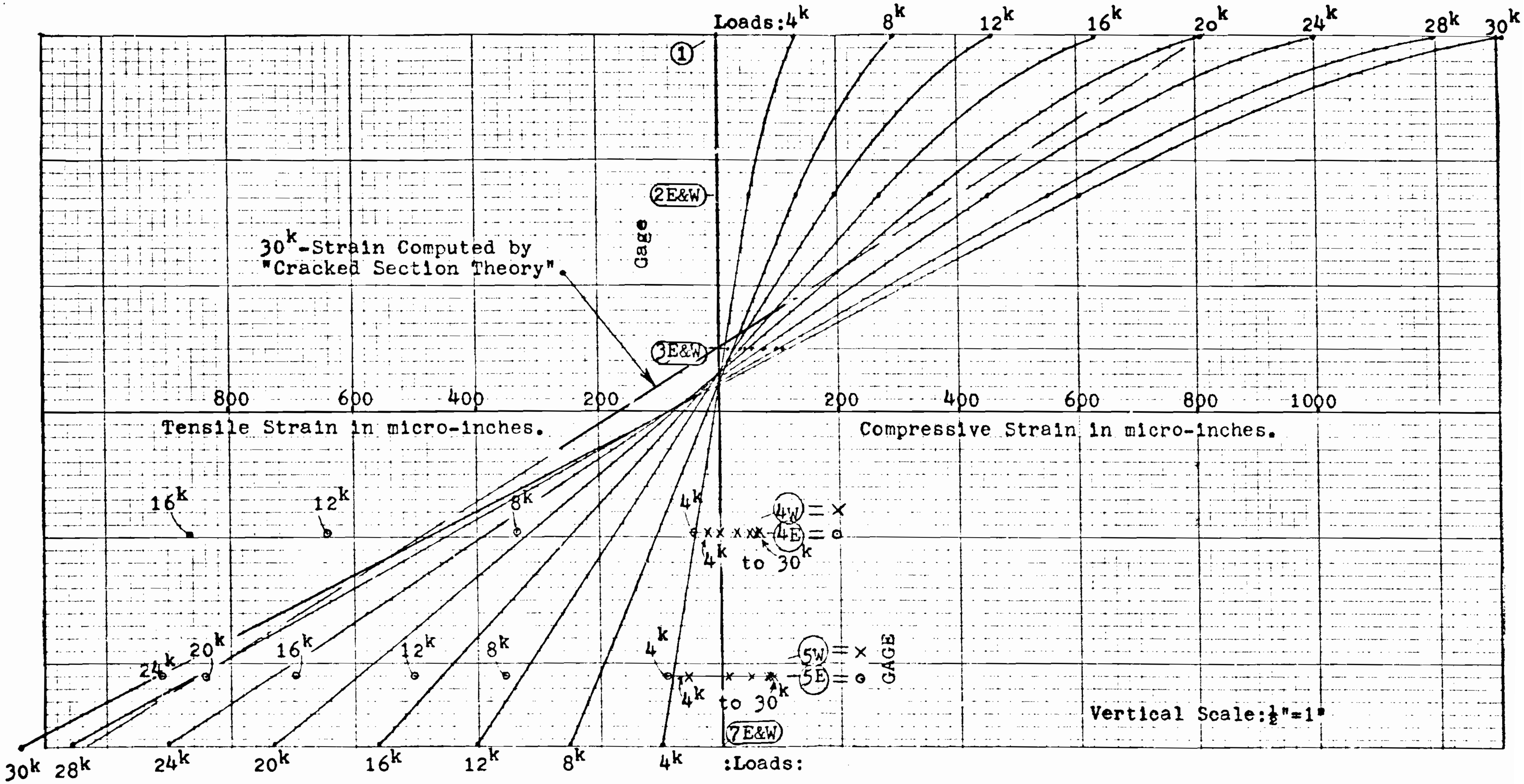

Fig.22-Strain Distribution in the Pure Moment Span of Beam 13.

lines were located in shear spans which formed diagonal tension cracks. The strain distribution diagrams were constructed with only those readings which fitted a reasonable shape, and in each case were the best fit possible (plotting the strains for individual sides did not improve the strain block shapes). The following gages were excluded from the averages: Beam 12, 2W & 3W; Beam 13-Shear Span, 3'E & W; Beam 13 - Pure Moment Span, 4 E & W; 5 E & W; Beam 14 - Shear Span with First Crack, 2 E & W before cracking, 4 E & W after cracking. The load-strain curves for the gages of each beam are shown in Figs. B-2 to B-6, Appendix B. A "made up" rosette consisting of one AX-5 (two element) gage and an A-7 (single element) gage were placed on Beam 13, Fig. 10. The readings proved to be confusing -- some compressive strain was indicated by the inclined gage 6W, Fig. B-5, Appendix B.

The load-deflection curves of Fig. 23 and 24 show the mid-span and third point deflections for the large beams, and the mid-span deflections for Beams 5A and 5B. Stiffnesses at mid-span, as computed by the Cracked Section Theory, are also indicated in the figures. These latter curves were computed using, for Series II, a modulus of elasticity of 3,750,000 psi., but an assumed $E_c = 1,000\ f'_c$ for Series I.

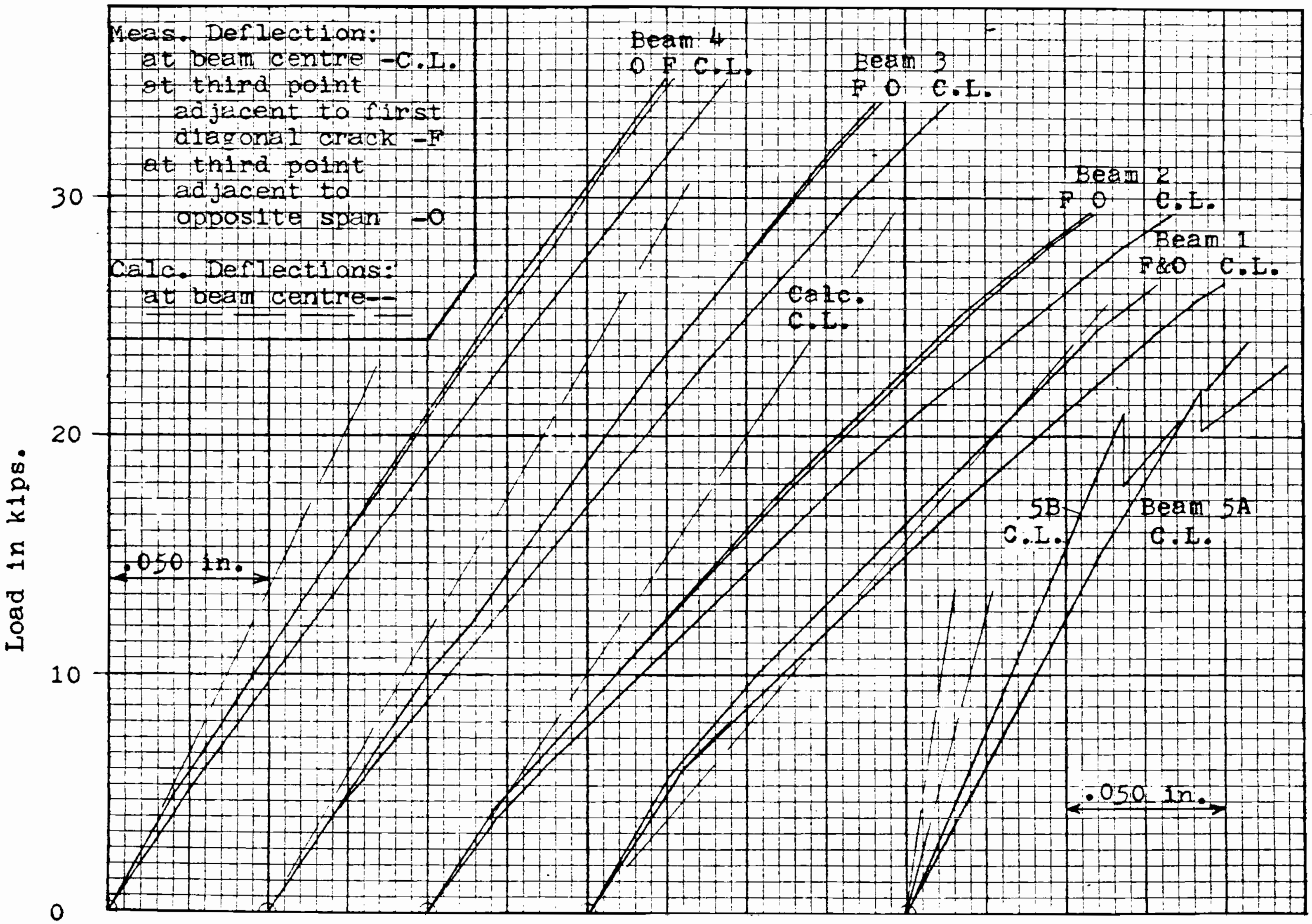

Fig.23- Load-Deflection Curves for SERIES I Beams.

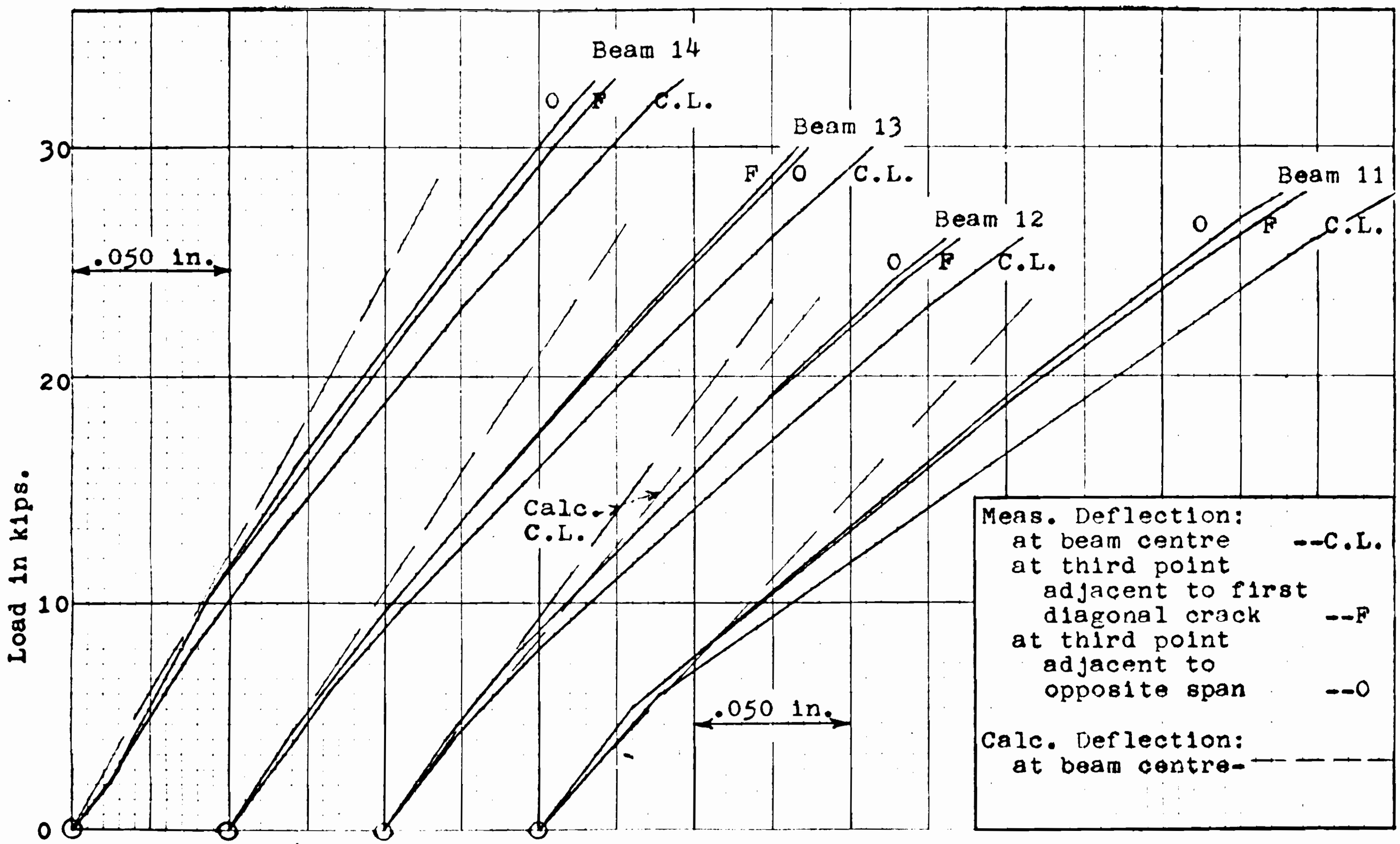

Fig.24- Load-Deflection Curves for SERIES II Beams.

DISCUSSION

Discussion of Results

STEEL RATIO: The results presented in Fig. 12 indicate a definite relationship between steel ratio and the nominal shear stress necessary to cause formation of a diagonal tension crack. As can be seen, there was a substantial increase in the cracking shear stress with increasing steel ratio. Decreased amounts of reinforcement raise the neutral axis, deepening the tension zone in the beams. This means higher steel stress, more flexural cracking and greater principal tensile stresses in the concrete. Accompanying these effects are increased local stress concentrations due to the presence of the flexural cracks. Thus, there is a greater probablilty that a diagonal tension crack will form.

The fitting curve shown in Fig. 12 passes through the averages of two values for Beams 5A and 14 -- had the opposite spans of the remaining beams developed diagonal tension cracks, average values would be higher than those shown. In order to eliminate all variables except that of steel ratio, the beams were all given the same dimensions. However, Beam 5A, introduced to supplement the results, had a smaller cross section but its cracking shear fits quite well into the curve at $p = 3.45\%$, Fig. 12. Beams 4 and 14, at $p = 3.9\%$, suggest a levelling off in a beam's resistance to diagonal tension cracking with the use of higher steel ratios. Beam 11, $p = 1.75\%$, would seem to be an exception to the general pattern; the diagonal tension crack formed from a very steep inclined crack, and required a higher load to precipitate it.

The National Building Code (1960), The Canadian Standards Association Code A 23.3-1959, and the American Concrete Building Code AC1 318-56 all allow a nominal shear stress of 90 psi. for the beams tested in this investigation, which gives safety factors of from 2.5 to 3.8.

It is of interest to make a comparison between the curves for the two concrete strengths in Fig. 12. Kesler (19) has presented the equation $f'_t = 9.5\sqrt{f'_c}$ for the modulus of rupture of concrete. The square root of the ratio of the cylinder compressive strengths is 1.11; ratios of values along the two curves of v_c are approximately 1.06. Using a constant value for "j" increases this latter ratio to approximately 1.11, emphasizing the relationship between the diagonal tension cracking resistance of a reinforced concrete beam and the tensile strength of the concrete. Size of aggregate and extent of shrinkage stresses are two important factors in the tensile strength of concrete; aggregate sizes differed between the two series of beams in this investigation, but method of curing, and presumably extent of shrinkage, were quite similar.

STRESS FUNCTION: The curves for σ_x', τ_{xy} and σ_y

computed from eqs. (7), (8) and (9) are shown in Figs. 5 4 and 3. The curves are smooth and symmetrical, and give values of a reasonable order for local stresses. The local influence of the uniformly applied load decreases rapidly, away from the loaded point, becoming negligible at a distance of one half the beam depth (c). Several of the σ_x' curves do not converge exactly to zero, probably due to the calculations not having been carried to enough cycles.

Measured values for the σ_x and σ_y stresses at the level y = +2 in a reinforced concrete beam supported by base blocks are compared, in Fig. 13, to those theoretically occurring in a homogeneous elastic beam. Although the measured stresses do not fit the theoretical curves perfectly, there appears to be a fair degree of similarity. There were numerous variations among the strain gage readings, so several sets of gage readings have been excluded from the averages -- the remainder deviated up to 60% from the average values of gage readings on either side of the beams. The value for σ_y at x = 12, although resulting from the average of two widely diverging values, has been included in order to illustrate that stress could probably have been quite high at this point. The measured σ_y stresses fit the stress function values within ± 35% except toward the extremities of the curve, where there is a much greater divergence. The measured σ_x stresses compare much better with the stress function values. The tolerance in reading the strains was ± 5 micro-inches -- which amounts to ± .05 psi; nearly all the measured σ_x values are within ± .05 psi. of the stress function. A single gage placed on coordinates x = 12, y = 0 gave results quite different from the theory.

Probably the major difficulty in presenting the curves for the measured stresses was in interpreting the strain gage readings. As will be described in the next section, "Discussion of Test Methods", there seemed to be a drift with time in the gage readings. Also, as the strains measured at this location were quite small, the tolerance of the strain indicator had a large influence on the accuracy of the readings. The load-strain curves from the gages at coordinates x = 18 and x = 16 showed sharp decreases in stiffness at about 26 and 29 kips respectively; it is thought that this is due to disturbances at the commencement of flexural cracking in the concrete at these locations.

One of the difficulties in attempting strain measurements of this sort is to implement the correct loading condition. The stress function is based on a uniformly loaded surface; this was approximated with a $1\frac{1}{2}$ inch thick steel block separated from the surface of the beam by $\frac{1}{4}$ inch of plaster. This was an extremely stiff block -- it probably behaved more as a rigid die, causing stress concentrations under the edges of the block. However, at the level of the strain gages -- 4 inches from the block -- this effect was not discernible in the σ_y readings. Another difficulty in the loading condition was in providing complete freedom in roller action at each end of the beam. One end was on a roller, but the base block end was on a fixed roller. The loading beam distributing load to the third points was also fixed at one end and on a roller at the other. Consequently, tensile strain on the lower surface of the beam would tend to cause "pull" on the support points, confusing the stress pattern. Two other factors must be mentioned -- the lack of homogeneity throughout the beam and the eccentric loading of the beam. For the range of strains measured, the concrete can be considered to be elastic, but not homogeneous. The presence of large reinforcing bars in the vicinity of the gages would undoubtedly distort the local stress pattern. From the load-strain curves Fig. B-1, Appendix B, it is apparent that the beam was being twisted slightly under loading, causing greater σ_y and smaller σ_x stresses on the east side.

The results of an additional set of readings taken at this same location, using a knife edge as a support point, are presented in Fig. 14. Also shown in this figure are curves for the theoretical values of these stresses, taken from Timoshenko and Goodier (18), p. 103. The measured σ_y stresses are lower and approximately parallel to the theoretical curve, but the measured σ_x stresses do not show much similarity to the theoretical values. Gage readings on either side of the beam deviated up to 60% or more from the average of the readings. The measured σ_y stresses fit the theoretical values within ± 60% except toward the extremities of the curve, where there is a greater divergence. Apart from the validity of the stress function, possible reasons for this could be strain gage inaccuracies, longitudinal "pull" on the knife edge (which was not on a roller support), twisting, and errors of interpolation in obtaining the theoretical curve from Sewald's values.

In the following graph, Fig. 15, a comparison between measured and theoretical stresses at y = +2 under base block and knife edge loadings shows that theoretically the knife edge loading does cause higher σ_y stresses at the point of application and that these taper off toward zero more rapidly than do those caused by the base block. However, it would appear that the measured σ_y stresses for the knife edge loading are smaller than those caused by the base block. Other comparisons between the theoretical local stresses caused by a base block and a knife edge loading showed that there are considerable differences within a half beam depth (c) (both horizontally and vertically) from the point of application of the forces, but beyond this zone, the stresses are nearly identical. Presumably, the use of different methods in applying the force on a reinforced concrete beam could influence the final position of a diagonal tension crack which passed into the above mentioned zone.

Extensive comparisons were made of the principal tensile stresses in a homogeneous elastic beam loaded by a base block, computed both by means of eqs. (7), (8) and (9) and by means of elementary beam theory. In the vicinity of the load point ($x = 42''$), the stress function gave either lower tensile stresses than those of elementary beam theory or even compressive stresses. Above mid-depth, the directions of the principal tensile stresses from eqs. (7), (8) and (9) varied little more than 4^o from those given by elementary beam theory. Beyond more than a half beam depth (c) horizontally from the point of application of the load, principal tensile stress given by the stress function differed little from that given by elementary beam theory. At the support point ($x = 12''$), the situation was similar -- principal tensile stresses given by eqs. (7), (8) and (9) were always less than those given by elementary theory, although the differences did extend somewhat more than (c) horizontally from the point of application of the force. Not investigated was the zone between $y = +4$ and $y = +6$, where principal tensile stresses could possibly be larger than those given by elementary beam theory. Fig.25 shows the stress trajectories of the principal tensile stresses in the vicinity of the support point base block. Trajectories of stresses computed by means of the stress function, eq. (6), are shown in full lines; those computed by means of elementary beam theory are shown in dotted lines. It can be seen that the stress function gives more horizontal directions to the principal tensile stresses in the vicinity of the base block, but these differences do not extend much farther than (c) from the base block.

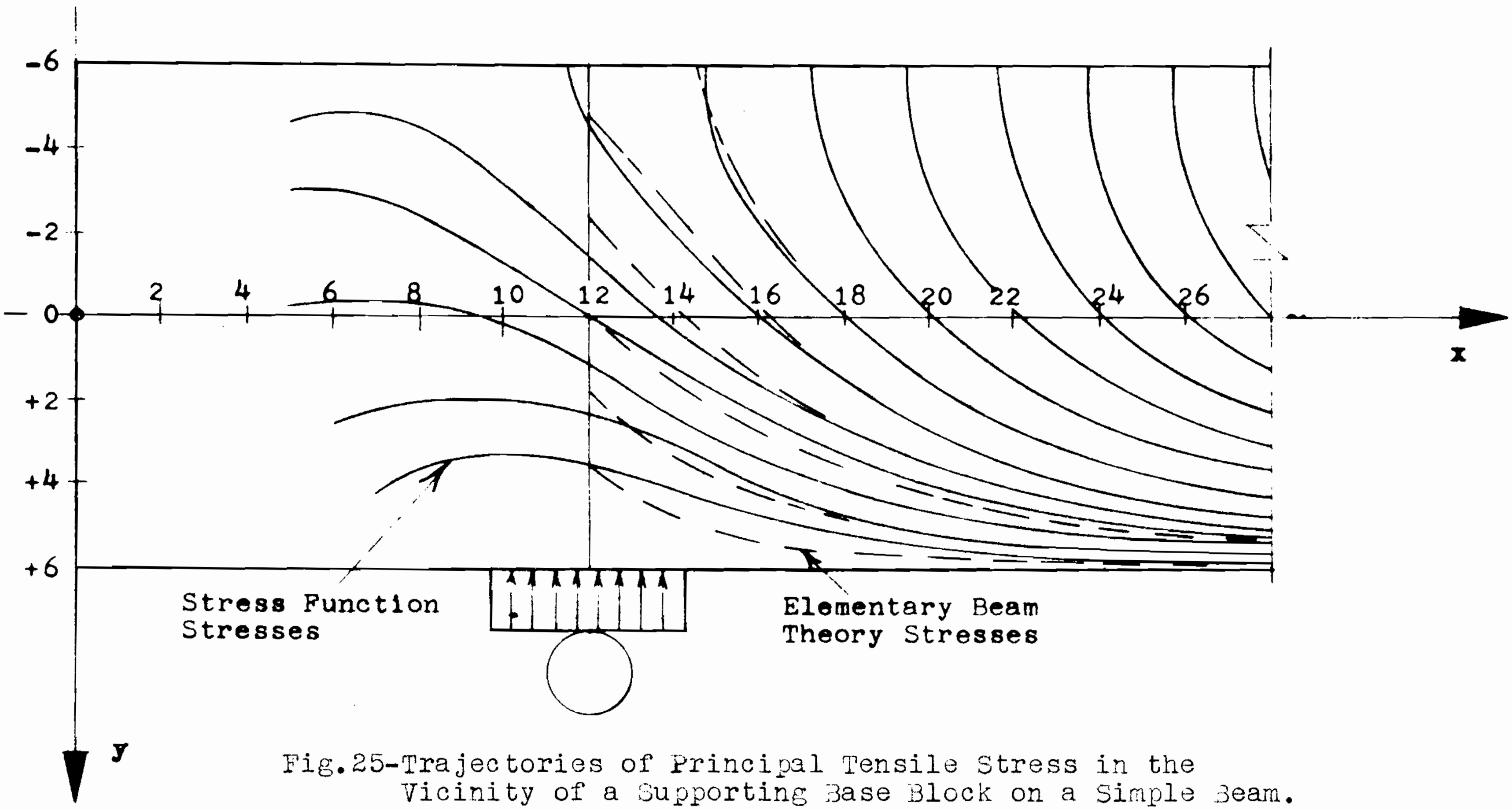

Fig.25-Trajectories of Principal Tensile Stress in the Vicinity of a Supporting Base Block on a Simple Beam.

SLIP: The measurements made of slip of the longitudinal reinforcing bars do not give any conclusive results for the purpose intended due to the type of failures that occurred in this investigation. The original purpose of the slip gages was to illustrate that very steep diagonal tension cracks could only develop with considerable slippage of the bars. Beam 11 developed the only steep diagonal tension crack -- slippage was not large and was of the same order as that of several other beams which developed very flat cracks, Fig. 17. The gage was about 4 inches from the crack.

The gages were arranged in order to measure slip of a bar relative to a point fixed in the concrete on the bottom of the beam and to eliminate the effect of the beam's tensile strain on the readings. However, the effect of possible flexural cracking at the point of anchorage is an unknown factor in these readings. The slip measured was of the order of .002 inches (Figs. 16 and 17), probably less than the width of the visible flexural cracks; this suggests that the deformed bars did not slip very much. Flexural cracking developed around the location of some of the gages, but in only three cases (the failure spans of Beams 11 and 12, and the span without the diagonal crack, Beam 3) could start of gage movement be associated with the probable load at which the flexural cracking began.

A few comments can be made on the load-slip curves. Slip usually started after the beam had undergone considerable loading, and increased steadily with further loading. The advances in gage readings were of two types -- steady (elastic-like) increases and sudden slippages. Usually, but not always, the greater slip was recorded in the failure spans, and this slip was away from, as often as it was toward, the diagonal tension crack. Occasionally sudden movements of the slip gages preceded diagonal tension cracking, as in the case of Beam 1, but this was not found to be a general pattern. The gages in the failure spans of Beams 1 and 3 show unusual reversals in the direction of slip prior to cracking. No consistent relationship could be discerned between gage movement and either gage location or amount of longitudinal reinforcement.

Slip measurements could probably be of more value if they were made at several points in a span and included more than one bar. A more adequate method of anchorage for the dial gage is also clearly necessary.

STRESS DISTRIBUTION: The original object of making strain measurements in the shear spans was to determine the strain distribution at the critical section, above a diagonal tension crack. After the formation of such a crack, the only forces acting on the shear block are support and load point shears (V), steel tension (T), and a compressive force (C) at the critical section, Fig. 26. The shear block thus behaves similarly to a two-hinged arch. Strain distribution at the critical section should be close to

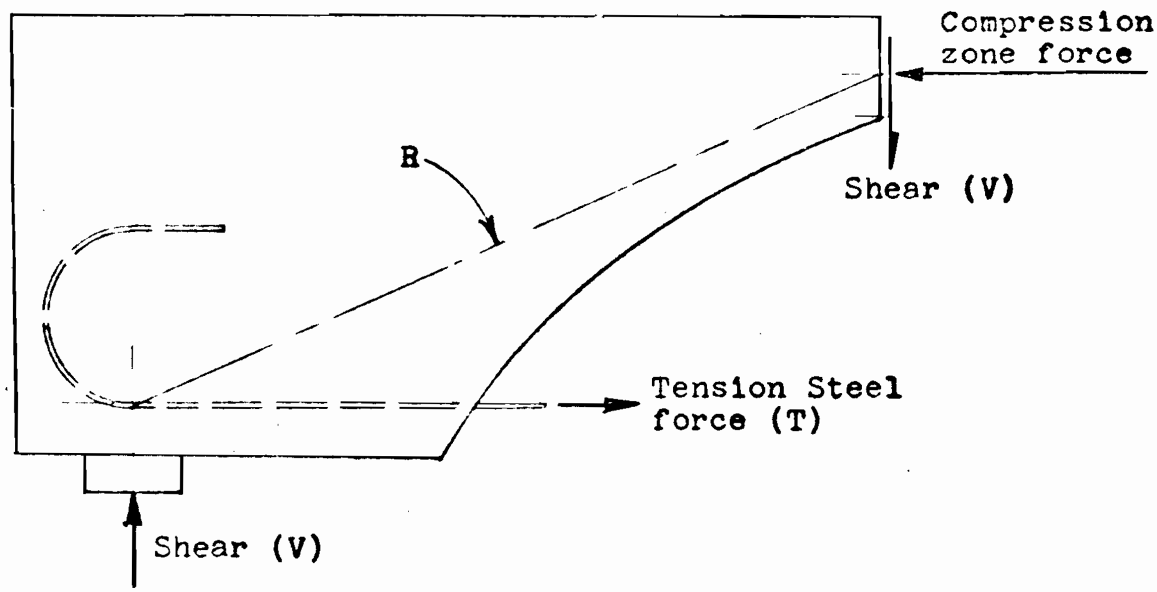

(a) Shear block.

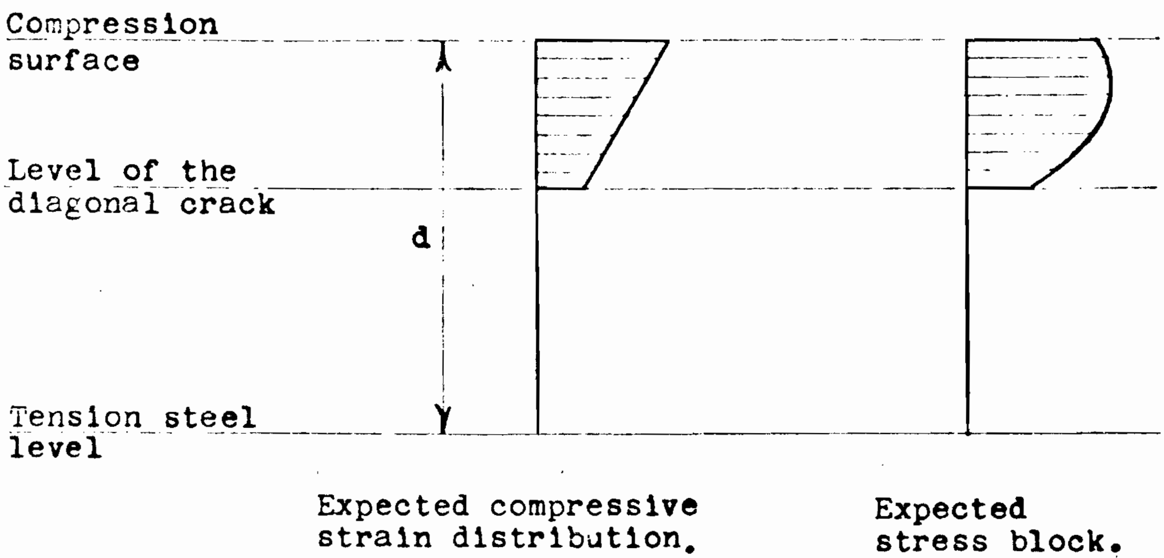

(b) Expected distribution of stress and strain at the critical section of a beam failing in shear compression.

Fig.26-Shear Block and Expected Stress Distribution at the Critical Section.

linear; and near failure, the stress distribution should be of a parabolic form. The amount of eccentricity of the compressive force C is indeterminate, but it is to be expected that a certain amount of strain should exist at the level of the crack, probably compressive strain as shown in Fig. 26. With a strain distribution such as this, stress distribution, near failure, would have a parabolic shape but would not be zero at the level of the crack. The only case for which stress or strain could be zero at the level of the crack, as assumed in current literature (see Fig. 1(c)), would occur when the compressive force C acts exactly on the edge of the kern of the critical section.

In this investigation, most of the beams failed at the formation of the diagonal tension crack, making it impossible to obtain the desired measurements. Therefore, gage lines were established in mid-span and strains read there.

The gages of Beam 12, Fig. B-2, Appendix B, indicated the presence of disturbances just prior to diagonal tension cracking -- no readings were obtained after cracking. However, excellent gage readings of the stress redistribution were obtained in both spans of Beam 14, Figs. 19 and 20, after diagonal tension cracking. The load-strain curves, Figs. B-3 and B-4, Appendix B, and the above mentioned strain blocks of the compression zones indicate the start of flexural cracking and the relatively elastic behavior until disturbances began just prior to diagonal tension cracking.

After crack formation, the compression zone strains underwent a very marked redistribution. The top surfaces went into tension, while the lower gages indicated increased compressive strains. As described later, in the "Discussion of Beam Behavior", the line of action of the resultant of the forces applied to the shear block passed through the block, but was sufficiently eccentric to the centroid of this section of the block to cause tension on the top surface.

The gage lines on Beam 14 had approximately the same relative position in either shear span. Just why the gages above the First Crack (34 kips) should show only half the strains shown by those above the Second Crack (38 kips), both before and after crack formation, is not known. With every set of strain gage readings, some gage readings were found to be erratic or impossibly out of line, so were neglected. From the average of two strain gage readings at each point shown in the strain blocks of Figs. 18 to 22, individual gage readings showed deviations of up to 20%. The strain gages on the reinforcing bars were the most consistent, rarely differing by more than 3% from an average value. In the first span of Beam 14 to form a crack (34 kips), the fact that gages 4 E & W were close to the crack and may have been damaged at crack formation probably explains their lack of agreement, after crack formation, with the strain distribution presented by the other gages. However, on this same beam gages 2 E & W, with reasonably similar readings, gave inexplicably low values before crack formation; after crack formation the readings agreed quite well with the strain distribution presented by the other gages.

The remaining strain blocks, Figs. 18, 21 and 22, show strain distribution in the failure span of Beam 12 and in the spans of Beam 13 which did not develop diagonal tension cracks. The strain distributions in the compression zones are quite triangular, and the load-strain curves, Figs. B-2, B-5 and B-6, Appendix B, are generally linear till the failure load is approached.

The steel strains for Beams 12 and 14 were not measured at the sections where the concrete strains were measured, so have been adjusted proportionally to the bending moments of the two sections. However, these adjusted strains do not fit a linear strain distribution pattern with the concrete strain. On the other hand, the steel strain (adjusted) in the shear span of Beam 13 fits a linear strain distribution,as does that of the pure moment span. The resulting neutral axes, in all cases except Beam 12, remain relatively steady during the tests. Included in each figure is the theoretical strain block for the 20 or 30 kip load, computed by means of the Cracked Section Theory ($E = 3,750,000$ psi.). Measured compression zone forces vary from 75 to 150% of the theoretical forces, and apparent neutral axes vary from one inch below to one inch above the theoretical neutral axes.

The strain gage line in the pure moment span of Beam 13, Fig. B-6, Appendix B, shows some unusual characteristics. Gages 4 and 5 were placed on the concrete in the tension zone. Little flexural cracking could be observed in the vicinity of the gages -- one short crack passed through gage 5E just before failure of the beam. Gage 5E on the concrete showed strains of a slightly larger value than those on the adjacent reinforcing bars; gage 4E, closer to the neutral axis and showing greater strain, must have been damaged by a flexural crack. 5W and 4W opposite to 5E and 4E respectively, indicated tensile strain, then changed to compressive strain shortly after flexural cracking began. Clark (20) and Watstein & Mathay (21) have noted a similar phenomenon -- that between flexural tension cracks there can exist, on the surface of the concrete, a state of compressive strain.

Plots of strain versus deflection were found to give a slightly more linear relationship (fewer bends occurred in the curves) than do the load-strain curves.

DEFLECTION: The load-deflection curves, Figs. 23 and 24, are quite linear and show clearly the point at which flexural cracking became general in the central span. With the exception of Beam 12, they show the increase in stiffness of the beams with increased amounts of reinforcement and with increased cylinder compressive strength. It is thought that the increase in stiffness of Beam 14 at the 2 kip load is due to preliminary loads applied before the test began. Generally, the decrease in stiffness associated with the start of flexural cracking in the central span occurred between 4 and 7 kips -- roughly what would be expected using the modulus of rupture from Kesler's (19) suggested equation. Measured deflections under either load point of each beam were slightly different, but there is no correlation between the load point of the greater deflection and that span which developed the diagonal tension crack. Beams 2 and 12 had less reinforcing steel in their failure spans than in their opposite spans -- but only Beam 12 showed greater load point deflection in the failure span, and this only after a high load had been attained. In about half the cases, a sharp decrease in stiffness can be noted a few increments of load prior to the formation of the diagonal tension crack.

Included in the figures are mid-span deflections computed from the Cracked Section Theory. The beams are all considerably less stiff than the theory would suggest: the large Series I beams are between 65% and 80% as stiff as the theoretical values, while Series II beams are about 67% as stiff. Measured mid-span deflections were also compared to theoretical deflections computed by Maney's*equation. For a beam loaded at the third points, this equation is:

$$\delta_{\mathcal{C}} = \frac{23}{216} \frac{L^2}{d} (\epsilon_1 + \epsilon_7)$$

where: $\delta_{\mathcal{C}}$ is deflection at mid-span.

ϵ_1 and ϵ_7 are the strains on the top surface and average tension steel strain respectively, measured in the pure moment span.

---

* This equation is given in "Principles of Reinforced Concrete Construction" by Turneaure, F.E. and Maurer, E.R.; John Wiley & Sons, Inc., New York; 4th Edition, 1932, page 163. See also Moretto (5), page 152.

L and d are length and effective depth respectively, of the beam.

As most of the strain gage lines of this investigation were located in the shear spans, ϵ_1 and ϵ_7 were obtained by direct ratio from the measured strain. In the case of this theory also, actual deflections were between 140% and 160% greater than those given by the equation.

Three factors could account for the large discrepancy between the theoretical values and the measured values. Probably the most important reason is the "plastic" behavior of concrete under stress. By assuming a small value for the modulus of elasticity, perhaps 1 to 2 million psi., the Cracked Section Theory could be adjusted to give values for stiffness more comparable to beam behavior. Secondly, shear deflection is neglected by both theories. In a homogeneous elastic beam of comparable dimensions, shear deflections are of the order of 4% of flexural deflections. Finally, the method used in this investigation to measure deflections would include settlement of supports, if such were to occur. A better arrangement would be a deflection frame supported from the ends of the beam itself, in order to measure deflection of the centroid of the beam.

Discussion of Test Methods

The concrete of the first pour was very stiff and difficult to place, with the result that there was much honeycombing around the reinforcing bars. Beams 1 and 2, having only one layer of bars, were free of honeycombing, but Beams 3, 4, 5A and 5B had varying amounts of their lower layers of bars exposed. As far as can be determined from crack patterns, deflections, and values of failure loads, this does not appear to have affected Beams 3, 4 or 5A. Examination of the slip gage readings, Figs. 16 and 17, shows movement indicated by the slip gage in the failure span of Beam 3 to be less than either that indicated by the gage in the opposite span or by the gages in several other failure spans. The slip gage in the failure span of Beam 4 hardly moved. Beam 5A was in worse condition than Beams 3 or 4 -- Beam 5B was much worse. Because a smaller shear span to depth ratio was used for Beam 5B than 5A, it was expected that diagonal crack formation in 5B would occur at a higher load. However, the average diagonal tension cracking load was the same for both beams. Possibly the poorer condition of Beam 5B reduced its cracking strength to that of 5A.

Examination of the beams for hairline cracks is not considered by the author to give a complete picture of what is taking place in the material for two reasons. Firstly, hairline cracks probably become visible in stages and are not seen immediately upon formation; considerable separation is required before they can be detected visually. Secondly, even if a fine crack does exist, it can be very difficult to detect. The smoothness of the surface, the quantity and angle of the light used to illuminate the surface, and the time taken in examining an area, are all important factors which dictate how early in its growth a hairline crack can be detected.

Although flexural cracking did not become visible until the range 10 to 20 kips, a sharp change of stiffness could be noted at 4 to 6 kips in all of the load-deflection curves -- presumably this is when the flexural cracking began in the centre span. Perhaps deflections are a more delicate measure of beam behavior than crack examination.

It was noted in several cases, particularly in that of Beam 4, Plates 9 and 10, that considerably more cracking had occurred on one side of the beam than the other. Although care was taken in the arrangements, it is possible that eccentric loading or eccentric positioning of the reinforcing bars could account for this phenomenon; another possible explanation would be the usual differences in ability to observe cracking due to inequalities in the surface textures on either side of the beam. The strain gages placed above the support block of Beam 14 did show greater σ_y stresses on one side than the other, Fig. B-1, Appendix B, thus indicating the presence of eccentric loading conditions.

Generally, it was difficult to match the flexural crack pattern on one side of a beam with that on the other side; sometimes the nearest flexural cracks on each side were up to two inches apart; sometimes a crack existed on one side only. The diagonal tension cracks on either side of a beam were, allowing for crushing and splitting, rarely more than one inch apart. Although location of the formation of the flexural cracks was by chance, any twisting of the beam by the loading arrangement would be a factor in confusing the pattern.

There were some variations among the beams in the rate of loading near failure; the increment of load was usually 500 or 1000 pounds, the period of loading 15 minutes for Series I, 20 minutes for Series II. It appears from the test results that rate of loading may have some effect on the load at which the diagonal tension crack forms. It was noticed that many of the beams could sustain the load increment for as long as 15 minutes before the diagonal tension crack appeared. Should a period less than this have been used, it is possible that a larger load could have been placed on the beam. Conversely, a slower loading might have resulted in a lower value. It would seem that time is required for the beam to become adapted to a load placed on it. Indications of the plasticity of reinforced concrete beams could be noted from the deflection gages, which generally took quite a few minutes to settle down to a steady reading. Beam 5A was loaded roughly two and a half times as fast as the others and does show a higher average diagonal tension cracking shear stress than Beam 4 (and thus all Series I beams).

It must be noted that in this investigation about half the beams contained two layers of reinforcing bars. It is probable that the spacing and width of flexural cracking is affected by both bar diameter and arrangement. In comparing beams with single and double layers of bars and containing zone "Z" diagonal tension cracks, no consistent relationship could be detected between either position of crack or cracking load and number of layers of bars. But those cracks which formed in zone "Y" were in beams with double layers of bars (except Beam 11).

The strain gages were very delicate measuring devices, but were not always reliable when used on concrete. By referring to the curves for strains above the base block of Beam 14, Fig. B-1, Appendix B, it can be seen that many curves showed at least one change of stiffness during the test. There were often discrepancies between zero readings before and after the test, due only partly to permanent set in the concrete. Trial strain readings on the concrete cylinders in connection with experiments in centring the cylinders in the testing machine indicated that strains of the order of 100 to 200 micro-inches were required to cause a permanent set of 10 micro-inches. No doubt the tolerance of the readings from the indicator was large in comparison to the relatively small strains that were measured. It is believed, however, that the two discrepancies mentioned above were mainly due to drift,with time,in the strain gage readings. This drift is probably caused by differences in the effect of temperature and humidity changes on the measuring and compensating gages. In fact, a similar set of readings for a knife edge loading, taken over a 40 minute interval, gave a nearly perfectly linear load-strain relationship. Occasionally a gage (such as gage 2E or 2W, Beam 14-First Crack (34 kips), Fig. B-3, Appendix B), gave a reasonably linear load-strain relationship, which was far from the value expected for that location. The gages are apparently susceptible to local stress variations in the concrete itself --

to stress concentrations due to such things as pieces of aggregate and air voids. It has been suggested that the nominal gage length should be considerably larger than the largest aggregate size; in this investigation, the aggregate was $\frac{1}{2}$ inch, the gages $\frac{3}{4}$ inch (7/16 inches in the case of the A X-5's).

Discussion of Beam Behavior

INITIAL INCLINED CRACKS: Several authors have noted that diagonal tension cracks originate from initial inclined cracks first appearing at or slightly above the level of the reinforcing bars, while others, notably Ferguson (10),have mentioned inclined cracks which appear at mid-depth. Practically anywhere along the length of the beams in the present investigation, a few hairline cracks first became visible at, or within two inches, of the level of the reinforcing bars. However, isolated cracks near mid-depth of a beam were rare; Beam 11 showed the only ones and these were about midway between the level of the reinforcement and the neutral axis (as computed by the Cracked Section Theory). A partial explanation for the fact that cracking was first detected above the level of the bars would be that the lower parts of some of the beams had rough surface textures or even honeycombing, making detection difficult.

It is suggested that at the level of the reinforcing bars, the presence of the bars is a factor in delaying opening of the cracks to a visible width, but that at higher levels in the beam where concrete strain is still relatively large, crack widening is hampered less directly by the bars. Cracking represents a local stress relief in the concrete; the width of the crack is possibly, among other things, a function of the amount of stress relief that has occurred. Immediately around the reinforcing bars, stress relief in the vicinity of a crack would depend on the amount of local bond failure along the bars. At slightly higher levels in the beam, more remote from the bars, the restraint imposed by the bonding of the concrete to steel would have a diminishing effect on crack widening. It has been demonstrated by Watstein and Mathey (21) that cracks would be wider at the surface of a beam than along the reinforcing bars, this effect being more pronounced at higher steel stresses. Thus a crack could first become visible above the reinforcing steel, then grow down to the bottom of the beam.

WARNING OF DIAGONAL CRACKING: There generally was not too much definite warning when a diagonal tension crack was going to form. Both the flexural and most of the initial inclined cracks would grow at very erratic rates. A few of the initial inclined cracks, at one increment prior to "opening up", or even at the final increment, would show a sudden rapid extension upward into the beam. In the case of Beam 2, Plates 5 and 6, Beam 11, Plates 11 and 12, and Beam 5B, Plate 23, the crack had clearly risen into the compression zone. Indications of internal disturbances just prior to diagonal tension cracking can be noted in several strain gage readings in Figs. B-2, B-3 and B-4, Appendix B: Beam 12, gages 5W, 5E (the crack passed through the centre line of both) and 4E; Beam 14-First Crack (34 kips), gages 1 and 4W; Beam 14-Second Crack (38 kips), gage 1. The load-deflection curves exhibited a tendency toward continuous decrease of stiffness during loading, but about half the beams showed a marked decrease of stiffness within two or three load increments before diagonal tension cracking. The slip gage readings do not show any clear pattern in this respect.

Diagonal tension cracks were observed to "open up" from a variety of inclined flexural cracks: tiny cracks; cracks which had grown up to the region of the neutral axis (as calculated by Cracked Section Theory); or occasionally cracks which had clearly progressed into the compression zone. The fact that a considerable number of the diagonal tension cracks exhibited a steep lower end and a much flatter upper end suggests that their growth was in two stages. But from the data of this investigation, no observed stage of crack growth would justify the establishment of the criterion of diagonal tension cracking as other than at that load at which the crack "opened up".

SHEAR BLOCK: An examination of Fig. 11 is of interest. In the case of Beam 14, two diagonal tension cracks formed, the reinforcing bars split out as far back as the support blocks, but the beam continued to carry load. A free body analysis can be made of the shear block (that portion of the beam above the crack; see Fig 26), which is acted upon by the load and support forces (V), the tensile force in the reinforcing bars (T), and the compression zone stresses at the critical section. Presumably a small part of the shear load could be carried by the reinforcing bars in dowel action; this must be transferred directly to the support point, not into the shear block. The resultant of these forces passes along the line marked R. Both diagonal tension cracks of Beam 14 passed below the line of action of the resultant of the applied forces (marked approximately in Fig. 11). The beam continued to carry load after the cracks formed, so the resultant forces could not have been too eccentric to the centroids of the shear blocks. Some eccentricity did exist at certain sections, however, for both tensile strain gage readings and tensile cracking were noted on the top surface of the beam, above the cracks. It can be seen from Figs. 19 and 20, and Figs. B-3 and B-4, Appendix B, that the compression zones above both the First Crack (34 kips) and the Second Crack (38 kips) underwent a sharp stress redistribution upon formation of the diagonal tension crack. The beam photographs, plates 17 to 20, do not indicate too well the existence of tension cracks on the top surface, but these were noted between coordinates 10 and 14 inches above the first crack (34 kips), the largest extending downward 2 inches. Above the Second Crack (38 kips), finer cracking could be seen between coordinates 8 and 10 inches.

Using the strain blocks above the diagonal tension cracks of Beam 14, and with the stress-strain curve for cylinder D, a calculation was made to determine the point of application of the resultant on the section at which strains were measured and a rough value for the shear force carried at that section. In the case of Beam 14-Second Crack (38 kips), the point of application of the resultant at this section fell quite close to what would be expected from an examination of line "R", Fig. 11, while the calculated shear force compared quite reasonably (within 18%) with the value actually applied. However, similar calculations for Beam 14-First Crack (34 kips) compared very badly with the actual values. The strains in this span were unusually low in comparison to those measured over the Second Crack, in the opposite span.

Although the first crack (34 kips) appeared to be somewhat more eccentrically located with respect to the line of action of the resultant, and more tensile cracking existed on the top surface above it, the gage readings showed greater tensile strain above the second crack (38 kips), and in fact failure was at the latter crack.

The diagonal tension cracks which developed in zone "Z" all passed above the line of the resultant of the applied forces, and in each case failure was simultaneous with crack formation. The failure was accompanied by a certain amount of splitting along the reinforcement and a "buckling" action in the compression zone. Whether the diagonal tension crack passed right up to the load point and the thin strut buckled or whether the formation and buckling were simultaneous is not known and is probably immaterial.

From the above, it seems clear that one of the criteria of whether a beam will continue to carry increased load after a diagonal tension crack has formed in it depends upon the location of that crack in relation to the line of action of the resultant of the applied forces on the shear block. Among the beams containing zone "Z" diagonal tension cracks, no consistent relationship could be noted between shear stress at crack formation and position of crack.

The diagonal tension crack of Beam 11 passed a relatively long way below the line of action of the resultant. It is believed that the rather low position of this crack and the unusually high diagonal tension cracking load are related. Of the two diagonal tension cracks of Beam 5A, one was well below the resultant, the other above it, failure resulting when this latter crack formed. Both diagonal tension cracks of Beam 5B were well below the resultant, but failure occurred by crushing as the second crack formed.

Just why a diagonal tension crack should pass above or below the line of action of the resultant is not known, but at the M/Vd ratio of this investigation -- 3 -- it was beams with larger steel ratios which formed "stable" cracks passing below. Even so, Beam 5A developed one crack below and one above the resultant.

Considerable bond stress must exist at the point where the reinforcing steel passes into the shear block. Evidence of this bond stress, combined with the splitting effect of the bars in dowel action, can be seen in the short diagonal cracks along the level of bars in Plate 21. It is believed that the very flat diagonal tension crack on one side of Beam 11, Plate 11, was caused by this effect -- the original hairline crack rose quite steeply, but the increased steel tension tore out a portion of the concrete toward the support point.

STRESS REDISTRIBUTION: The mechanics of stress redistribution in a reinforced concrete beam upon formation of a diagonal tension crack has been described in the "Review of Earlier Research". Just as in the case for a diagonal tension crack, the stress in the steel directly under a steeply inclined flexural crack must be roughly constant and must be governed by the bending moment at the section through the head of the crack. Furthermore, if the growth of the inclined crack is gradual, the stress redistribution too must be gradual.

An analytical study of diagonal tension failures by means of stress trajectories defies solution. A theoretical study can be made of the stress trajectory pattern, but the intrusion of flexural cracking not only rearranges the pattern but introduces local stress concentrations. The position of the diagonal tension crack must be influenced by a very much more complex stress system than that which existed in the beam prior to the commencement of flexural cracking.

POSITION OF DIAGONAL CRACK: A glance at Fig. 11 shows clearly that the diagonal tension cracks did not develop at the theoretical point of maximum principal tensile stress, i.e. near the load point, but they did arise from the steel somewhere in mid-span, usually much closer to the support point than the load point. It is suggested that the reason for this is the contribution of the reinforcing steel to principal tensile stress resistance, and the relationship of this contribution to the angle of inclination of these principal tensile stresses, as will be described below. In passing horizontally along a given level from load to support point in the tension zone of a homogeneous beam, the angle with horizontal of the principal tensile stresses increases from zero to some value less than forty-five degrees. This would also be true of an uncracked reinforced concrete beam, but as flexural cracks form, this pattern could be expected to be somewhat disturbed. As flexural cracking progresses, however, the presence of the principal tensile stresses must influence the direction of cracking. An examination of the crack patterns of a loaded beam shows this to be true -- that cracks near the load point are vertical; those closer to the support point become increasingly more inclined.

Flexural cracks become less frequent closer to the support point because the bending moment decreases in this direction. From the load-deflection curves, Figs. 23 and 24, it can be seen that a sharp decrease in stiffness occurred in the 4 to 6 kip range -- obviously this occurred while the flexural cracking was becoming general throughout the central span. From this, it would be expected that, by the time the 27 kip load was reached, cracking could have proceeded to within 5 to 6 inches of the support point. As mentioned in the section dealing with "Warning of Diagonal Cracking", it seems that most of the diagonal tension cracks developed from some type of flexural crack, either large or small. Certainly such flexural cracking could have been present at the location of the diagonal tension crack. But even if the diagonal tension crack did not form from an existing flexural crack, the concrete stress must have been of such magnitude as to readily permit cracking.

It is suggested that, in moving from load to support point, the trajectories of the directions of the principal tensile stresses dip down to the reinforcing steel level at increasingly steeper angles. Consequently, the reinforcing steel, contributing mainly horizontal resistance to this stress, becomes increasingly less effective. This factor would tend to produce diagonal tension cracking nearer to the support point. However, coupled with this is the influence of the bending moment -- the prerequisite stress necessary to produce flexural cracking decreases toward the support point. Also, as pointed out previously, the support point pressure may cause more rapid decrease of principal tensile stress in the immediate vicinity of the base block than could be expected from the constant decrease of bending moment toward this support point. The result is the formation of the diagonal tension crack somewhere in mid-span -- in this series of tests a substantial number of cracks formed in zone "Z", rising from the reinforcing bars at around two-thirds of the span length from the load point. Extending this hypothesis, it would be expected that variation in steel ratio would affect the position of the diagonal tension crack. No clear trend of this sort can be noted among the diagonal tension cracks in zone "Z", although those cracks which formed in zone "Y" are in beams with the higher steel ratios (except Beam 11).

POTENTIAL CRACKS: Although the diagonal tension cracks developed at a considerable distance from the load point, a few of the beams displayed some very large, steep flexural cracks closer to the load point, in the same span. The opposite spans of several of the beams had well-developed inclined cracks -- for instance, failure appeared imminent in both shear spans of Beam 2. Unfortunately, due to the diagonal tension failures of the first spans, it was impossible to ascertain just what the cracking loads of the opposite spans would have been.

CURRENT EQUATIONS: A comparison of the diagonal tension cracking capacities of the beams in this investigation has been made with those values predicted by equations given in several reports. The curves of v_c versus p, shown in Fig. 27, were computed from the following equations: Moody et al.(9), eq. (1a); Whitney (12), eq. (2) and Morrow & Viest (11), eq. (1). In addition, equations from two recent reports were used: Bower and Viest (14), using the suggested value for the position of the diagonal tension crack; and Diaz De Cossio and Siess (13) (not shown in Fig. 27). The predicted cracking shear stresses are nearly all below the results of this investigation. The Morrow-Viest values are the closest; the Whitney curves are remarkably parallel but 40 to 60 psi. low. The Morrow-Viest, Bower-Viest, and De Cossio-Siess curves can be adjusted by varying the assumed position of the diagonal tension crack. Thus, using the actual position of the cracks, the first of the above equations can be improved considerably, but the other two develop an inclined and very jagged shape. The use of the average of the true positions of the cracks places the De Cossio-Siess curve much too high and the Bower-Viest curve about 10% low. These two equations can be made to fit the test results quite closely by assuming the crack to cross the reinforcing bars at mid-span and at a quarter span length from the support point, respectively.

A comparison was also made between predicted values of shear-compression capacity and actual bending moment at

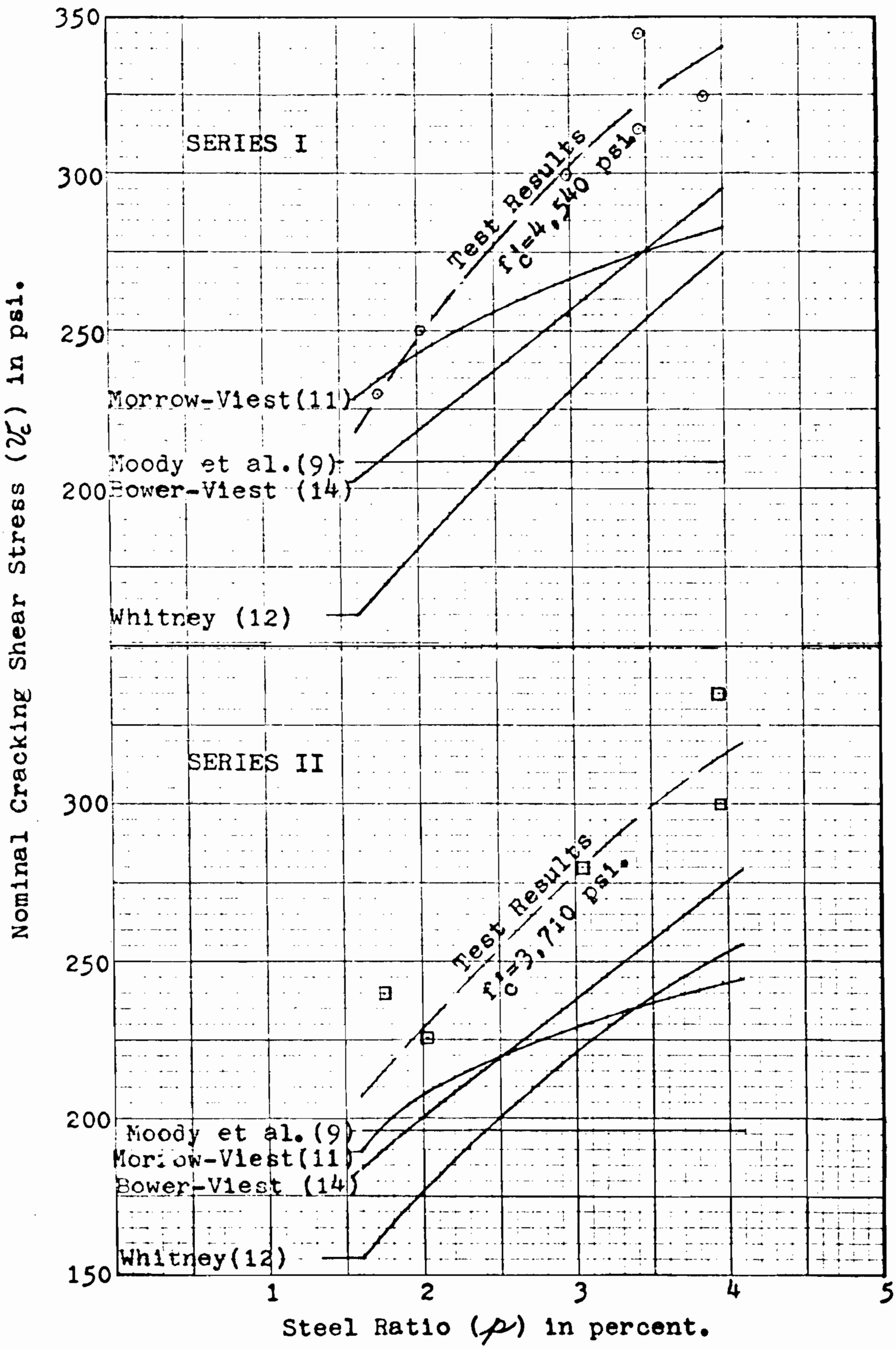

Fig.27-Nominal Cracking Shear Stress Predicted for Test Beams by Equations from Current Literature.

failure; these equations are from Moody et al.(9), eq.(3); Laupa et al.(8), eq. (18); and Morrow & Viest (11), eq.(2). Although the failures were definitely due to diagonal tension, the predicted values of load at shear compression failure are almost the same as the diagonal tension cracking loads. Ultimate bending moment for the only case of a shear compression failure, Beam 14, lies far above any of the predicted values. Beam 11, which carried an unusually high load, lies somewhat above the predicted values. In carrying out the computations with the Laupa et al. equation, a measured value for n of 8 was used for Series II and an assumed value of 6.6 for Series I concrete. With these values, the Laupa et al. equation is comparable to the other two equations. However, this equation for shear compression capacity is quite susceptible to variation in the modular ratio; assuming a value for n of, say 10, increases the predicted values considerably above those given by the other two equations.

TERMINOLOGY: There is quite a variety of terminology used in the literature, in describing shear investigations. Both the reports of Morrow and Viest (11) and that of Moody et al.(9) refer to "shear" failure as being failure by destruction of the compression zone above a diagonal tension crack, but at a greater load than that required to cause the crack to form. "Diagonal tension" failure is designated as the failure that occurs as the crack is formed. Moody et al. (9) refer to "ultimate moment" capacity in a shear failure; many authors refer to this as the "shear compression" capacity. Sometimes the term "shear strength" has been used -- or even simply "strength".

The interpretation of the diagonal tension cracking load is subject to some variation -- in beams with smaller M/Vd ratios it is arbitrary as to just how large an inclined crack must become before it can be labelled a diagonal tension crack. The equations in the literature for predicting the cracking load are based on"the first well defined inclined crack", "a major inclined crack", or "the initial diagonal tension crack" that develops in the span. Some authors report more than one diagonal crack in a shear span (effective span). Perhaps this haziness in definition would account for some of the differences among the various equations given in current literature.

Another point in connection with this haziness in defining a diagonal tension crack is to be found in some of the results presented by Moody et al.(9), page 323, and Morrow and Viest (11), page 843. These tabulated results show values of cracking load (P_c) and ultimate load (P_u). Several of the beams at larger M/Vd ratios (2.5 - 3.5) have a P_u recorded which is only slightly larger than the P_c value. These beams were loaded relatively rapidly, but as mentioned earlier in this discussion, it is possible to get a diagonal tension failure after a constant load has been maintained for several minutes. Considering the rate of loading and the varied definitions of a diagonal tension crack, it would be of interest to know if some of these recorded failures could be considered as a combination of diagonal tension cracking and shear compression failure.

Further Research

It would be of interest to the author to have a comparison between the stresses computed from the stress function, Eq. (6), and stresses measured on a homogeneous beam of an elastic material such as steel. Also of interest would be further calculations with the stress function, in order to ascertain the effects of a variation in the shear span length (keeping all other variables constant), on the local stresses caused by the base block.

In the past, a considerable number of studies done on "shear" failures have been of an empirical nature. Clearly, a more generally applicable, rational approach to failure behavior is needed. Diagonal tension cracking strength is usually correlated with cylinder compressive strength of concrete. Although the tensile strength of concrete can be empirically related to its compressive strength, it would be much more satisfactory in the laboratory to study diagonal tension strength in relation to the tensile strength of concrete. Shrinkage is a very important consideration when studying either plain or reinforced concrete, but with care this can be controlled, as is done when curing modulus of rupture specimens. There is need for a study of the part played by shrinkage on diagonal tension cracking of reinforced concrete beams.

Up to the present, all testing done has been with concrete beams reinforced with round bars, coinciding with general construction practice. However, the state of stress around each individual bar is very complicated -- certainly stress is not uniform throughout the width of the lower part of the beam as is commonly assumed. This aspect could be simplified in order to assess more accurately the factors affecting cracking. Such a simplification might include the replacement of the longitudinal tension bars with a steel plate of the same width as the beam itself. This plate could be embedded on the bottom face of the beam, bond surface being supplied by means of shallow longitudinal and evenly spaced fins. By this means, the shear stress between steel and concrete would be considerably more evenly distributed to the concrete section.

With other variables such as d, M/Vd ratio, type of loading, and shape of beam, it would be of interest to study the relationship between deflection and diagonal tension cracking. Deflections appear to give a fairly clear indication of the initiation of flexural cracking; they can be a powerful tool in studying flexural behavior.

Finally, slip measurement of longitudinal reinforcing bars merits further study. The arrangement used in this investigation requires improvement, particularly the method of anchorage.

SUMMARY AND CONCLUSIONS

This investigation included the testing of eight simply supported, reinforced concrete beams having a cross section 7 by 10 inches and a M/Vd ratio of three, plus tests of two beams 5 by $8\frac{1}{2}$ inches. None contained web reinforcement. With all other variables held constant, the reinforcing steel ratio was varied; the results demonstrated that with increased amounts of steel, the beams had increased resistance to diagonal tension crack formation.

Under load, beam behavior was characteristic of reinforced concrete flexural member until formation of the diagonal tension crack. The load at which flexural cracking began could be clearly discerned on the load-deflection curves. The flexural cracks gradually climbed and spread, but generally little definite forewarning in the form of visible hairline cracking could be found before failure occurred. The diagonal tension cracks appeared quite suddenly and, in ten out of thirteen cases, precipitated complete failure. Those beams that did have diagonal tension failures all developed very similar cracks, Fig. 11.

Included in the discussion of this investigation is a hypothesis concerning location of diagonal tension cracks. After flexural cracking has begun, the reinforcing bars carry part of (or all) the principal tensile stress that previously existed in the concrete. Toward the support point, the direction of the principal tensile stress becomes increasingly more oblique to the longitudinal direction of the reinforcing bars, reducing the bars' effectiveness in carrying this load as a tensile force. However, closer to the support point, both the decreasing bending moment, and perhaps local effects of the base block, produce decreasing principal tensile stresses. The result is the formation of a diagonal crack somewhere in mid-span -- in this investigation, the cracks were close to the support point.

Cylinder compressive strength tests showed that all the beams from a batch of concrete could be described by a single compressive strength with satisfactory accuracy. Tests conducted to determine a stress-strain curve for the concrete of Series II indicated a wide variation in the value of E_c -- from 3,000,000 to 5,000,000 psi.

The electric strain gages, when used on concrete surfaces to measure strain, were found to be very delicate and somewhat temperamental measuring devices. A drift with time, possibly due to temperature and humidity changes, was apparent in some of the readings. The presence of large lumps of aggregate and air voids probably explains much of the wide divergence between gages placed on opposite sides of a beam at a given location.

A stress function, eq. (6), in the form of a trigonometric series has been developed to describe the state of stress in a rectangular homogeneous beam under concentrated loading. The stress components are given by eqs.

(7), (8) and (9); stresses computed for a beam of similar proportions to those tested in this investigation are shown in Figs. 3, 4 and 5. In mid-span these give stresses identical to those given by elementary beam theory; close to the load point they include both flexural and local stresses caused by the applied force. However, these local stresses do not extend much more than a half beam depth horizontally from the point of application of the force. Strain measurements made on a reinforced concrete beam in the vicinity of the base block had a certain similarity to the theoretical σ_y stresses, while the measured σ_x stresses compared fairly well with the theory. Comparisons were made between the stresses given by eqs. (7), (8) and (9) for a 5 inch wide base block and those given by a stress function describing the state of stress caused by a knife edge loading. Within a distance (c) of the load point there are considerable differences between these two extremes in loading conditions; beyond a distance of (c) these two loading conditions produce almost identical stresses.

Slip of longitudinal tension bars was measured with an arrangement shown in Fig. 7(b), in order to show that steep diagonal tension cracks could only develop with considerable slippage of the bars. However, a majority of the diagonal tension cracks formed at very flat angles, obviating any verification of the above hypothesis. An examination of the magnitude of the readings taken suggests that the above method of slip measurement is not too reliable, as flexural cracking in the region of the anchorage could easily distort the results.

Originally, strain measurements were to have been made at the critical section above a diagonal tension crack in order to demonstrate that longitudinal strain at this point must have a trapezoidal, and not triangular, distribution. These measurements could only be obtained on a beam which did not fail at the formation of the diagonal tension crack (the shear block must retain a substantial load-carrying capacity). It had been expected that the use of an a/d ratio of three would assure this type of behavior; such was not the case, as eight out of nine beams having this ratio failed in diagonal tension. It would seem that, to assure diagonal tension crack formation without complete failure, a smaller a/d ratio than three is required. Strain measurements, made on one of the beams that did not fail when the crack formed, gave a very interesting demonstration of stress redistribution at crack formation.

Comparisons of Cracked Section Theory values for deflection and strain with measurements made of these same values, indicated that the beams in this investigation were between 65% and 80% as stiff as suggested by the theory, while the size of the flexural strain blocks varied from 75% to 150% of the theoretical size.

The following conclusions may be drawn from the results of this investigation:

1. Increased resistance to diagonal tension crack formation was associated with increased amounts of longitudinal tension steel in simply supported, reinforced concrete beams having M/Vd ratios of three. These beams were rectangular and without either web reinforcement or compression steel.

2. The state of stress in a rectangular, homogeneous, elastic beam under concentrated loading may be evaluated with the stress function and its stress components given by eqs. (6), (7), (8) and (9).

   Strain measurements made in the vicinity of a support point on a reinforced concrete beam indicated that measured σ_y stresses were somewhat similar, and that measured σ_x stresses were reasonably comparable to the stress components of this function.

3. Measurements, to determine the extent of the slippage of longitudinal tension bars in concrete beams failing due to steep diagonal tension cracks, were attempted; however, such measurements were not obtained for the beams of this investigation because of the types of cracks which developed.

   It is considered that the particular arrangement used in this investigation (see Fig. 7(b)) is inadequate for the purpose of obtaining accurate slip measurements due to the unreliability of the anchorage of the measuring device.

BIBLIOGRAPHY

1. Hognestad, Eivind: "What Do We Know About Diagonal Tension and Web Reinforcement in Concrete?" University of Illinois Engineering Experiment Station, Circular Series No. 64, March 1952.
   (This bulletin contains a very extensive bibliography on shear investigations.)

2. Talbot, A.N.: University of Illinois Engineering Experiment Station, Bulletin Nos. 4, 8, 12, 14, 28, 29.

3. Richart, Frank E.: "An Investigation of Web Stresses in Reinforced Concrete Beams", University of Illinois Engineering Experiment Station, Bulletin 166, June 1927.

4. Richart, Frank E., and Larson, L.J.: "An Investigation of Web Stresses in Concrete Beams, Part II, Restrained Beams", University of Illinois Engineering Experiment Station, Bulletin 175, April 1928.

5. Moretto, Oreste: "An Investigation of the Strength of Welded Stirrups in Reinforced Concrete Beams", ACI Journal, Nov. 1945, Proceedings Vol. 42, pp. 141-162.

6. Clark, Arthur P.: "Diagonal Tension in Reinforced Concrete Beams", ACI Journal, Oct. 1951, Proceedings Vol. 48, pp. 145-156.

7. Zwoyer, E.M., and Siess, C.P.: "Ultimate Strength in

Shear of Simply-Supported Prestressed Concrete Beams Without Web Reinforcement," ACI Journal, Oct. 1954, Proceedings Vol. 51, pp. 181-200.

8. Laupa, Armas ; Siess, Chester P., and Newmark, Nathan M.: "Strength in Shear of Reinforced Concrete Beams", University of Illinois Engineering Experiment Station, Bulletin 428, March 1955.

9. Moody, K.G., Viest, I.M., Elstner, R.C., and Hognestad, E.: "Shear Strength of Reinforced Concrete Beams",

   "Part 1 - Tests of Simple Beams", ACI Journal, Dec. 1954, Proceedings Vol. 51, pp. 317-332.

   "Part 2 - Tests of Restrained Beams Without Web Reinforcement". ACI Journal, Jan. 1955, Proceedings Vol. 51, pp. 417-434.

   "Part 3 - Tests of Restrained Beams With Web Reinforcement", ACI Journal, Feb. 1955, Proceedings Vol. 51, pp. 525-539.

   Moody, K.G., and Viest, I.M.; "Shear Strength of Reinforced Concrete Beams. Part 4 - Analytical Studies", ACI Journal, Mar. 1955, Proceedings Vol. 51, pp. 697-730.

10. Ferguson, Phil M.:"Some Implications of Recent Diagonal Tension Tests", ACI Journal, Aug. 1956, Proceedings Vol. 53, pp. 157-172.

11. Morrow, JoDean; and Viest, I.M.:"Shear Strength of Reinforced Concrete Frame Members Without Web Reinforce-

ment", ACI Journal, Mar. 1957, Proceedings Vol. 53, pp. 833-869.

12. Whitney, Charles S.:"Ultimate Shear Strength of Reinforced Concrete Flat Slabs, Footings, Beams and Frame Members Without Shear Reinforcement", ACI Journal, Oct. 1957, Proceedings Vol. 54, pp. 265-298.

13. Diaz De Cossio, Roger; and Siess, Chester P. : "Behavior and Strength in Shear of Beams and Frames Without Web Reinforcement", ACI Journal, Feb. 1960, Proceedings Vol. 56.

14. Bower, John E., and Viest, Ivan M. :"Shear Strength of Restrained Concrete Beams Without Web Reinforcement", ACI Journal, July 1960, Proceedings Vol. 57.

15. Al-Alusi, A.F.:"Diagonal Tension Strength of Reinforced Concrete T-Beams with Varying Shear Span", ACI Journal, May 1957, Proceedings Vol.53, pp.1067-1077.

16. Hanson, J.A.:"Shear Strength of Lightweight Reinforced Concrete Beams", ACI Journal, Sept. 1958, Proceedings Vol. 55, pp. 387-403.

See also the discussion of the above paper, ACI Journal, Mar. 1959, Proceedings Vol.55, pp. 1057-1068.

17. Taub, J., and Neville, A.M. :"Resistance to Shear of Reinforced Concrete Beams. Part I - Beams Without Web

Reinforcement", ACI Journal, Aug. 1960, Proceedings Vol. 57.

18. Timoshenko, S. and Goodier, J.N. : "Theory of Elasticity", McGraw-Hill Book Company Inc., New York, 1951, Second Edition.

19. Kesler, C.E.: "Statistical Relation Between Cylinder, Modified Cube and Beam Strength of Plain Concrete", American Society for Testing Materials, 1954, Proceedings Vol. 54, pp. 1178-1187.

20. Clark, Arthur P. : "Cracking in Reinforced Concrete Flexural Members", ACI Journal, 1956, Proceedings Vol. 52.

21. Watstein, D., and Mathey, R.G.: "Width of Cracks in Concrete at the Surface of Reinforcing Steel Evaluated by Means of Tensile Bond Specimens", ACI Journal, 1959, Proceedings Vol. 56.

APPENDIX A: FACTORS FOR THE STRESS COMPONENTS ABOVE A BASE BLOCK

An examination of eqs. (7), (8) and (9) revealed that the variable "y" formed the more complex portion of the equations, so the stress calculations were separated into two major steps. The trigonometric-hyperbolic terms within the largest parentheses of eqs. (7), (8) and (9) were called $\overline{X}$, $\overline{T}$ and $\overline{Y}$ respectively. Thus the equations became:

$$\sigma_x = \sum_{m=1}^{m=\infty} \overline{X} \cos \alpha x \tag{7'}$$

$$\tau_{xy} = \sum_{m=1}^{m=\infty} \overline{T} \sin \alpha x \tag{8'}$$

$$\sigma_y = -2rw/\ell - \sum_{m=1}^{m=\infty} \overline{Y} \cos \alpha x \tag{9'}$$

Tabulated calculations were used to compute both the factors $\overline{X}$, $\overline{Y}$ and $\overline{T}$,and the stress components. In the following tables the factors are given for y = 0, $\pm$ 2, $\pm$ 4 and $\pm$ 6 inches; they are carried to 20 cycles. Beam dimensions are as given in "THEORY - Computations".

Cycles	y = 0			y =+6	y =-6
	$\overline{X}$	$\overline{T}$	$\overline{Y}$	$\overline{X}$	$\overline{X}$
1	.0002	.5792	.0098	-3.5678	3.5670
2	.0009	.0635	.0140	- .2089	.2051
3	.0043	-.1479	.0320	.3464	- .3652
4	-.0295	.0094	-.1418	.0505	.0899
5	-.0083	-.1000	-.0295	.2254	- .1820
6	-.0084	-.0453	-.0242	.1224	- .0728
7	-.0175	.0296	-.0436	- .0115	.1313
8	.0238	-.0112	.0524	- .0638	- .1268
9	.0072	.0282	.0144	- .1302	.0614
10	.0057	.0208	.0106	- .1203	.0547
11	.0119	-.0045	.0209	- .0610	- .1080
12	-.0057	.0064	-.0095	.0077	.0927
13	-.0019	-.0052	-.0030	.0651	- .0239
14	-.0013	-.0059	-.0021	.0841	- .0469
15	-.0039	.0003	-.0059	.0656	.0736
16	.0005	-.0020	.0008	.0261	- .0503
17	.0001	.0004	.0002	- .0139	.0047
18	.0001	..0010	.0001	- .0343	.0295
19	.0007	0	.0009	- .0336	- .0336
20	0	.0003	0	- .0189	.0163

Cycles	y =+2			y =-2		
	$\overline{X}$	$\overline{T}$	$\overline{Y}$	$\overline{X}$	$\overline{T}$	$\overline{Y}$
1	-1.1510	.5160	.0718	1.1512	.5160	-.0522
2	- .0594	.0571	.0275	.0606	.0567	.0005
3	.0878	-.1332	-.0154	- .0818	-.1358	.0798
4	- .0244	-.0029	-.1408	- .0176	.0203	-.1490
5	.0150	-.0992	-.0851	- .0274	-.0908	.0235
6	- .0026	-.0497	-.0558	- .0106	-.0393	.0038
7	- .0136	.0177	-.0254	- .0156	.0435	-.0720
8	.0195	.0082	.0513	.0227	-.0324	.0717
9	.0142	.0395	.0473	- .0004	.0253	-.0115
10	.0137	.0320	.0390	- .0017	.0192	-.0106
11	.0113	.0093	.0240	.0157	-.0211	.0360
12	- .0030	.0010	-.0051	- .0110	.0172	-.0243
13	- .0065	-.0110	-.0138	.0015	-.0050	.0038
14	- .0075	-.0124	-.0150	.0035	-.0076	.0074
15	- .0062	-.0074	-.0112	- .0068	.0084	-.0124
16	- .0017	-.0030	-.0031	.0037	-.0054	.0067
17	.0008	.0012	.0014	- .0002	.0004	-.0004
18	.0018	.0027	.0031	- .0016	.0023	-.0027
19	.0017	.0021	.0027	.0017	-.0021	.0027
20	.0008	.0011	.0012	- .0006	.0009	-.0010

Cycles	y = +4			y = -4		
	$\overline{X}$	$\overline{T}$	$\overline{Y}$	$\overline{X}$	$\overline{T}$	$\overline{Y}$
1	-2.3307	.3243	.1191	2.3305	.3243	-.0995
2	-.1270	.0368	.0380	.1264	.0364	-.0100
3	.1929	-.0878	-.0525	-.1955	-.0910	.1181
4	-.0008	-.0094	-.1437	.0172	.0216	-.1585
5	.0753	-.0773	-.1351	-.0715	-.0659	.0677
6	.0270	-.0441	-.0877	-.0242	-.0293	.0269
7	-.0109	.0086	-.0156	.0139	.0470	-.1082
8	.0035	.0204	.0648	-.0027	-.0450	.1072
9	-.0024	.0491	.0923	.0046	.0249	-.0367
10	.0027	.0447	.0822	.0013	.0213	-.0332
11	.0047	.0209	.0421	.0073	-.0385	.0723
12	-.0016	-.0022	-.0063	-.0080	.0328	-.0577
13	-.0065	-.0223	-.0376	.0021	-.0085	.0132
14	-.0097	-.0278	-.0457	.0053	-.0156	.0253
15	-.0082	-.0206	-.0336	-.0092	.0232	-.0376
16	-.0034	-.0078	-.0123	.0066	-.0154	.0243
17	.0018	.0039	.0058	-.0006	.0013	-.0020
18	.0046	.0094	.0141	-.0040	.0080	-.0121
19	.0045	.0087	.0128	.0045	-.0087	.0128
20	.0025	.0046	.0067	-.0021	.0040	-.0057

APPENDIX B: LOAD-STRAIN CURVES

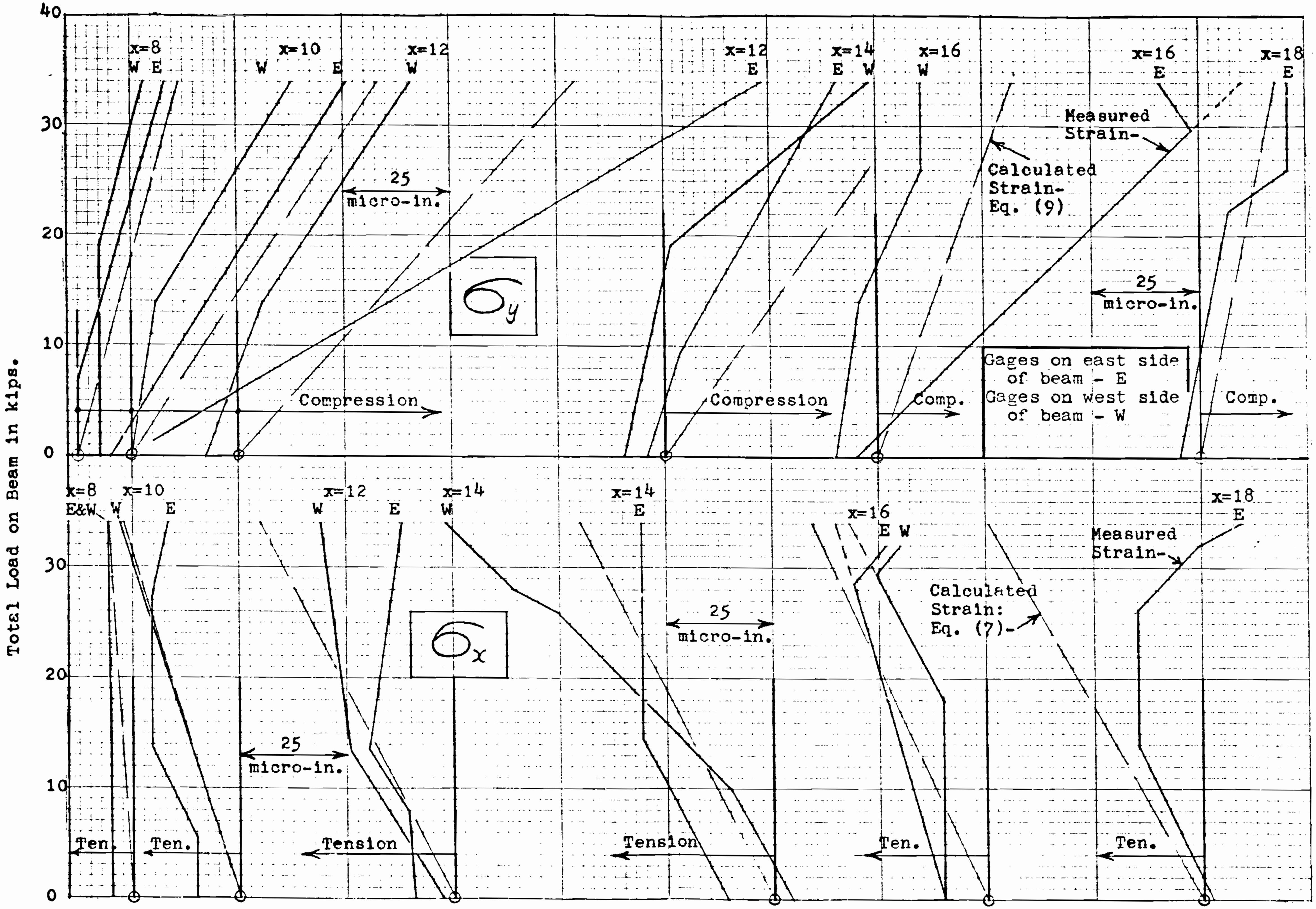

Fig. B-1: Load-Strain Curves for σ_y and σ_x at y= +2 in., above a Base Block Support.

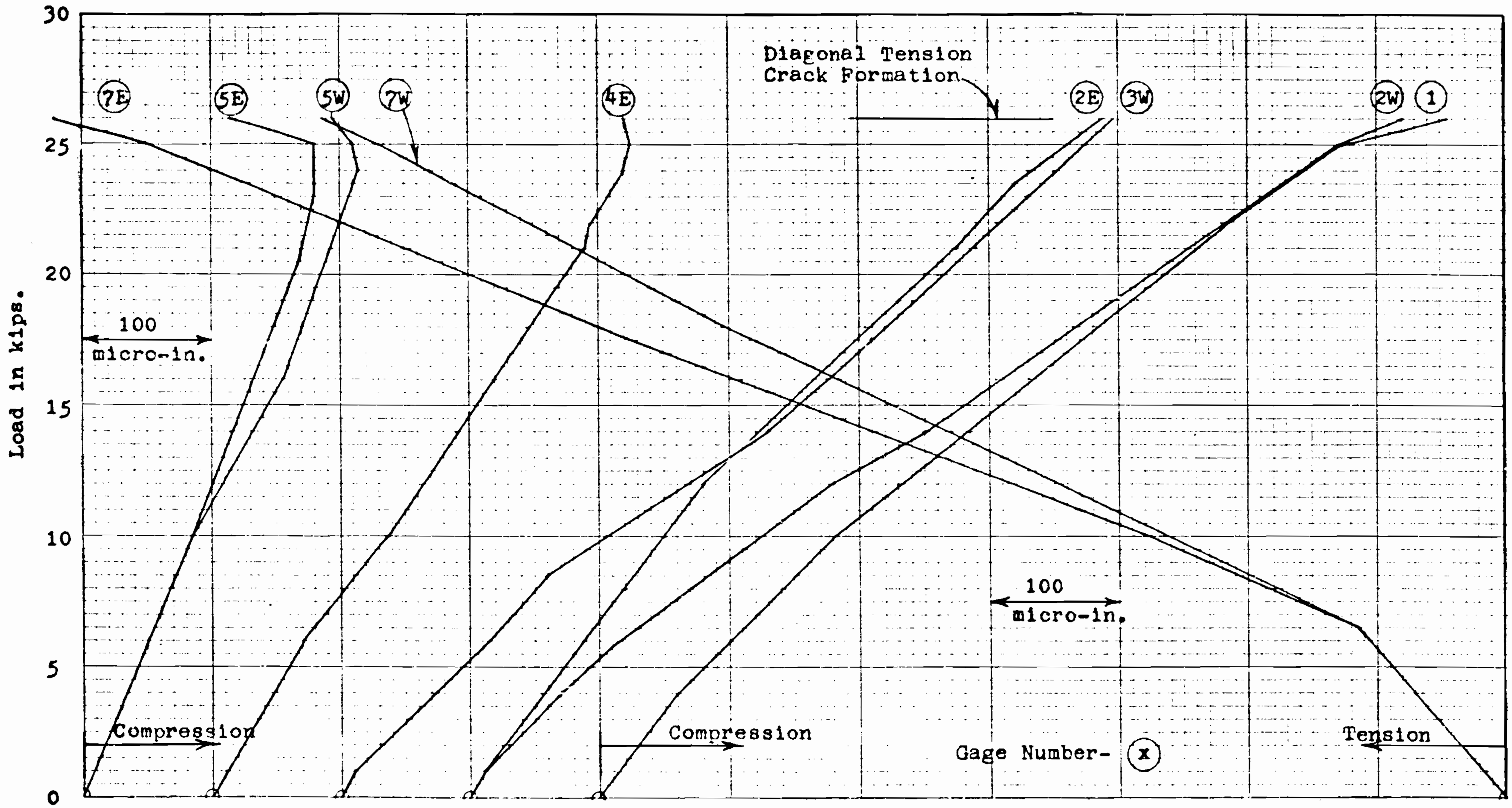

Fig. B-2: Load-Strain Curves for the Shear Span of Beam 12.

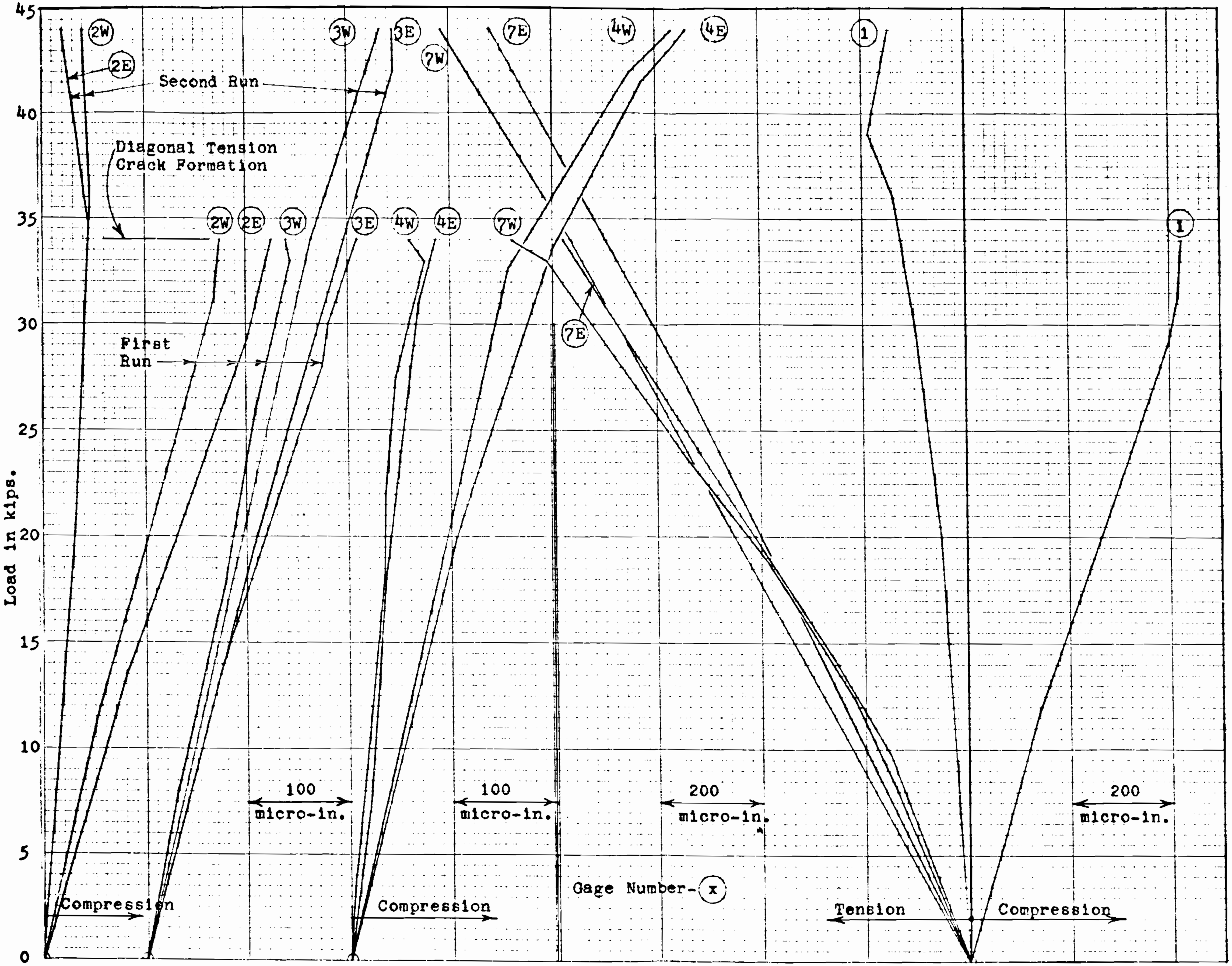

Fig. B-3: Load-Strain Curves for the Shear Span Forming the First Diagonal Tension Crack, Beam 14.

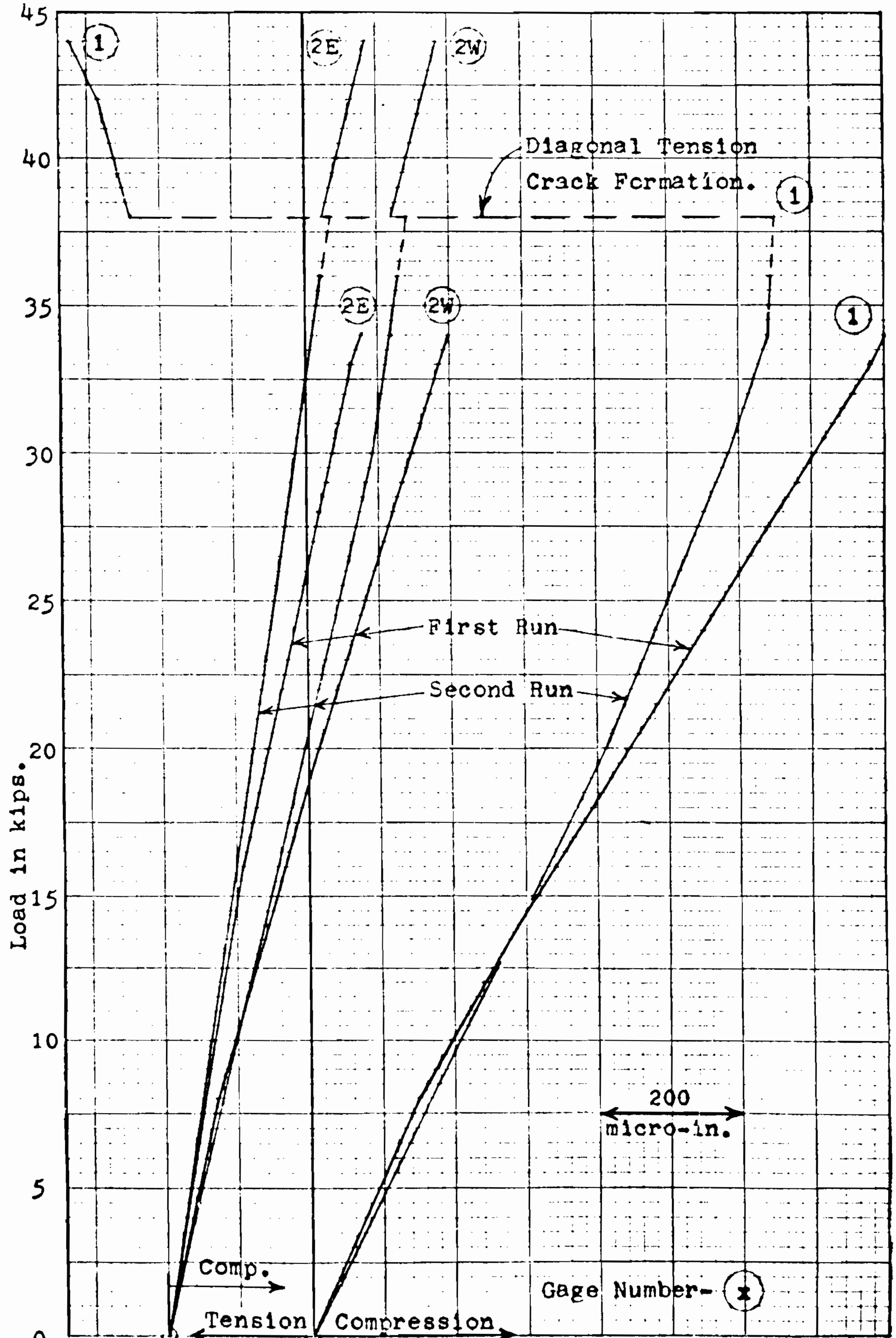

Fig. B-4: Load-Strain Curves for the Shear Span Forming the Second Diagonal Tension Crack, Beam 14.

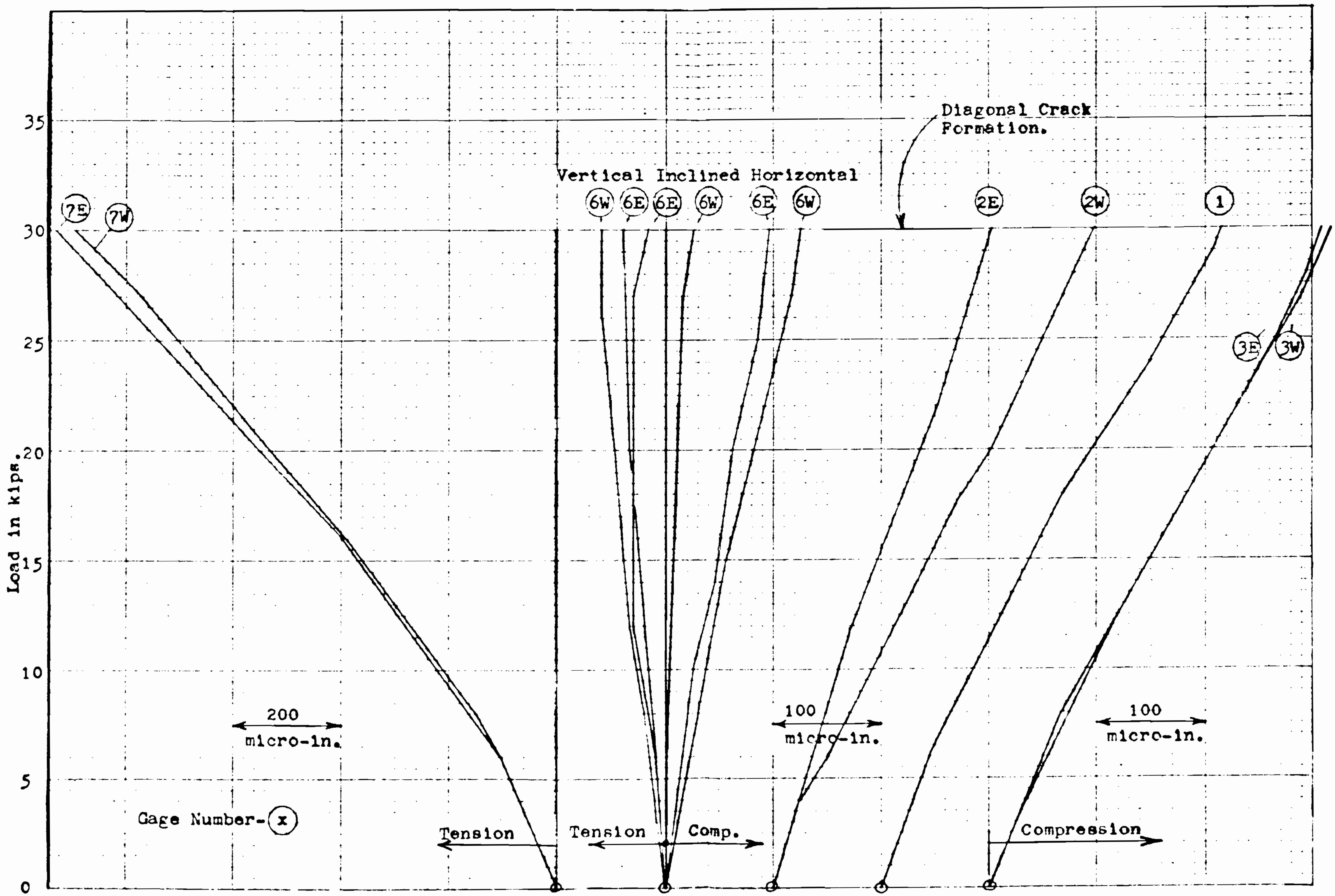

Fig. B-5: Load-Strain Curves for the Shear Span of Beam 13.

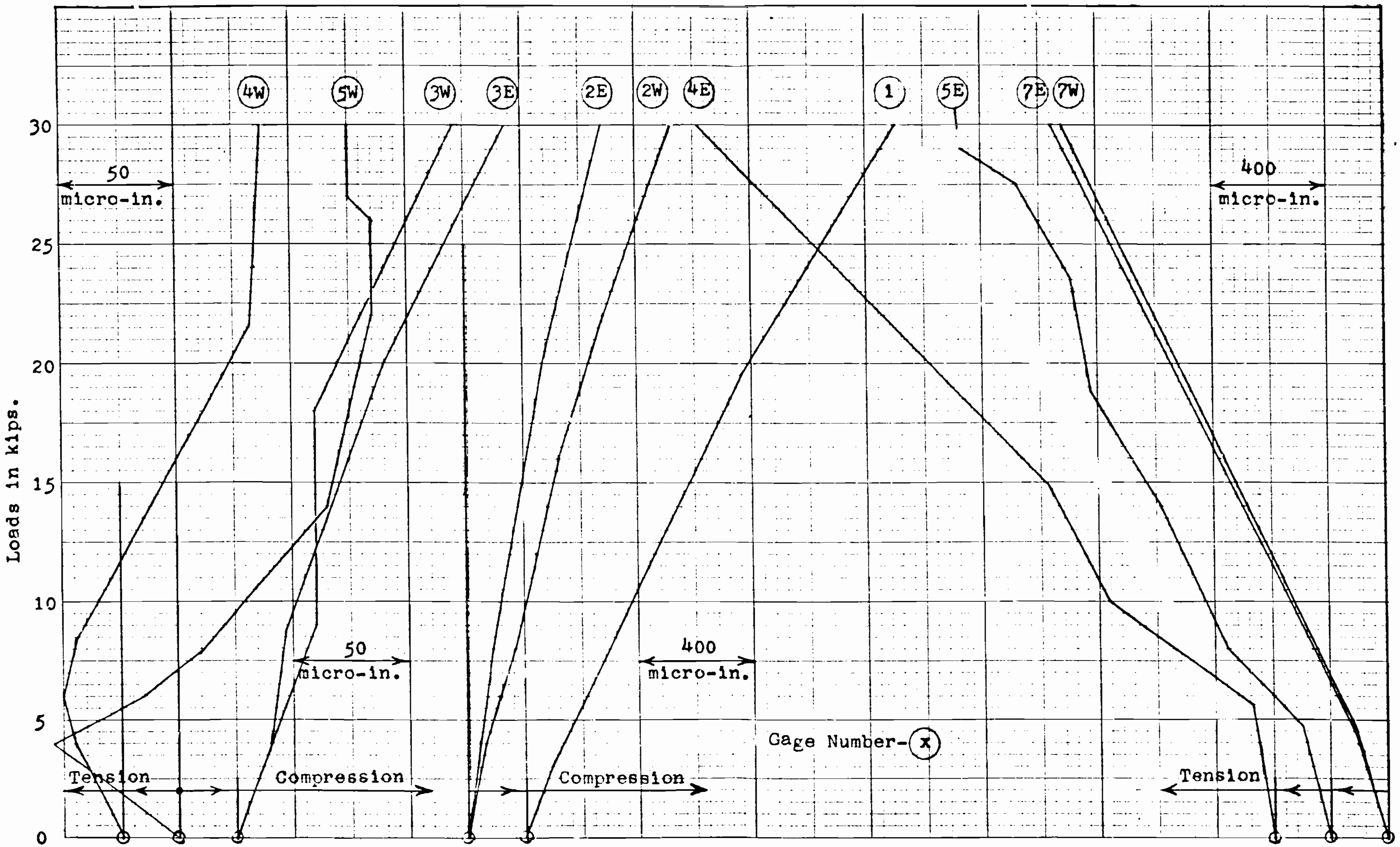

Fig. B-6: Load-Strain Curves for the Pure Moment Span of Beam 13.